Charles University in Prague
Faculty of Science
Institute of Hydrogeology, Engineering Geology and Applied Geophysics

Study program: Applied Geology


**Mgr. Jana Trhlíková**

# Mechanical behaviour of cemented fine-grained soils – simulation of undisturbed samples

Ph.D. THESIS

Supervisor: Ing. Jan Boháč, CSc.

Prague, 2013

Supervisor: Ing. Jan Boháč, CSc.
Institute of Hydrogeology, Engineering Geology and Applied Geophysics
Faculty of Science, Charles University in Prague

Supervisor - consultant: Doc. RNDr. David Mašín, Ph.D.
Institute of Hydrogeology, Engineering Geology and Applied Geophysics
Faculty of Science, Charles University in Prague

## Declaration

I hereby declare that this submission is my own work and that, to the best of my knowledge and belief, it contains neither material previously published or written by another person nor material which to a substantial extent has been accepted for the award of any other degree or diploma of the University or other Institute of higher education, except for the already published results, which are included in the list of references.

In Prague,.....

…….
Signature

**Acknowledgement**

I would like to express my gratitude to my supervisor Ing. Jan Boháč, CSc. and my supervisor - consultant Doc. RNDr. David Mašín, Ph.D. for their advices. I am very grateful to my colleagues for providing a very friendly working environment.

# Table of contents

# Abstract

The mechanical behaviour of natural clays is influenced by the degradation of the structure developed during and after deposition. In order to model the influence of structure artificially cemented specimens have been prepared. A series of one-dimensional compression tests of cement treated kaolin specimens were analysed. The effect of bonding and debonding on compression of the specimens was observed. The compression of cemented specimens was not monotonic, depending on disturbance of the structure. Cement content and curing period were found the main factors influencing the compressibility of cement treated kaolin clay. The possibility of using cement treated kaolin to model naturally cemented soil was confirmed.

For the purpose of the research described in this dissertation, artificial cementation bonds were created in a model clayey material by adding 4% of Portland cement to kaolin clay. The mechanical behaviour of the model material at compression and shearing was compared with the behaviour of the pure reconstituted kaolin clay. Triaxial CIUP tests were carried out in determining the shear strength. Submersible LVDT´s and bender elements were used for measuring of the shear modulus to identify the destructuration of the specimens. The experimental behaviour was successfully simulated by the hypoplastic model.

Finally, the shear modulus of cemented soils at very small strain ($G_0$) was studied. For artificially cemented clay, $G_0$ was found to be independent of the mean effective stress until the yield stress. After yield, a significant effect of structure degradation on $G_0$ was observed. The experimental data were interpreted by an equation, which relate $G_0$ of cemented soils to mean stress, apparent overconsolidation ratio and the state of structure (sensitivity). The equation was also found to represent $G_0$ of cemented sands.

# Chapter 1

# Introduction

Natural clays contain structure (combination of fabric and bonding), which influences their properties (Burland, 1990). According to the literature based on laboratory testing of natural soil specimens (Burland, 1990; Leroueil & Vaughan, 1990; Feda, 1995; Callisto & Rampello, 2004) the effect of structure is to increase strength and decrease compressibility.

Soil structures can be assigned to two basic classes, sedimentation structure and post-sedimentation structure. The first, sedimentation structure, includes all structures that develop during and after deposition as a result solely of one-dimensional consolidation. The second, post-sedimentation structure, develops when some geological process subsequent to normal consolidation intervenes to modify the sedimentation structure. These post-sedimentation structures result from processes such as cementation at deposition, weathering and tectonic shearing (Cotecchia & Chandler, 2000).

Testing of a soil with post-sedimentation structure, naturally cemented soil, is very difficult, because this structure is progressively destroyed as the soil is deformed during sampling and preparation. An alternative is to use artificially cemented specimens made up through the addition of a cementing agent to the soil.

## *1.1. Cementation of soils*

### 1.1.1. Introduction

The formation of natural soils starts with weathering of Earth surface. The products of weathering may remain in situ, forming the residual soils or the process may continue with erosion, transport and deposition of the particles to sedimentary area, forming the deposited soils. Freshly deposited soils are normally consolidated with low bulk density and high permeability. After weathering and deposition, physical, chemical, biochemical and biological alteration of soils occure in order to set the stability under the changing conditions in the

subsurface. The process of hardening and welding of a soil leads to the formation of a sedimentary rock.

The diagenesis is general term for mechanical and chemical changes of soils in the period from the formation to the beginning of metamorphism or weathering. The mechanical changes are connected with compaction of soil with increasing burial depth under younger sediments, associated with decrease of porosity and water content.

The chemical changes are connected with reactions between minerals and the pore water. The effect of the chemical diagenesis can be destructive due to the development of secondary porosity, or constructive, with the pores of soil filled with cement. The cement forms an integral and important part of the soil, leading to changes to the original mineralogy and nature of the soil. Consequently, different properties of soils in natural states are interpreted as a result of different grading, mineralogy, water content and structure.

Structure of soils, the combination of fabric and bonding, is associated with processes and mechanisms operating in various micro- and macroenvironments. During chemical diagenesis soils may acquire additional cementing bonds. Early cementation protects grains against compaction and pressure solutions, further cementation leads to the hardening and welding of soil. Therefore, the presence of cementation in soils has been proved not only by microstructural analyses, but also by testing of the mechanical behaviour of soils.

Typically, cementing bonds at soils are brittle and diminish during sampling and specimen preparation. Artificial cementation is therefore considered as a good option to examine in detail the effect of cementation on mechanical behaviour of soils. The most common admixtures forming the cementing bonds in soils are Portland cement and lime, the other admixtures include gypsum, calcite, wax and resins.

This chapter is concerned with the origin and mineralogy of natural cement, the stability of cementing bonds and evidences from literature. The artificial cementation is discussed from the chemical and microstructural point of view.

### 1.1.2. Natural cementation

The cementation may be defined as a precipitation of micro crystals in the pore spaces of soils, binding the grains together in a fabric, forming a strong and rigid structure. That results in an increase of soil stability against disaggregation by water and solutions and against reorientations during burial and tectonic activity.

Formation of cement is a combined result of mineralogy, particle size and shape, water chemistry during deposition, pressure, temperature and organic content (Mitchell, 1993). The textures and compositions of natural cements may reflect the sedimentary and diagenetic environments in which a soil was formed. Natural cementation often displays a characteristic evolution of the diagenetic system with several cement generations and secondary leaching.

#### 1.1.2.1. Genesis of natural cement

Cement, the secondary component of soils, precipitates from pore water. The identification of the cement origin is often difficult. The cements can originate either from minerals derived from grain solution (isochemical diagenesis in a closed system), or it is a product of crystalization from circulating groundwaters or fossil waters, enriched from outside (allochemical diagenesis). Generally, pore waters are modified by reactions with clay minerals, solution of unstable grains, precipitation of authigenic minerals, mixing with waters from other sources, decomposition of organic matter and by microbial activity (Tucker, 2001).

A large number of ionts, contained in pore water, is released from clay minerals. Clay minerals have a considerable quantity of cations available for exchange, expressed by the cation exchange capacity (CEC). The common process of illitization, the change of smectite to illite at temperatures higher than 50°C, comprises chemical reactions connected with release of Si, Ca, Na and Mg cations to the pore waters. The transformation of montmorillonite (or mixed-layer illite-montmorillonite) to illite is suggested as a source of silica cement (Towe, 1962). On the contrary, the cation exchange with clays may lead to the decrease of the Mg content in the pore water with time.

Another source of ionts may be primary minerals. Solution of unstable minerals appears under the changing physico-chemical conditions. Primary minerals react with solution containing carbon dioxide (hydrolysis), acids (acidolysis), salts of strong acids (salinolysis) and salts of weak acids (alcalinolysis). Some minerals, such as carbonates (e.g. calcite) and evaporites (e.g. halite), dissolve rapidly and significantly change the mineral composition of pore waters. Minerals such as silicates (e.g. feldspars and clay minerals) dissolve much more slowly and their solution has only a minor effect on the water composition. The solution of minerals is increased by respiration by microorganisms and organic matter decomposition, leading to the formation of carbonic and organic acids (van der Perk, 2006).

A transitional process between mechanical and chemical diagenesis is pressure solution. According to Riecke´s principle, the solution of minerals is enhanced under

compressional stress. Thus the stress at the contacts between two grains of a different composition may result in partial pressure dissolution of one particle, the other particle usually maintains its shape. The dissolved matter is often precipitated immediately next to the grain contacts, where minimum stress conditions prevail (Einsele, 1992).

Chemical precipitation is active in the medium of water, mostly when there are mixing two solutions of different composition, temperature, $CO_2$ content, etc. The important factors affecting the precipitation of cement are temperature, Eh (redox potential), pH (acidity-alkalinity) and salinity of surface waters and pore waters. The intensity of cementation is controlled by water energy and circulation. The quantity of cement depends on the supersaturation of pore fluids, the porosity and the permeability of soils.

#### 1.1.2.2. Factors of cement stability

The same processes leading to the cement formation may lead to its destruction. Changing conditions may affect the stability of the initially attained structure by inducing new particle associations, new pore sizes and different pore fluid properties. Such changes may affect the ability of the soil to carry effective stresses as well as its permeability and consistency (Pamukcu & Tuncan, 1991). Consequently, cementation is one of the phenomena causing the development of soil sensitivity.

The chemical stability of cements is affected by temperature, pressure and chemistry of pore waters (characterized with pH, electrolyte concentration and type, salinity and dielectric constants). Cementing minerals frequently reflect the changing conditions, unstable minerals are dissolved and replaced by stable minerals. Circulating pore fluids enable solution and redistribution of cements in a long period of time. Slowly moving pore fluid (e.g. rate of convection about 1 m/year) is heated during its downward flow and it cools within upward moving. The cooling pore fluid precipitates minerals with “prograde solubilities“ (quartz, etc.) and dissolves minerals with “retrograde solubility“ (carbonates, etc.).

The typical transformation of silica phases proceeds with increasing burial depth and temperature from opal-A through opal-CT to quartz, leading to solution-reprecipitation of cement (Mitsui & Taguchi, 1977; Tada & Iijima, 1983; Kim et al., 2007). The data indicate that the transformation of opal-A to opal-CT starts at the temperature range between 22-33°C. The rate of opal-CT dissolution outpaced precipitation once temperature increased above ~55°C (Spinelli et al., 2007). The opal-CT transformation to quartz is completed at around 72°C (Tada & Iijima, 1983).

The solubility of cements is further affected by chemistry of pore waters (Table 1.1). Hematite cement is insoluble in water unless the water becomes highly reduced. The anhydrite precipitation is probably controlled by the temperature and salinity of the pore fluids (Dworkin & Land, 1994). However, there are many exceptions.

*Table 1.1 Characteristics of pore fluids affecting the solubility and precipitation of cements*

| | temperature | pH | salinity | ion activity | reduction/ oxidation | $CO_2$ pressure |
|---|---|---|---|---|---|---|
| anhydrite | x | | x | | | |
| hematite | | | | | x | |
| carbonates | x | x | | x | | x |
| quartz | x | x | | | | |
| clays | x | x | | x | | |

The cementation may be unstable in the zone of weathering. Cyclical wetting and drying and freezing and thawing may lead to mechanical collapse of some structures, particularly those with open fabrics where particles are only weakly bonded (Mitchell, 1993). Mechanical failure of cements also occurs during the onset of plastic (virgin) deformation caused by tectonic movements or increased pressure. Even very soft cement is load-bearing, the yielding and failure of cement depends on its stiffness (Dvorkin & Yin, 1995).

Generally, dissolution and recrystallization of mineral phases can change the distribution and geometry of pores, but it hardly creates a significant increase in overall porosity (Einsele, 1992). The increase in permeability and porosity (secondary porosity) of sediment can be caused by separate dissolution of cement and mechanical failure of cement bonds.

#### 1.1.2.3. Classification and occurrence of natural cementation

The cementation occurs in all types of sediments, soils and sedimentary rocks. Classification system of cements is based on the mineral composition and on the cement volume in the pore space of the sediment. The basic mineral groups of cements are silica, carbonates, authigenic clay minerals, iron oxides and hydroxides, sulphates and zeolites.

The origin of the silica cements is attributed to ground waters, pressure solution (under increasing overburden load) and to solutions of silica dust, other silicates and biogenic silica. The silica cements are represented by quartz, chalcedony and opal. Quartz is the most abundant form of diagenetic cement in clastic sedimentary rocks, especially in sandstones (Grant & Oxtoby, 1992; Haddad et al., 2006). A minor amount of opal cement, coating grains

and present at grain contacts, was indicated in mudstones (Spinelli et al., 2007). The cementation by calcite and opal-CT was proved in pelitic sediments (Mederer, 1988) and claystones (Kim et al., 2007).

The second important group of cements includes carbonates. The source of the $CaCO_3$ may be the pore water itself or dissolution of biogenic carbonate skelets. The common first-generation cement is calcite, which is precipitated in rivers and desert sands and soils at the present. A film of amorphous calcite, strongly bonding clay, was identified by Cotecchia & Chandler (1997). It is also the most abundant cement in carbonate rocks. Calcite precipitation results often in a displacement of grains or in a splitting of grains due to precipitation in the grain cracks (Tucker, 2001).

Calcite is often altered by metastable aragonite cements. Aragonite and high Mg calcite are the most common cements of recent beachrocks or beach sandstones (Ginsburg, 1953; Vieira & De Ros, 2006). The other carbonate cements are dolomite and siderite, less common is magnesite and ankerite. Dolomite and magnesite arise from pore waters rich in Mg ions, siderite arises mostly as the later cement from pore waters rich in Fe ions. The dolomite and lesser ankerite cements were found in layers of sandstones and siltstones (Klein et al., 1999). A sandy rock layer cemented by carbonates, formed at contacts between particles by reprecipitation, was reported by Fukue et al. (2003).

Forming of quartz overgrowths and calcite cementation commonly followed after the precipitation of clay rims. Cementing clay minerals are kaolinite, illite, chlorites and smectites. The type of clay mineral depends on the pH of pore fluids and on the ion activity. Clay and light carbonate cementation at grain contacts is often present in aeolian soils (Mitchell, 1993).

Hematite coatings and impregnations represent iron cements. Another important iron mineral is goethite, forming a frequent microcrystallic cement. The presence of iron oxides acting as a cement between the kaolinite particles were found in kaolin deposits (Cravero et al., 1997).

Sulphates are recent cementing agents often derived from anthropogenic sources, represented by gypsum and anhydrite, less common is baryte. Anhydrite cement precipitates typically in the deep-burial environment. An example of anhydrite, the common but volumetrically minor cement, was found in sandstones (Dworkin & Land, 1994). A combination of anhydrite and baryte cements in sandstones was reported by Gluyas et al. (1997).

Sediments with a high content of volcanic rock fragments and feldspars may have cements formed from clay minerals and zeolites. The pore-filling laumontite, a zeolite formed at higher temperatures from low-temperature clinoptilolite, is usually associated with chlorite and smectite. Smectite and zeolite, filling pore-space of hemipelagic sediments, were observed by Buatier et al. (2002).

According to the cement volume in the pores and the development, the cements can be grouped in four categories: pore-filling, grain-coating, contact and filler (Figure 1.1). Examples of each cement categories are shown in Figure 1.2. The pore-filling cements (Figures 1.1a and 1.2a) fill the pores between clasts, typically by authigenic clays or carbonate cements. This type of cement is usually formed in the deep phreatic zone (the saturated zone) with very low water circulation.

The meniscus (grain-coating) cements (Figures 1.1b and 1.2b) covers clasts as a thin film, the considerable part of pores remains empty. Sediments with this type of cementation ranges from well-cemented to moderate cemented. Overgrowths usually form on the quartz grains of sandstones or limestones, and are sometimes separated from grains by clay or hematite (Folk, 1980). The presence of opal, quartz or hematite overgrowth is common for sediments in the vadose zone (the unsaturated zone above the groundwater table).

Precipitation or recrystallization of authigenic minerals, which takes place only on contact points of grains serving as nuclei, creates contact cements (Figures 1.1c and 1.2c). The contact cement is characteristic of weakly cemented sediments. The typical contact cement is created by silica phase.

The last type of cements are the filler cements (Figures 1.1d and 1.2d), infilling pores with older cement by new precipitates. The pore-filling cements and filler cements are typical for lithified, well-cemented sediments such as limestones (Lindholm, 1974), sandstones (Cookenboo & Bustin, 1999; Gluyas et al. 1997), siltstones, claystones, mudstones, shales and ironstones (sedimentary rocks with more than 15% of iron).

Characterisation of the natural cement type may be difficult. Changes in diagenetic environments lead to formation of different cements with different cementation textures. Four kinds of cements, carbonate (calcite), clay (smectite and illite), phosphate (carbonate-fluorapatite) and hydrocarbon (bitumen) and eight types of cementation textures were identified in storm-influenced marine sediments by Liu & Greyling (1996). Vieira & De Ros (2006) described seven main morphologies of carbonate cements (exclusively composed of high-Mg calcite) and six other diagenetic features in beachrocks. Isotopically and texturally

distinct types of calcitic cements, including calcite and travertine, were found in carbonate rocks (Ellis, 1986).

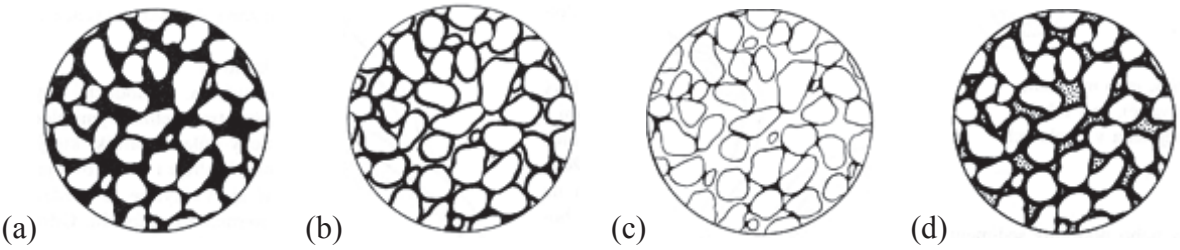


*Figure 1.1 Four categories of cements classified according to the volume in pores (Petránek, 1993). (a) pore-filling cement; (b) grain-coating cement; (c) contact cement; (d) filler cement.*

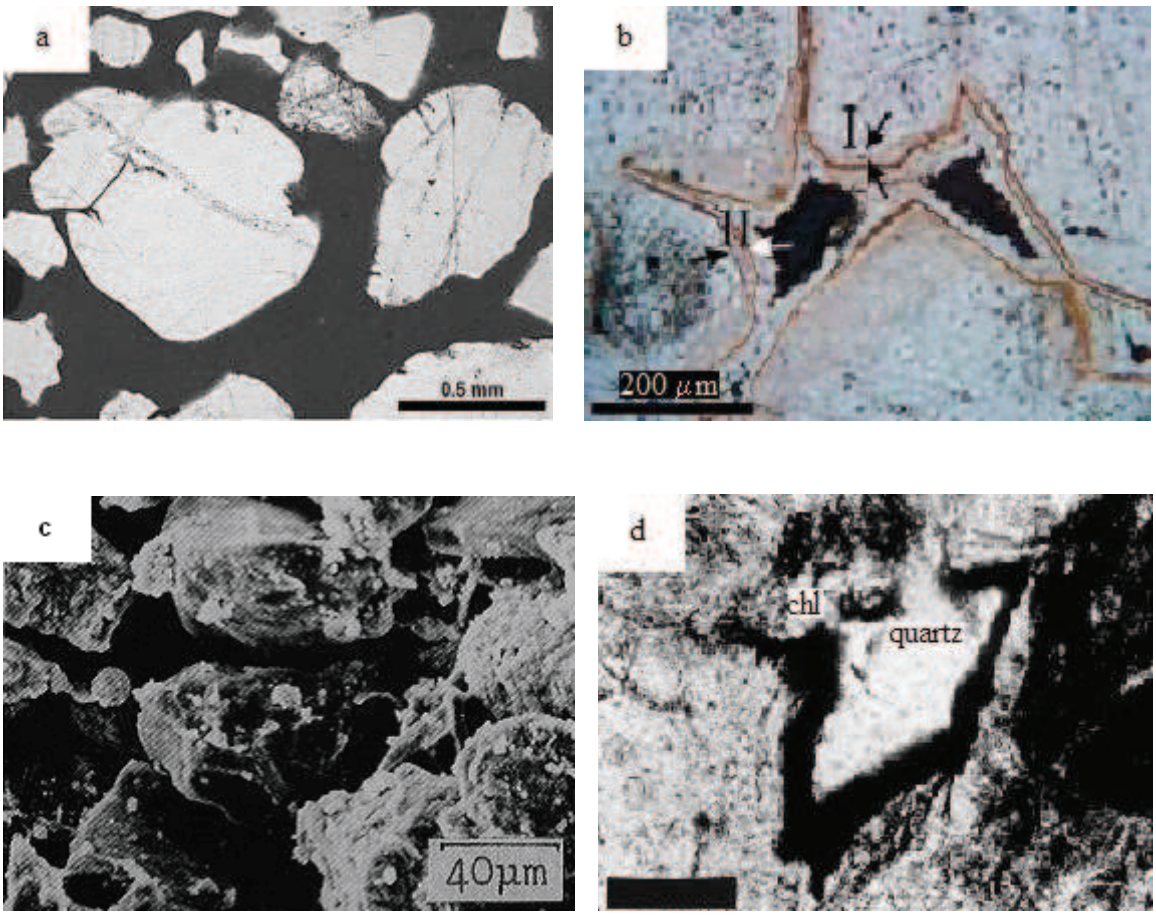


*Figure 1.2 Examples of cements classified according to the volume in pores and the development. (a) Dark, cryptocrystalline cement completely filling the pore space between quartz grains (Vieira & De Ros, 2006). (b) Subangular quartz grains with overgrowth cementation (Haddad et al., 2006). (c) Dominant sand and silt grains with clay particles and amorphous material acting as cement between grains (Guorui, 1991). (d) Quartz cement fills a pore first lined by chlorite cement and then coated by oil (Cookenboo & Bustin, 1999).*

### 1.1.3. Artificial cementation

Natural cementation, its formation, stability and effect on mechanical behaviour of sediments, arises many questions. An artificially cemented specimen formed from soil with cementing agent may help to study all aspects of cementation. The advantage of the artificial cementation is the homogeneity of cement type and no apparent variability as an effect of sampling and specimen preparation.

The preparation of cemented specimen contains problematic issues such as the type of binder, the amount of binder, the amount of water and the curing period. Solutions for these issues are usefull also for the stabilisation of soils (to improve qualities of foundation soils, pavement base layers, etc.) and for radioactive waste deposition. Therefore, different types of cement agents are investigated by scientists to compare their performances as modifiers for soils with different grain size distribution and density.

#### 1.1.3.1. Types of binders

Lime, Portland cement, fly ash, gypsum, calcite, wax and resins have been used as a cementing agent. The interaction of soil with cementing agent includes dissolution and dissociation of additives and soil particles, followed by transfer and exchange of ions, changes in pH and temperature of the environment and precipitation of cement. According to its phases and the cementing agent, which has been used, the artificial cementation may be more or less similar to the processes of cementation in nature.

One of the most common cements existing in nature is calcite. Ismail et al. (2002) reported an usage of a technique called Calcite In-situ Precipitation System (CIPS) to achieve the calcite cementation in sands. The mechanical behaviour of a calcareous sand cemented artificially using calcite was compared with the mechanical behaviour of natural calcarenite samples with a comparable range of density and level of cementation. The mechanical behaviour of both the materials was almost identical. The technique was also used by Sharma & Fahey (2003, 2004) to study the effect of cementation on the deformation characteristics of cemented calcareous soils.

The artificial formation of another natural binder, hematite, was studied by Labuda et al. (2007). The study explored the formation of hard and dense hematite under conditions relevant to those found in steam generators as an analog of the formation of hematite in sedimentary rocks. The structure of the used solids, recovered from the steam generators of a

power plant, closely resembled the structure of red siltstone. The produced hematite formed a hard composite material as well as in nature.

Cementing agents such as lime, Portland cement and fly ash differ from natural cements, but they represent popular binders in the ground improvement techniques. Hence, in such applications, proper understanding of mechanical behaviour of treated soil is essential. Studies show that the mechanical properties of treated soils correspond with the properties of natural structured soils. The interaction of binder and soil leads to chemical and microstructural changes, forming soil with cementation. Thus the mixtures may help to study the effects of cement on mechanical behaviour of soil.

Lime is added to problematic soft clay soils either in the form of quicklime ($CaO_{(s)}$) or as hydrated lime ($Ca(OH)_{2(s)}$). The lime and the soil system with water pass through several different reactions such as hydration, cation exchange and pozzolanic reactions. The lime-clay reaction mechanism was studied by Boardman et al. (2001) on two refined clay minerals, kaolinite and sodium-montmorillonite. The pozzolanic reaction, affecting the long-term changes, took place after 7 days of curing and the montmorillonite produced more reaction products owing to the relative position of silicon and aluminium in the crystal lattices.

The hydration and the pozzolanic reactions are typical also for the soil-Portland cement interaction. The reactions and the effect of each factor are described in detail in the following chapter. A comparison of cement and lime modification was carried out with laterite (Osula, 1996), sulfate rich soils (Puppala et al., 2006) and clayey soils (Tremblay et al., 2001). Osula (1996) examined the performances of lime and cement as modifiers for laterite with kaolinite as predominant clay mineral. The modification was evaluated against plasticity, grain size and liquid limit. The effect of lime was higher than the effect of cement in all aspects.

The other two studies were concerned with mechanical improvement of clays. The stiffness properties of lime and cement treated clays with sulfates were studied by Puppala et al. (2006). Cement treated clays showed considerable increase in small strain stiffness in comparison with lime treated clays. The results agree with observation that the cement binder produces stronger bonds between soil particles than does the lime stabilizer (Chang & Woods, 1992).

Tremblay et al. (2001) tested lime and cement stabilisation of four inorganic soils and three organic soils. The compression behaviour of inorganic clay treated with lime or Portland cement was similar. The stabilisation of organic samples with lime was not very effective in comparison with Portland cement.

Fly ash, a material with good pozzolanic properties, is frequently used in conjunction with lime and cement treatment. Quartz sand and natural silt cemented with a cement fly ash slurry were studied by Lo et al. (2003). The formed specimens showed behaviour patterns of weakly cemented soils.

The artificially cemented sand mixed with gypsum plaster was prepared by Coop & Atkinson (1993). The quantities of gypsum that had to be added to achieve realistic strengths were so great, that the fines content was increased from 1% to 24%, resulting in a reduction in specific volume. The reduction of specific volume has a significant influence on the mechanical behaviour of the cemented soil, such as stress-strain behaviour and the peak strength at strains beyond those required to fracture cement bonding, which must be avoided when comparing with the corresponding uncemented soil.

Epoxy resin and polyester resins systems are adhesives able to bond different materials and the bond strength is considerably high (Shaw, 1982). The type of bonding is very specific and distant from natural bonding. Both resins are classed as thermosettings materials, the molecular chains are locked permanently together, when cured. Further increase in temperature leads to the lost of strength and the resins become more rubbery.

#### 1.1.3.2. Development of artificial structure in soils with Portland cement

The addition of Portland cement to a soil results in several different chemical reactions causing immediate and long-term changes to the soil. The most important reactions are hydration and pozzolanic reactions.

A complicated set of reactions, which follows after mixing of Portland cement with water, is known as cement hydration process. The hydration reactions of pure cement compounds were summarized by Ye (2003). The principal product is calcium silicate hydrate gel, formed as a result of hydration of siliceous compounds of Portland cement. The other products are ettringite or monosulfate aluminate hydrate crystals, calcium hydroxide (Portlandite), alumina hydroxides and garnets. The hydration of Portland cement is connected with the excess of heat and release of the ions $Ca^{2+}$ and $OH^{-}$ (products of the dissolution of Portlandite), $SO_4^{2-}$, $K^{+}$ and $Na^{+}$ to the solution.

The products lead to the formation of hard solid phase (Figure 1.3). The calcium silicate hydrate gel forms fibers on the cement grain surface and the calcium hydroxide precipitates from solution as large crystals into the empty pores.

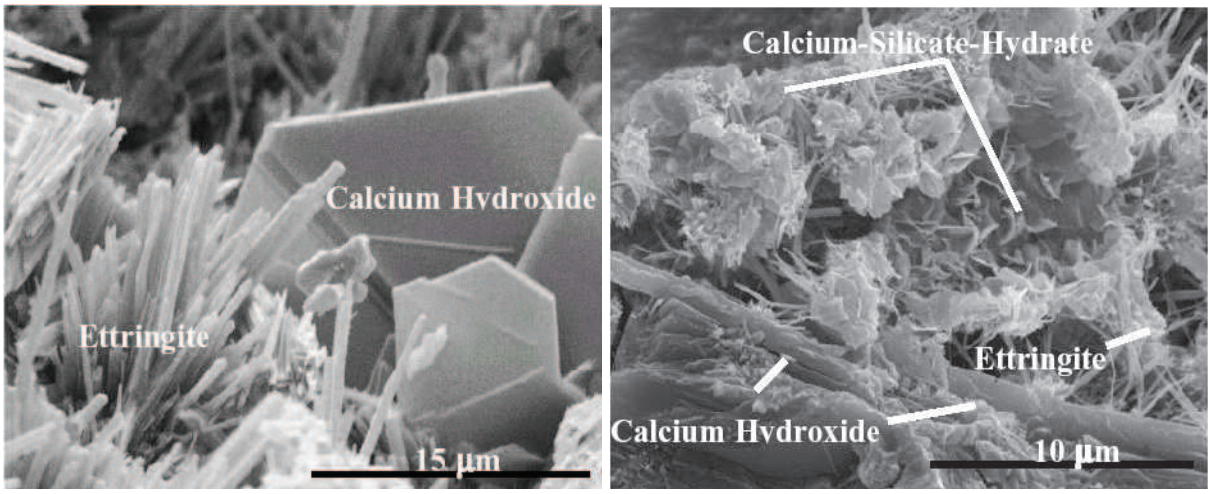


*Figure 1.3 Morphology of the cement hydration products (Stutzman, 2001)*

The pozzolanic reaction is most pronounced in clays, which contain Si, Al and Fe rich phases ready to react with Portlandite. The reaction of Portland cement with sand is affected mainly by the presence of clay.

The modification of clay is brought about by the solution of the silicates and aluminates, leading to the release of Si, Al, Mg and Fe ions. The solution proceeds at the high pH environment caused by the highly reactive lime-product of cement hydration, pH typically changes from around 8 to 13 (Read et al., 2001; Chew et al., 2004). The composition of solution indicates which components of clay have been soluted. The increase in Fe indicates that the dominant solution may be solution of the chlorite component (Pusch et al., 2003). Mg and Al hydroxides are formed by the solution of montmorillonite, clinochlore and illite (Read et al., 2001). Clays such as montmorillonites and illite are rich in Si-O tetrahedral phase, kaolinite is rich in Al-O octahedral phase (He et al., 1995).

The solved material associates with the $Ca^{2+}$ ions, the reaction produces cementing agent coagulating softer parts. The dominating products of pozzolanic reaction between clays and Portlandite are calcium silicate hydrate ($C_2SH_x$, $C_3S_2H_x$) and calcium aluminate hydrate ($C_3AH_x$, $C_4AH_x$) in various concentrations. Gehlenite hydrate and hydrogarnet may be produced in Al rich clays (He et al., 1995). The Mg and Al hydroxides supply a gel-like hydrotalcite phase. The presence of $Ca^{2+}$, $OH^-$ ions and bicarbonate in pore water induces calcite precipitation (Read et al., 2001).

Many physical and chemical factors contribute to the interaction of water, cement and soil. The reactive surface area, pore water chemistry, the potential effect of reaction catalysts or inhibitors, the rate constants, the porosity, soil minerals and soil pH are main effects

associated with the soil. The effect of binder is controlled by the type of cement, cement content, curing time, curing temperature and pH.

#### 1.1.3.3. Level of cementation

The qualitative degree of cementation of a soil can be characterised following the points made by Hight et al. (1992b) in terms of

(a) state – by comparing the void ratios of the cemented clay and the reconstituted clay under the same stress
(b) strength – by comparing the strength of the intact and reconstituted soil, i.e. by sensitivity
(c) yield stress – by comparing the apparent overconsolidation with that attributable to mechanical overconsolidation.

According to Chang & Woods (1992), the degree of cementation may be specified as cementation level C, which is defined as:

$$C = V_c / V_p \tag{2.1}$$

where $V_c$ is volume of the cementing material and $V_p$ is the total volume of the initial void space in the specimen. The value of C ranges from 0% (uncemented) to 100% (fully cemented). The structure of cemented sand may vary in three stages, specified by means of the cementation level (Table 1.2).

*Table 1.2 Microstructure of cemented sand (Chang & Woods, 1992)*

| Stage | Cementation level (%) | Characterization |
|---|---|---|
| I | C < 20 – 25 | cement partially covers the surface of soil particles with some initial bonding at various contact points between soil particles |
| II | 20 – 25 < C < 60 – 80 | cementing of soil particles is very significant, most contact points between soil particles have developed chemical bonds as manifested by cement rings |
| III | C > 80 – 90 | cement fills most of the void space between soil particles, development of chemical bonds has been completed and the additional cement acts mainly as a filler |

The level of artificial cementation in clays strongly depends on the water content (Lorenzo et al., 2005). Water is required for good and efficient mixing of cement with clay and during hydration process of cement. The presence of air in the partially saturated clay results in the decrease of the free dispersion of the cementing ions. Conversely, the clay with high water content eventually requires a large amount of cement to bind together dispersed soil particles. The optimum clay water content is higher than the liquid limit of the clay. Figure 1.4 shows the schematic diagrams of untreated and treated clay particles with different water content suggested by Lorenzo et al. (2005).

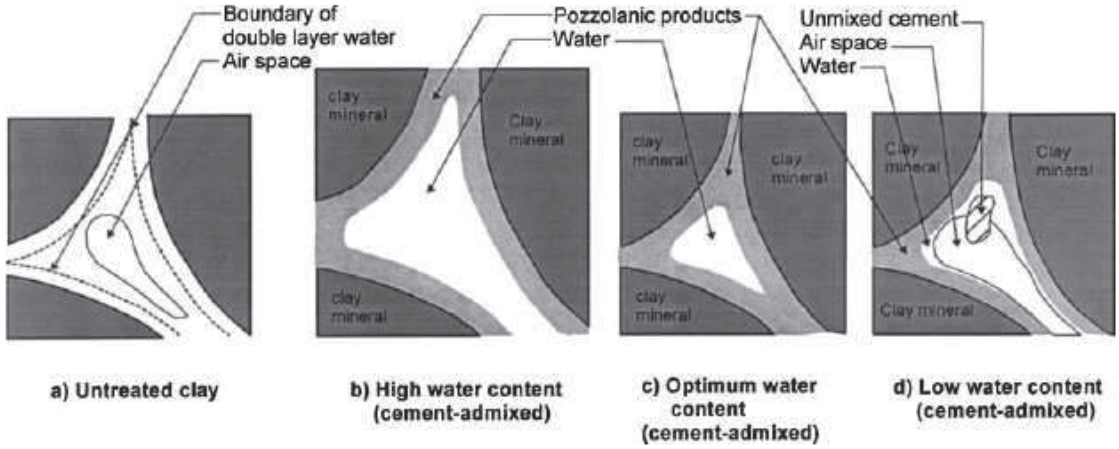


*Figure 1.4 Schematic diagram of untreated and cement treated clay particles showing the effect of mixing water content (Lorenzo et al., 2005)*

## *1.2. Mechanical behaviour of cemented soils*

### 1.2.1. Introduction

Physical and mechanical properties of sediments are closely related to the mineralogical and chemical composition as well as to consolidation and cementation. All contribute in some degree to the microstructure of soil. The relationships between the microstructure of the soil, its geological history and its mechanical response have been studied by many researchers. Analyses of the mechanical behaviour of different undisturbed natural soils have shown similarities, while the comparison of the same undisturbed and reconstituted soil has shown differences. The results show that the microstructure affects the mechanical behaviour of soil in the range from very small to large strains (Sangrey 1972; Clough *et al.* 1981; Burland 1990; Leroueil & Vaughan 1990; Hight et al. 1992b; Feda 1995; Burland *et al.* 1996; Cotecchia & Chandler 1997; Cuccovillo & Coop 1999).

The microstructure of a soil results from particle associations and arrangements (fabric) and from cementing between particles and particle groups (bonding). An important part of the microstructure is represented by cementing bonds, which usually change the characteristics of cemented soils to characteristics of porous weak rocks (Leroueil & Vaughan, 1990). Even light cementation significantly increases the strength and the stiffness of soils, the dilative tendency and the resistance to liquefaction. The effect of cementation on the mechanical behaviour of terrestrial cohesive soils is shown in Table 1.3, which has been listed by Boone & Lutenegger (1997).

The mechanical effect of cementation on the soil behaviour is directly linked to the number of interparticle contacts at which cementation bonds are developed and it is limited by the strength of bonds. The current influence of cementation can be quantified with the parameter sensitivity ratio, defined as the ratio of the size of the boundary to all possible states, state boundary surface, for the cemented soil to that for the corresponding reconstituted soil (Cotecchia & Chandler, 2000). The sensitivity depends on mechanical conditions such as deposition and consolidation rates during formation of cement and on the properties of the cement. Similarly, the cement content, type of cementing agent, the grain size distribution, curing time, density and the cementation-stress history are the major parameters governing the sensitivity of artificially cemented soils (Yun & Santamarina, 2005).

The irreversible process of debonding leads to the degradation of soil microstructure and its mechanical properties. The transition from stiff to less stiff response, connected with

development of irrecoverable plastic strains, is marked by the yield point, a change in stress-strain behaviour under monotonic stress changes. The progressive damage to bonding during plastic straining is often denoted as destructuration. Experimental studies have shown that yield in cemented soils may be determined in all types of laboratory tests.

The literature review is focused on compression and shear behaviour of cemented soils and the possibilities of mathematical modelling of the observed mechanical behaviour. A part of this chapter is a comparison of the effect of natural and artificial cementation, mainly the cementation with Portland cement, which was used for the simulation of the cemented specimens in this work. The influence of cement content and curing period on the behaviour of artificially cemented soils is discussed.

*Table 1.3 Cementing agents and suspected effect on geotechnical engineering properties of soils (Boone & Lutenegger, 1997)*

| Cementing agent | Suspected effect on geotechnical engineering properties | Deposit location | Deposit type[a] | Source |
|---|---|---|---|---|
| Unspecified | Particle bonding; increases strength, $\sigma_p'$ | Lilla Edet, Sweden | GM | Bjerrum and Wu 1960 |
| Carbonates, iron oxides, silicates, aluminates, and organic matter | Aggregation of fines; increases in shear strength | — | — | Lambe 1960; Soderblom 1966 |
| Unspecified | Particle bonding; increases $S_u$; decreases strain at failure ($\varepsilon_f$) | Skabo, Sweden | GM | Bjerrum and Lo 1963 |
| Carbonates | Particle bonding | New Liskeard, Ont. | GL | Townsend 1965 |
| Organics, carbonates, gypsum, Al and Fe compounds | Particle bonding; increases $\sigma_p'$, strength | — | — | Bjerrum 1967 |
| Iron oxides, salt | Increases $\sigma_p'$ | Labrador | GM | Kenney et al. 1967 |
| Aluminum and iron hydroxides | Particle bonding; increases strength | Toulnustouc River, Que. | GM | Conlon 1966; Quigley 1968 |
| Carbonates | Cementation bonding | St. Jean de Vianney, Que. | GM | Moum and Zimmie 1972 |
| Salt, carbonates, iron oxides | Increases $\sigma_p'$, strength; decreases $\varepsilon_f$ | Outardes region, Que. | GL | Loiselle et al. 1971 |
| Salt, carbonates, Al and Fe hydroxides | Increases strength at low stresses | St. Lawrence River valley | GM | Sangrey 1972*a* |
| Salt, carbonates, Al and Fe hydroxides | Increases strength at low stresses | Mattagami, Que. | GL | Sangrey 1972a |
| Amorphous Al and Fe; Mg and Ca; salt | Increases $S_u$ and sensitivity ($S_t$); Mg decreases $S_t$ | Drammen, Norway | GM | Moum et al. 1971 |
| Carbonates, amorphous Si, Al, Fe oxides | Results in cementation and related to $S_t$ | Canadian glacial and glacial-marine clays | GL, GM | Quigley 1980 |
| Carbonates | Increases strength, brittle behaviour | Northampton, Mass. | GL | Bemben 1982 |
| Carbonates | Directly related to $S_t$ | Hawkesbury, Ont. | GL | Quigley et al. 1985 |
| Carbonates | Affects $\sigma_p'$, $S_u$ | James Bay, Canada; Taranto, Italy | GM; L | Jamiolkowski et al. 1985 |
| Carbonates | Variation in $S_u$ and compressibility | Hertfordshire, U.K. | TILL | Little 1989 |
| Carbonates | Affects $\sigma_p'$, $S_u$, $G_o$, OCR, $K_o$ | Fucino, Italy | L | Burghignoli et al. 1991 |

[a]GL, glaciolacustrine; GM, glacial marine; L, lacustrine; TILL, basal or water-laid glacial till or lacustrotill.

### 1.2.2. Compression and swelling

The compression behaviour of either naturally or artificially cemented soil has been studied in literature based upon both one-dimensional and isotropic compression data (see Liu & Carter,

1999). Differences as well as similarities have been observed. According to Burland (1990), the properties of a reconstituted soil represent the intrinsic properties, which are inherent to the soil and independent of its natural state. Thus the intrinsic compression line (ICL), obtained from tests on reconstituted soil, is commonly used as a reference line for studying the compression characteristics of a cemented soil.

The schematic comparison of one-dimensional compression of cemented and reconstituted soil according to Leroueil & Vaughan (1990) is shown in Figure 1.5(a). Figure 1.5(b) shows representative compression curves from isotropic compression tests (Rotta et al., 2003). Despite the different mineralogical composition and particle size, cemented soils follow a simple general pattern with the overconsolidation characteristics. The cementing bonds bear up against compression until the load trespasses their strength. Thus the cemented soils show stiffer response on compression than the reconstituted samples of the equivalent soils until yield is reached.

The yield, threshold of major plastic strains, represents the beginning of the progressive debonding. The abruptness of yield increases with the void ratio at which it occurs and with increase in the bond strength and yield stress (Leroueil & Vaughan, 1990). The effect of cementation is much greater at higher void ratios than at lower ones. Microstructure is not removed immediately, the unstable structural elements degrade with post-yield strains due to further loading.

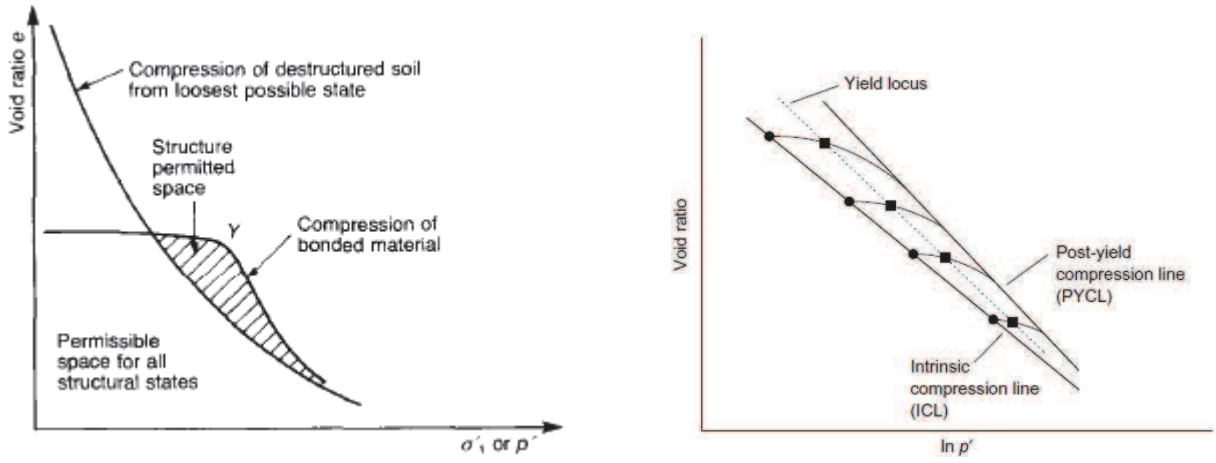


*Figure 1.5 Comparison of structured and destructured compression. (a) oedometer test (Leroueil & Vaughan, 1990). (b) isotropic compression tests (Rotta et al., 2003)*

The yield points and the post-yield compression curves define the boundary for the possible states of cemented soils attainable in one-dimensional or isotropic compression.

After the yield, the paths of the specimens of different initial void ratios all follow a post-yield compression line that is unique for each degree of cementation (Rotta et al., 2003). The post-yield compression line, yield locus and the intrinsic normal compression line may converge at higher stresses (lower void ratios), as indicated in Figure 1.5(b).

Tests on artificially cemented soils show that the change of compression curve inducing apparent overconsolidation is increasing with increasing cement content (Kamruzzaman et al., 2009; Rotta et al., 2003; Feda, 2002; Tremblay et al., 2001). Schematic comparison of the isotropic compression of weekly and strongly cemented sand according to Cuccovillo & Coop (1999) is shown in Figure 1.6. The difference between the behaviour of a weekly and strongly cemented and the corresponding reconstituted soil is reflected in the additional void ratio sustained by soil microstructure. The post-yield isotropic compression curve of well-cemented soil is much steeper than the isotropic compression line of reconstituted soil and they may converge. The convergence is slow, thus the cemented microstructure of soil remains stronger beyond yield and perhaps at all stages of loading. In contrast, the compression curve of weakly cemented soil remains close to the compression curve of reconstituted soil and is essentially parallel. Similar results were obtained for one-dimensional compression behaviour of well-cemented and weakly-cemented clay by Burland (1990).

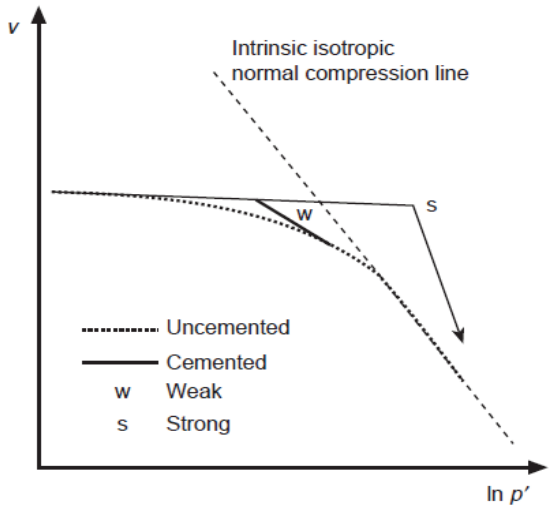


*Figure 1.6 Schematic comparison of the isotropic compression of weakly and strongly cemented carbonate sand (Cuccovillo & Coop, 1999)*

According to the results of tests described by Feda (2002) the influence of cement addition is noticeable on compression curve even with cement content of 2%. For all ranges of cement, the change of void ratio is very small in the pressure range before the respective apparent overconsolidation pressure (yield stress). At the post-yield stress regime, the

reduction of void ratio appears in all cases due to the breaking of cementation bonds. Figure 1.7 shows that after yield, the treated curves shift parallel with the increase of cement content having higher post-yield void ratios.

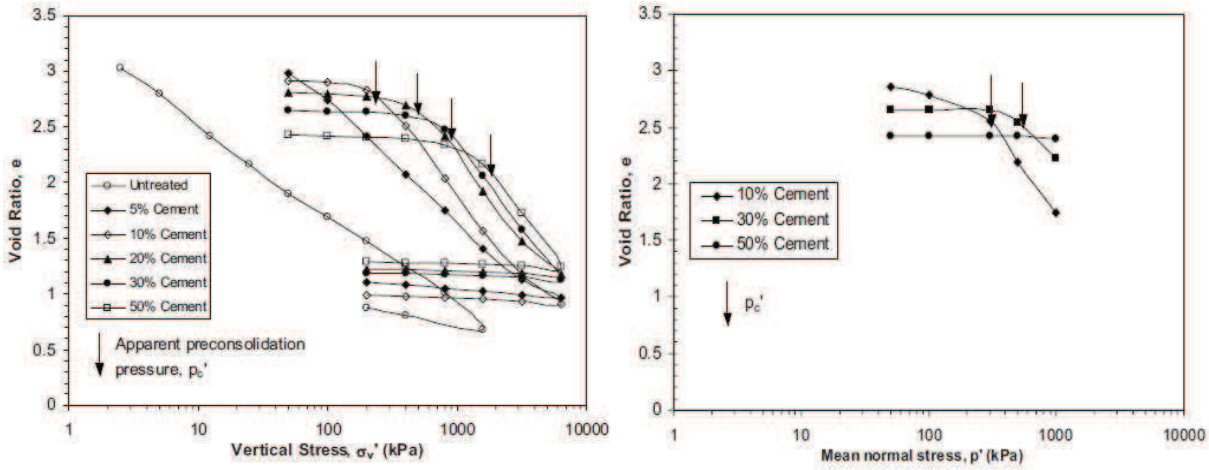


*Figure 1.7 Effect of cement content on compression behaviour of clay at 28-day curing (Kamruzzaman et al., 2009): (a) one-dimensional compression; (b) isotropic compression*

An important factor during the formation of cement bonds is the initial void ratio. The differences in initial void ratio and water content of a natural soil result from the burial to different depths and from a deposition of cementitious material during sedimentation. Similarly, the void ratio of artificially cemented soils is dependent on the curing stress and the cement content. The significant increase of cement content decreases the initial void ratio (Figure 1.7) due to the reduction of water content resulting from hydration and pozzolanic reaction. The reduction of void ratio during curing increases the yield stress of specimens with the same cement content (Rotta et al., 2003).

Changes in the pore space of loess treated with various amount of lime were studied over a long period by Metelková et al. (2012). According to their results the initial macroporosity increases with the amount of lime as a result of flocculation. With curing time the macroporosity of specimens decreases and the mesoporosity increases due to the formation of new mineral phases.

Another important factor, which influences the yield stress of artificially cemented soil, is the curing period. The effect of curing time on the compression behaviour is shown in Figure 1.8. The longer curing period leads to the higher apparent overconsolidation. The significant increase in yield stress is observed at the cement content ≥ 10% (Kamruzzaman et al., 2009).

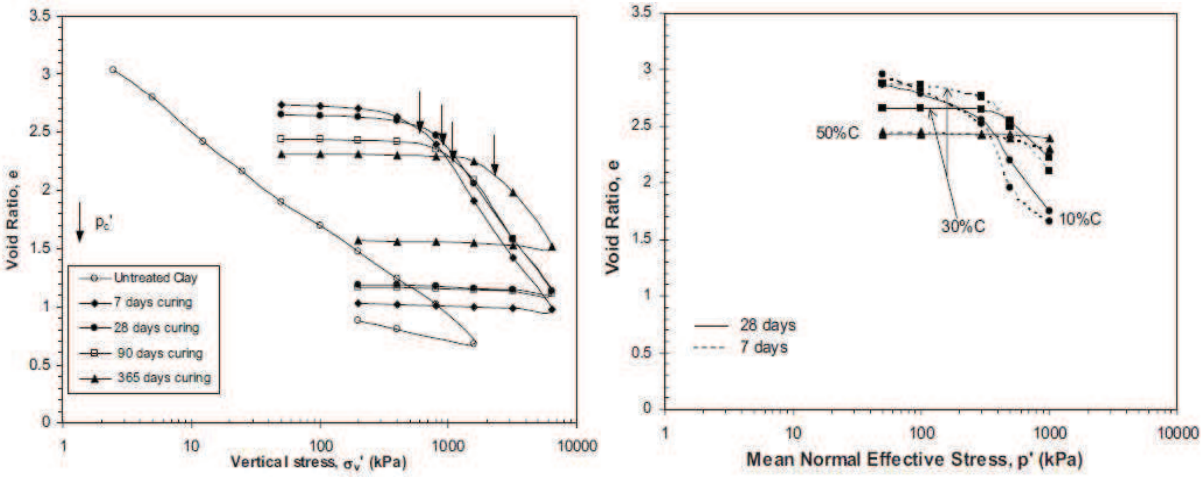


(a) (b)

*Figure 1.8 Effect of curing time on compression behaviour of clay (Kamruzzaman et al., 2009): (a) one-dimensional compression (30% of cement); (b) isotropic compression*

The one-dimensional compression of soils is usually characterised with compression index $C_c$. The stress-strain curves of both naturally and artificially cemented soils in one-dimensional compression are non-linear, therefore no single value of $C_c$ can be ascribed to the cemented soil. The value of $C_c$ for weekly cemented soil is close to the value typical for normally consolidated soil (Feda, 2002). Mixtures with higher cement content have a low $C_c$ up to the yield stress. After yield, the compression of cemented soil gradually increases and the ratio of the plastic strain increments for cemented soil is higher than for reconstituted soil (Kamruzzaman et al., 2009; Feda, 2002).

Figure 1.9 shows the effect of initial void ratio $e$ and the sensitivity $S$ of the clay on the compression index $C_c$ of the structured soil, determined from the post-yield behaviour. The sensitivity reflects the difference between the structured and destructured states. A progressive disruption of the fabric and bonding is connected with the increasing $C_c$. The effects of microstructure are most apparent when void ratio is high (Leroueil & Vaughan, 1990).

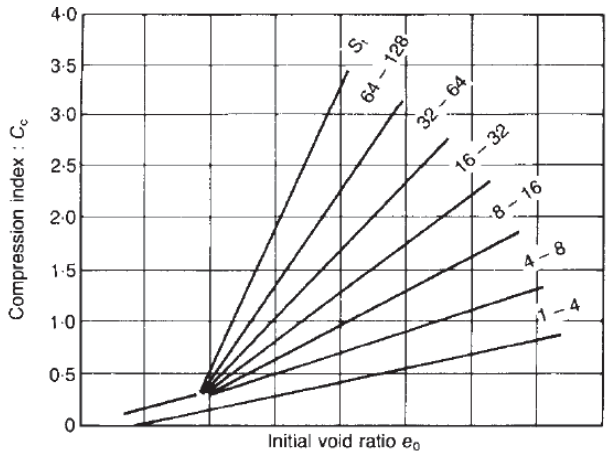


*Figure 1.9 Relationship between compression index $C_c$ and initial void ratio for structured soft clays (Leroueil & Vaughan, 1990)*

Similarly, the swelling index $C_s$ of cemented soil is much smaller than that of uncemented soil (Burland, 1990; Kamruzzaman et al., 2009). The difference between swelling indexes of reconstituted ($C_s^*$) and cemented soil ($C_s$) indicates the strength of cementation, the ratio $C_s^*/ C_s$ (the swell sensitivity) may provide a measure of bonding in the soil (Burland, 1990).

### 1.2.3. Shear strength

The shear behaviour of cemented soils depends on the initial resistance of cemented microstructure and disturbance during testing. Generally, cementation increases the peak strength, initial stiffness and brittleness of soils.

The domain of states in which the shear behaviour of a soil is controlled by bonding is defined by the initial yield locus. The behaviour of cemented soil in this domain may be defined with cohesion $c' > 0$. Figure 1.10 shows two closed yield surfaces, the intrinsic reference yield locus, which represents reconstituted soil, and the initial natural yield locus, which represents the soil with cemented microstructure. Yield is taken as the point at which there is a significant reduction in the gradient of the $q'$ - $\varepsilon_s$ curve. The yield of cemented soils is attributable to the breakage of bonds. According to Rocchi et al. (2003), when the two surfaces coincide, natural clays behave like 'ideal' materials, suitably described by the critical-state soil mechanics framework.

Frictional behaviour is associated with states beyond the yield surface but still within the intact state boundary surface (SBS) as shown in Figure 1.11. Figure 1.11 presents the yield states of the cemented clay and stress paths of the cemented and the reconstituted clay

normalized with $p_e^*$, mean effective stress on reconstituted NCL at the same specific volume as the natural clay. The current state boundary surfaces of both cemented and reconstituted soils have a 'dome' shape. The effect of cementing is shifting of the state boundary surface (Cotecchia & Chandler, 1997).

The location and shape of the bounding surface itself is affected by the level of disturbance. As a result of destructuration, the initial bounding surface of cemented soil shrinks towards that of the corresponding reconstituted soil (Hight et al., 1992b). It is accompanied by a progressive bond degradation and volumetric compression (Cuccovillo & Coop, 1999).

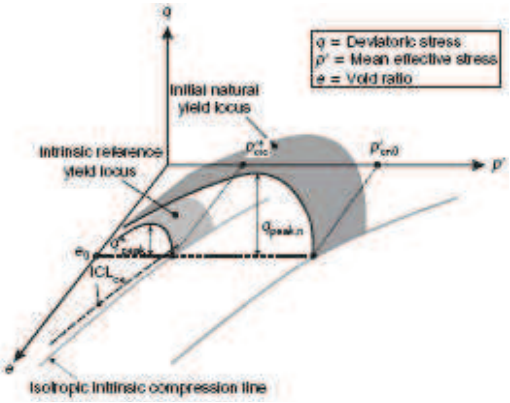


*Figure 1.10 Idealised initial natural and intrinsic reference yield loci (Rocchi et al., 2003)*

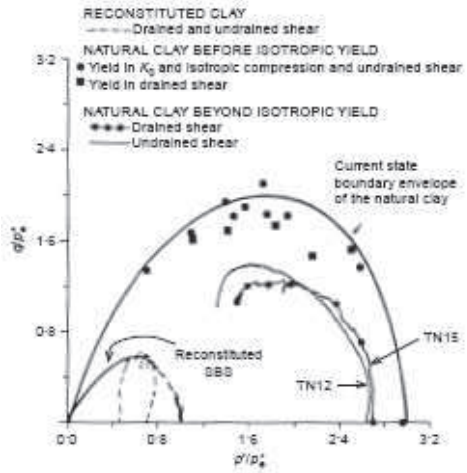


*Figure 1.11 Normalized stress paths and yield states of the natural and the reconstituted clay (Cotecchia & Chandler, 1997)*

Based on the initial state of the sample relative to the yield curve of the cement bonds, three modes of shear behaviour could be identified during shearing of cemented soil (Leroueil

& Vaughan, 1990; Coop & Atkinson, 1993; Cuccovillo & Coop, 1999). The three observed modes are shown in Figure 1.12.

At confining pressures which are low relative to the strength of the bonds, the behaviour is elastic up to a well defined yield. A peak state occurs at low strains well outside the state boundary surface of the uncemented soil. The stress-strain curve shows clearly evident peak strength followed by strain softening towards a much lower destructured or critical state strength. The maximum rate of dilation does not occur at peak, as it would for such a soil, but at significantly larger strains. This indicates that the peak strength is controlled by cemented microstructure rather than density. The presence of bonding prevents the soil from dilating up to yielding. After yielding, the gradual degradation of the bonds inhibits the dilation of the soil, which is later recovered by a more rapid increase of the dilatancy.

At intermediate pressures, yield occurs before reaching the critical state and no peak strength is seen. The failure is essentially frictional, approached after large strains accompanied by significant contraction. At the highest pressures, the behaviour is ductile from the start as the bonding has been broken during compression. The behaviour tends towards that of the uncemented soil, with no yield point. The unbonded soil reaches smaller peak strength at a larger failure strain.

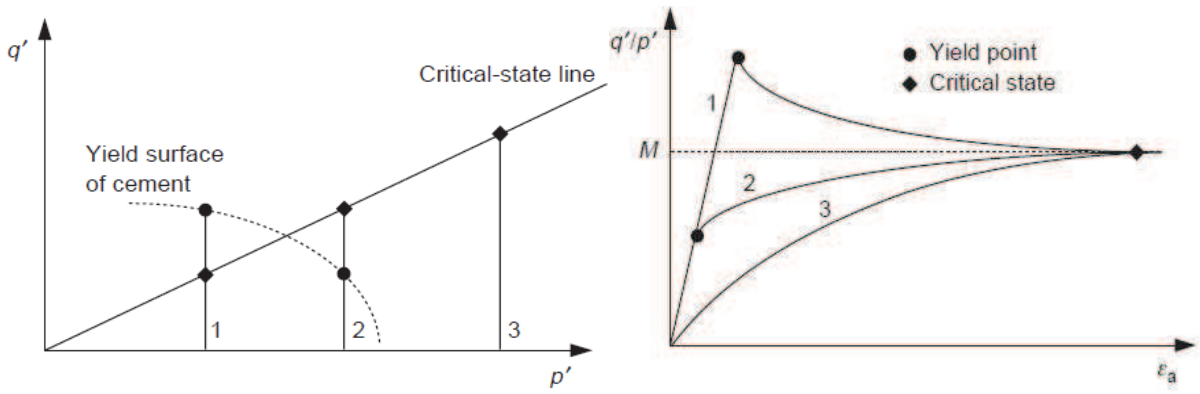


*Figure 1.12 Idealized behaviour of cemented soil (Coop & Atkinson, 1993)*

The failure envelopes of cemented soils, derived from the values of peak deviator stress, are above the critical state line (CSL) of the corresponding destructured soil (Burland, 1990; Leroueil & Vaughan, 1990). The cementation gives a cohesion intercept $c'$ to the strength envelope. Figure 1.13 shows a comparison of the peak strength envelopes and the limit state curves for the bonded, destructured and reconstituted clay normalized with respect to the yield mean stress $p_p'$. The peak strength envelope (upper part of the limit state curve) of

the intact clay is above the reconstituted and destructured clay, reflecting the strength of the bonds (Saihi et al., 2002).

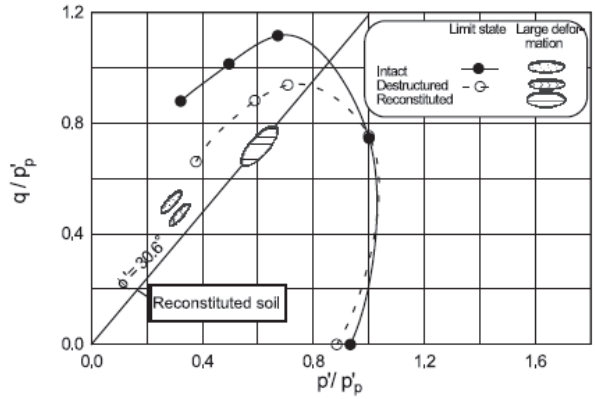


*Figure 1.13 Normalized limit state curves and large deformation states for the intact (bonded), destructured and reconstituted clay (Saihi et al., 2002)*

The critical state of soil corresponds to relatively large straining when the soil is essentially reconstituted and to reach this state the cementing material must fracture. This means that the critical states of cemented and uncemented material will be about the same and the principal influence of cementing will be on yielding and on the small strain stiffness (Atkinson, 1993). Cuccovillo & Coop (1999) obtained for cemented sands at the critical states similar stress ratios to those of corresponding reconstituted soil. Conversely, according to Cotecchia & Chandler (1997), the structural differences between the cemented and reconstituted states of clays remain even at the critical state. Also the normalized stress conditions at large deformation in Figure 1.13 are quite different for intact, destructured and reconstituted clay. The results indicate that the cemented microstructure influences soil behaviour even at large deformations. According to Burland (1990), shearing in triaxial compression does not induce sufficient destruction of the microstructure to bring the soil to the intrinsic critical state.

Uddin & Buensuceso (2002) proposed a conceptual model for the evaluation of the stress-strain behaviour of artificially cemented clay. Figure 1.14 shows the behaviour of the soft clay based on the conceptual model. Lime treatment changes the strength and deformation characteristics from normally consolidated clay behaviour to that of a heavily overconsolidated clay for stress states inside the yield loci $Y_1$ (zone I). It is suggested that the behaviour in this zone is rigid up to failure. The yield loci $Y_1$ was obtained from the bilinear characteristics of the strain paths during anisotropic consolidation.

Outside the strain path yield loci (within zone II), the behaviour consists of three phases: an initial pseudo-elastic phase, a work-hardening phase up to failure, and a strain-softening phase up to the residual states. A schematic comparison of the drained and undrained shearing behaviour of untreated and lime treated clay in this zone is shown in Figures 1.15 and 1.16 respectively.

The pseudo-elastic behaviour is characteristic for stress states from consolidation pressure $p_0$ up to the yield locus, distortional ($Y_2$) or volumetric ($Y_3$). Within the pseudo-elastic phase, the developments of pore pressures and volumetric strains are very small. The distortional and volumetric yield loci are defined from the relationships of mean normal stress during anisotropic consolidation and the shear strain and volumetric strain respectively.

The work-hardening phase starts as the stress path crosses the distortional or volumetric yield locus and exists up to the failure of the treated clay. The behaviour is characterized with relatively large increase of deformations and pore pressures during CID and CIU tests respectively. The stress-strain behaviour of treated clay can be described with the use of critical states concepts until the failure state.

The failure states are followed by strain-softening phase, with a very large reduction in strength observed after considerable straining. The behaviour of the clay is unstable within this phase and cannot be properly described with the use of critical states concepts.

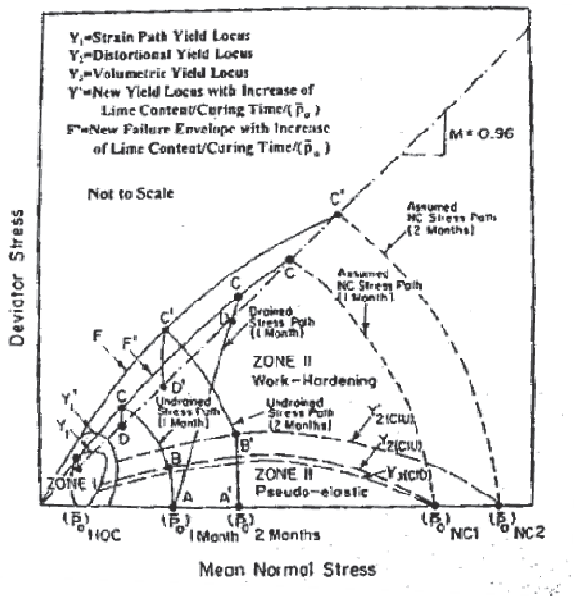


*Figure 1.14 Schematic diagram of the behaviour of lime treated clay (Uddin & Buensuceso, 2002)*

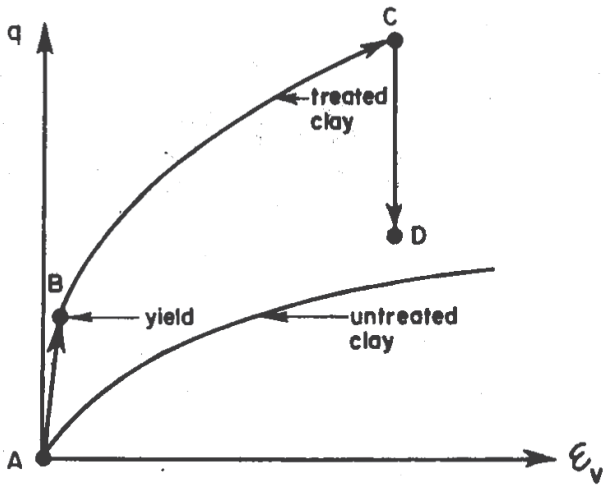


*Figure 1.15 Schematic diagram of q-$\varepsilon_v$ relationship from CID test for lime treated clay (Uddin & Buensuceso, 2002)*

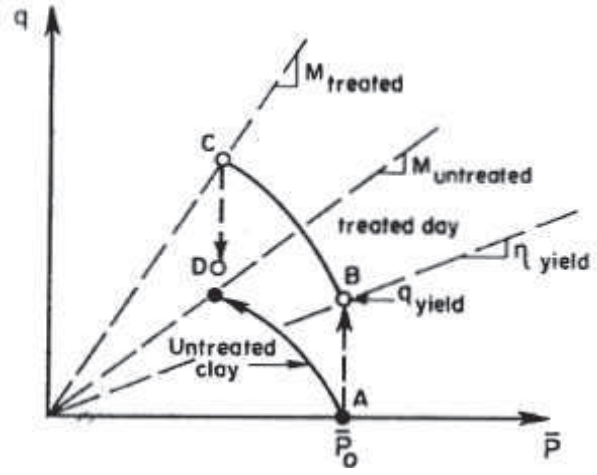


*Figure 1.16 Schematic diagram of undrained stress path for lime treated clay (Uddin & Buensuceso, 2002)*

The formation of cemented microstructure in Portland cement or lime treated soils leads to a notable increase of strength in dependence on cement or lime content and curing period (Uddin & Buensuceso, 2002; Kamruzzaman et al., 2009). An increase in the cement content or curing period results in an expansion of the yield curve of the cement bonds. Consequently, the strength of the cemented soil is higher at higher content of the additive and curing period (Figure 1.17). Test results reveal that at higher cement content, the cemented clay showed strain softening behaviour up to higher compression and the differences of peak deviator stresses are minor in that range of mean effective stress. This is due to the effect of cementation leading to the minor volume changes during the consolidation stages of the specimens (Kamruzzaman et al., 2009).

The curing period affects the linearity of the failure envelope (Kamruzzaman et al., 2009). A more linear failure envelope from shearing is shown by specimens with shorter curing period, as destructuration is completed during the consolidation stage. Conversely, the different curing period has no influence on the destructuration envelope, derived from the ultimate states of cemented specimens.

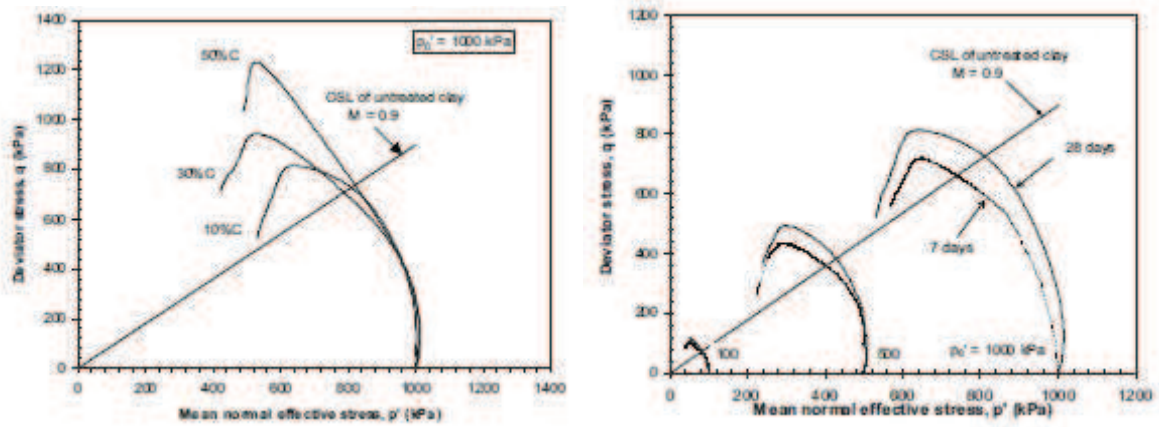


*Figure 1.17 Effect of cement content and curing time on the stress paths of cement treated specimens (Kamruzzaman et al., 2009)*

According to Uddin & Buensuceso (2002) the stress states of artificially treated clay ultimately lie very close to the CSL of the corresponding reconstituted clay. However, the destructuration envelope of cemented specimens obtained by Kamruzzaman et al. (2009) lay above the CSL of reconstituted soil and was shifted upward with the increase of cement content. At the destructuration state, the behaviour of the artificially cemented specimen was different from that of the natural clay. According to the authors, the hydration and pozzolanic reaction between cement and clay particles creates permanent changes of the treated clay fabric, which could not be reversed or destroyed during the shearing.

### 1.2.4. Shear stiffness

The cementation provides strong enhancements to the shear strength and shear stiffness properties. Figure 1.18 presents the patterns of behaviour expected of unbonded and bonded soils and soft rock. Unbonded soils are less stiff and show no bond yield. The curve of bonded soil indicates that the bonds contribute to an increase in the initial stiffness. The soil shows the first yield, representing the limit of linear elastic behaviour and the bond yield, representing the limit of recoverable behaviour similarly to the curve of soft rocks (Malandraki & Toll, 2001). Moving the state of the soil towards the intact isotropic boundary does not change the

value of stiffness determined by the bonds but decreases the range of strains over which bonding enhances stiffness (Cuccovillo & Coop, 1999).

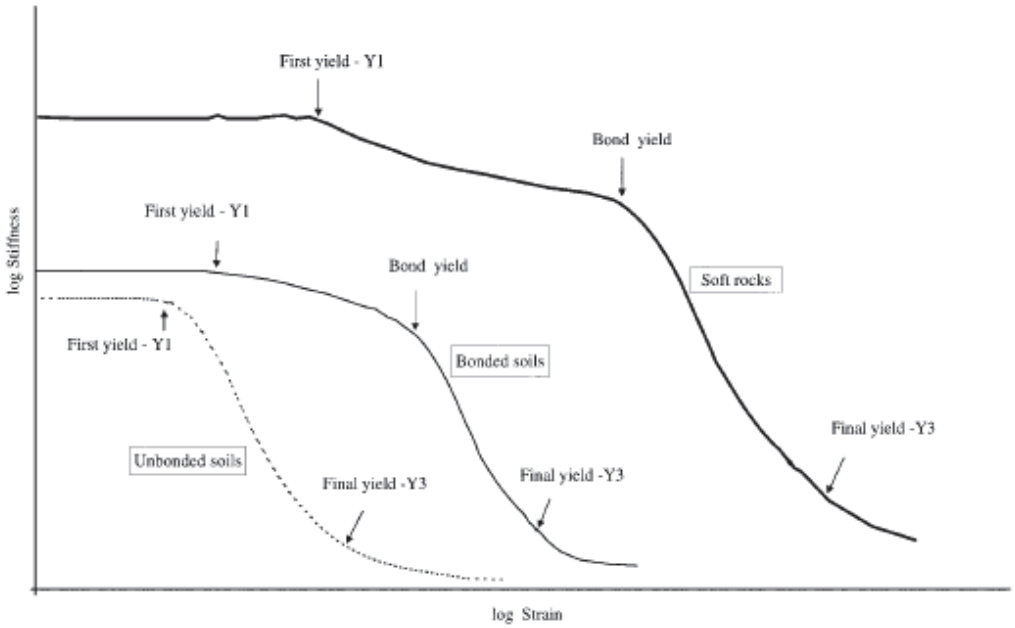


*Figure 1.18 Comparison of stiffness variation with strain for unbonded and bonded soils and soft rocks (Malandraki & Toll, 2001)*

Numerous studies published in the literature are concerned with the shear stiffness of naturally or artificially cemented sands. A consistent finding is that increasing cementation increases the very small strain stiffness ($G_0$) of sands (Acar & El-Tahir, 1986; Saxena et al., 1988; Chang & Woods, 1992; Sharma & Fahey, 2004).

The disagreement was found in the dependence of $G_0$ on confining pressure. According to the studies made by Acar & El-Tahir (1986) and Delfosse-Ribay et al. (2004), shear modulus of cemented sands increases with confining stress in the whole stress range. Conversely, Cuccovillo & Coop (1997), Baig et al. (1997), Fernandez & Santamarina (2001) and Sharma & Fahey (2004) reported the values of $G_0$ to be for cemented sands practically independent of the mean effective stress and dependent on cementation until a threshold stress, at which the destructuring takes place. The latter findings are consistent with the predictions of a micromechanical model for cemented granular material developed by Dvorkin *et al.* (1991), leading to the conclusion that the stiffness of the cemented system is strongly increased by cementation and independent of confining pressure.

The connection between deterioration of bonding and initiation of the pressure dependency of $G_0$ was reported for naturally cemented carbonate sand (i.e. calcarenite; Cuccovillo & Coop, 1997) and loose cement treated sand (Yun & Santamarina, 2005). After

yielding, Cuccovillo & Coop (1997) reported the decrease of very small strain stiffness as the bonding degrades, even if the mean effective stress and density increase. Conversely, the data of Yun & Santamarina (2005) for artificially cemented sand indicate the increase of very small strain stiffness with increasing stress after yielding, similarly to uncemented specimens (Figure 1.19). The reported values of $G_0$ of cemented sand were still higher even after yield. In both cases, it is expected that $G_0$ of cemented sand is gradually converging towards the values for uncemented sand due to complete degradation of cementation at high stress levels.

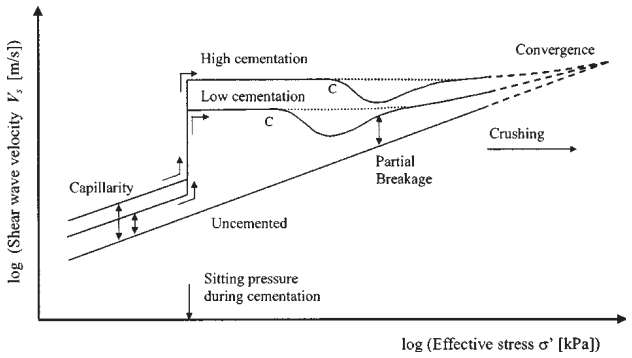


*Figure 1.19 Shear wave velocity of cemented and uncemented soils versus effective stress (Yun & Santamarina, 2005)*

The studies of very small strain stiffness $G_0$ of cemented clays are less common. Nevertheless, the obtained very small strain stiffness behaviour of cemented clays is qualitatively similar to the behaviour of cemented sands. The initial very small strain shear stiffness is increased by natural (Jovičić et al., 2006) and artificial (Puppala et al., 2006) cementation. The cementation solely controls $G_0$ at low stresses prior to yield stress and the dominant effect of stress prevails at higher stresses (Jovičić et al., 2006; Hird & Chan, 2008). After yield, the values of $G_0$ measured on artificially cemented clay by Hird & Chan (2008) were found to increase with increasing stress as for uncemented clay. On the contrary, the reduction in $G_0$ during compression after yield associated with degradation of natural clay microstructure was reported by Cafaro & Cotecchia (2001).

Figure 1.20 shows the variation of shear modulus with increasing percentages by weight of cementing agent (flyash). The values were obtained with bender elements measurements. The shear modulus of the kaolinite and flyash mixture increases with increasing percentage of additive up to around 20% and then decreases. This may indicate that the clay tends to acquire a flocculated microstructure at lower percentages of additives and consequently the stiffness increases. Conversely, at higher percentages of the additives the

microstructure may be dispersed producing the effect of reduced stiffness (Pamukcu & Tuncan, 1991).

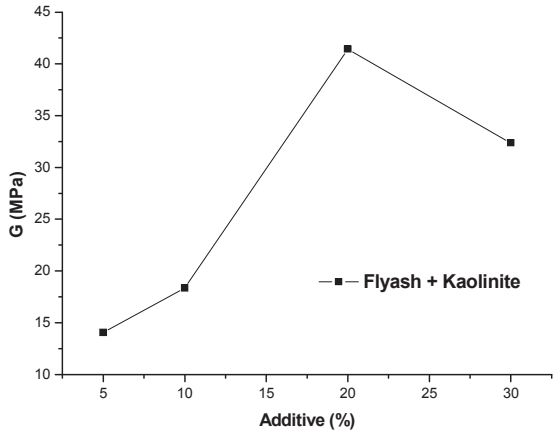


*Figure 1.20 Variation of shear modulus with percentage of additive for flyash and kaolinite consolidated at 200 kPa (Pamukcu & Tuncan, 1991)*

### 1.2.5. Numerical models

The similarities between the pre-failure behaviour of cemented and reconstituted soils indicate that constitutive models developed for reconstituted soils could be applied to naturally or artificially cemented soils only with a little modification. Constitutive modelling for such soils must take into account the nonlinearity of the soil behaviour as well as the evolution (degradation) of the additional soil stiffness and strength components related to the bonds between particles.

Generally, cemented soil can be modelled by the effective stress principle irrespective of whether the soil is weakly or strongly cemented (Cuccovillo & Coop, 1997; Gens & Nova, 1993; Toll & Malandraki, 1993). According to Gens & Nova (1993) a measure of the effect of the bonds is the difference in size of the yield surface of soil with bonding and the intrinsic yield surface of the corresponding soil with no bonding. As an hypothesis in most of the constitutive models the shape of the yield surface in cemented soils is assumed to be identical to that corresponding to reconstituted soil. The behaviour inside this yield limit is elastic and it is assumed that soil elastic properties are not affected by the structure (Koliji et al., 2008). Hardening is related to the evolution of the unbonded yield surface and softening is connected with the shrinking of the yield locus due to bond degradation (Gens & Nova, 1993).

Various constitutive models incorporating bonding and destructuration differ mainly in the precise form of detructuration law and in the form of the reference model used for the reconstituted soil. Several of the models do not include anisotropy supposing that the effects

of anisotropy and destructuration are combined and the large strain anisotropy disappears once destructuration is complete. A part of the existing models is concerned in accurate modelling of small strain behaviour.

According to Muir Wood (2004) the bonded material might be described by an extended Cam clay type of model in which the yield surface has an increased size as a result of the bonding (Figure 1.21). With plastic straining or chemical weathering the yield surface gradually shrinks to the Cam clay-like surface, appropriate to the remoulded, structureless material. Callisto et al. (2002) selected a simple form of the damage law in the model, assuming that the irrecoverable distortional and volumetric deformations eliminate cemented microstructure in the same way. Modified Cam Clay model was used by Lollino et al. (2005).

Vatsala et al. (2001) presented a model, which considers the strength of the soil to be a superposition of two components of the frictional strength of soil particles and the cementation bond strength, acting in parallel for the same strain response. The two components are described separately and then put together to get the overall response. An elastoplastic, strain softening model is proposed for the bond component.

Baudet & Stallebrass (2004) presented the Sensitivity Three-Surface Kinematic Hardening soil model, which uses a fixed relationship between change in sensitivity and plastic strain to represent destructuration. Stable elements of microstructure arising from fabric are simulated by allowing the sensitivity to decrease to an ultimate value greater than unity. The model does not include anisotropy.

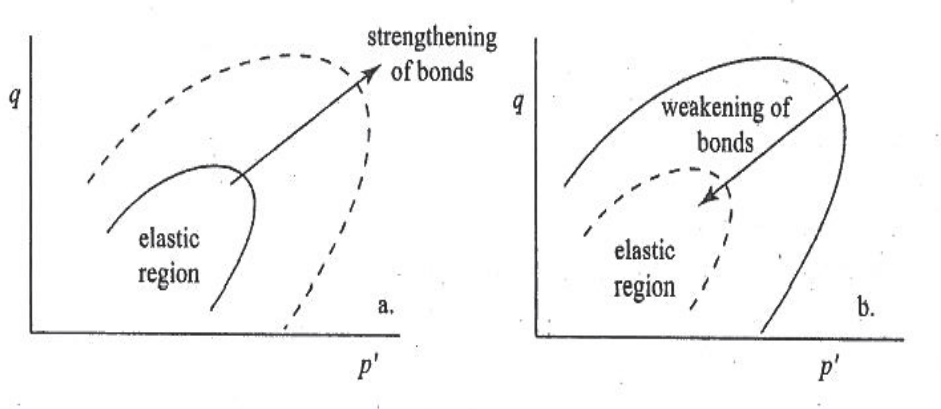


*Figure 1.21 Effect of cementation or bonding as feature added to elastic-hardening plastic model (Muir Wood, 2004)*

Some of the existing models combine large strain anisotropy and destructuration with the anisotropy not attributable solely to bonding. Constitutive modelling of anisotropy and destructuration is represented by the rotational hardening elasto-plastic model with

destructuration (Wheeler et al., 2003). The anisotropy of plastic behaviour is represented through an inclined yield surface and a rotational component of hardening. The yield surface for the natural soil with bonding is assumed to be of the same shape and orientation as the yield surface of the unbonded soil (Figure 1.22).

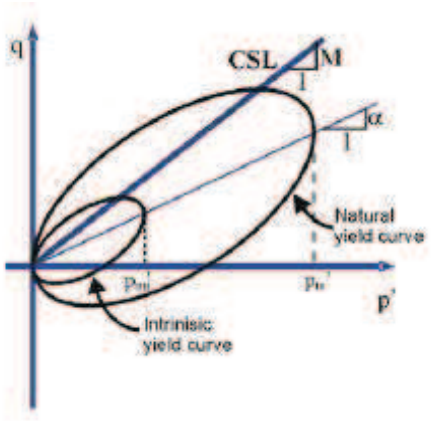


*Figure 1.22 Effect of cementation and anisotropy on yield surface in triaxial stress space (Wheeler et al., 2003)*

A nonviscous multi-laminate constitutive model incorporating structural anisotropy to simulate destructuration effects as well as the evolution of the compressional and strength anisotropy of soft natural soils is presented by Cudny (2003). The formulation of the model for soft soils applies the directional distribution of the overconsolidation or bonding over the sampling planes in the multi-laminate framework and connects the distribution with the microstructure of the soil.

Rocchi et al. (2003) proposed a viscoplastic constitutive model, which tracks changes in the yield locus from the initial position (soil with metastable structure) to the intrinsic position (destructured soil) with the flow and hardening rules.

A hypoplastic constitutive model for clays with meta-stable structure was presented by Mašín (2007). The effects of cemented microstructure were incorporated based on the modification of the barotropy and pyknotropy factors into hypoplasticity.

# Chapter 2

# Aims of the thesis

The general aim of this thesis is to study the mechanical behaviour of cemented fine-grained soil. The study is based on the comparison of the mechanical behaviour obtained for artificially cemented kaolin clay with the behaviour of the pure kaolin clay.

The thesis has three major objectives:

1) To create cement bonds in reconstituted kaolin specimens with the addition of Portland cement, to evaluate the effects of various cement contents and various periods of curing on the compressibility and to select the model material for further testing.

2) To obtain results for the compression and shearing behaviour of the cemented kaolin clay with the selected amount of Portland cement, to characterize the behaviour in the range from very small to large strains and to compare the results with the results for pure kaolin clay.

3) To evaluate the obtained results for shear modulus at very small strains by examining the results of previous research and to determine the shear modulus at very small strains with respect to the dependence of shear stiffness on structure.

# Chapter 3

# Characterization of specimens

## 3.1. Introduction

According to the literature review in the previous chapter, the effects of cementation can be studied either on the intact samples of high quality or on the artificial specimens. The disadvantage of intact samples is the disturbance, which is likely to occur during sampling, in situ testing and reconsolidation in laboratory testing. The evidence of intact samples disturbance is given by Hight et al. (1992a), Hight et al. (1992b) and Clayton et al. (1992). To avoid the problem of disturbance, the structured soil was prepared by artificial cementation as a mixture of soil, Portland cement and distilled water. A fine-grained soil was chosen for the testing.

The preparation and microstructure analyses of pure and artificially cemented specimens are summarised in this chapter. Experimental methods used in the study combined X-ray diffraction identification and electron microscope study (SEM).

## 3.2. Materials

Soil specimens were prepared by mixing commercially available kaolin clay (LB Minerals, s.r.o., Kaznějov) with distilled water and Portland cement CEM I 42.5 R. Typical index and other properties of the used materials, kaolin clay and Portland cement, are given in Table 3.1. The advantage of the kaolin clay is the minimal variability between specimens in the nature of the particles. Portland cement has been selected as a suitable binder due to its efficiency in mechanical improvement and availability. Moreover, kaolin clays contain predominantly kaolinite, which has a highly pozzolanic behaviour at presence of Portland cement, leading to a rapid increase in cementitious product content (Chew et al., 2004).

*Table 3.1 Characteristic values of kaolin clay (provided by Lasselsberger, CZ) and Portland cement (provided by Českomoravský cement, CZ)*

| kaolin clay | | Portland cement | |
|---|---|---|---|
| Water content (%) | max. 1 | Initial setting time (min) | >= 60 |
| pH | 6.63 | pH | 12 |
| Specific gravity | 2.65 | Specific gravity | 3.13 |
| Grain size distribution: | | Grain size distribution: | |
| 0.2 mm (%) | 0.005 | > 90 μm (%) | 5 - 15 |
| < 2 μm (%) | min. 20 | | |
| Atterberg limits: | | Composition: | |
| Liquid limit (%) | 60 - 70 | Clinker (%) | 95 - 100 |
| Plastic limit (%) | 30 - 40 | Minor constituents (%) | 0 - 5 |

### 3.2.1. Kaolin clay

Generally, kaolin clays are residual, highly weathered tropical soils. They result from weathering of minerals contained principally in acid rocks poor on iron, at stable humid and warm condition with a low mobility of $SiO_2$ at low pH. The selected kaolin clay was formed from arkoses and arkosic sandstones at the Pilsen basin area (Czech Republic) during Carboniferous tropical climate.

The studied kaolin is a white soft powder with very fine grains, used as a filler (kaolin KKA KA). The chemical composition of the kaolin specimens was obtained by X-ray fluorescence (Lasselsberger laboratory, CZ). The results are shown in Table 3.2. The clay consists overwhelmingly of $SiO_2$ and $Al_2O_3$ (87.8%), which are the main components of the mineral kaolinite. The mineral composition, obtained from rational analysis Hoffman-Haacke (by Lasselsberger laboratory, CZ) is shown in Table 3.3. The dominant mineral is kaolinite (69%), the other contained minerals are quartz and mica.

*Table 3.2 Chemical composition of studied kaolin clay (provided by Lasselsberger, CZ)*

| $SiO_2$ | $Al_2O_3$ | $TiO_2$ | $Fe_2O_3$ | CaO | MgO | $Na_2O$ | $K_2O$ | $P_2O_5$ | Volatile |
|---|---|---|---|---|---|---|---|---|---|
| 59.97% | 27.78% | 1.06% | 0.49% | 0.04% | 0.19% | 0.10% | 1.40% | 0.07% | 8.90% |

*Table 3.3 Mineralogy of the studied kaolin clay (provided by Lasselsberger, CZ)*

| Compound name | Content |
|---|---|
| Quartz ($SiO_2$) | 15.5% |
| Kaolinite ($Al_2Si_2O_5(OH)_4$) | 69% |
| Mica ($K(Mg,Fe,Al)_3(AlSi_3O_{10})(OH)_2$) | 14.1% |
| Rest | 1.4% |

Kaolinite is a 1:1 dioctahedral aluminosilicate with two basal cleavage faces: an alumina octahedral sheet and a silica tetrahedral sheet (Figure 3.1). Figure 3.1 further shows the features of the surface charges of kaolinite summarised by Wang & Siu (2006a). According to the authors, the highly pH dependent edge charges are important to the interparticle forces and associated fabric formations. It is also important for the formation of cement as the broken edges are regarded as major reactive sites.

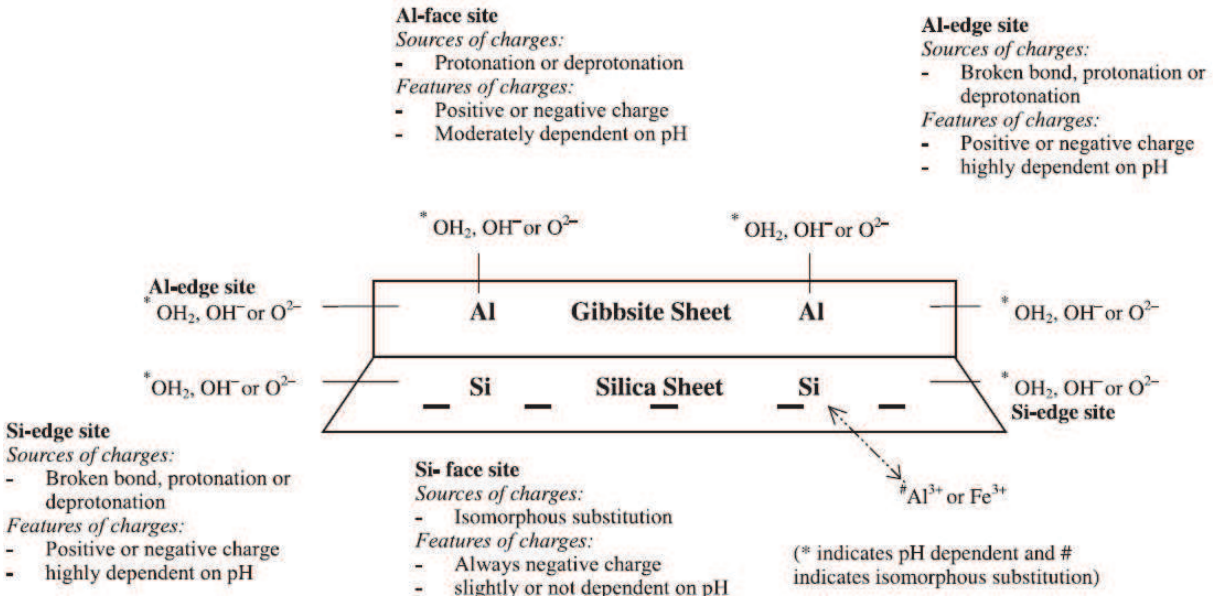


*Figure 3.1 Mineral composition and surface charge characteristics of kaolinite (Wang & Siu, 2006)*

Kaolin clays are nonexpendable soils with hydrophilic behaviour and thus readily water dispersible. Kaolin physical and physiochemical properties are dependent on particle-size distribution, structural order and shape, mineral composition, kaolin delamination and structure (interparticle forces and associated fabric). A comparison of typical values of parameters for different kaolin clays is shown in Table 3.4. Wang & Siu (2006a, 2006b) reported the effect of structure on the volumetric change under isotropic compression, small-

strain shear modulus and liquid limit of kaolinite soils. Consequently, the mechanical properties of kaolin clays are sensitive to the addition of cementing agent.

*Table 3.4 Values of parameters for some kaolin clays*

| | *LL* | *PL* | $\lambda$ | $\Gamma$ | *N* | *M* | $\phi'$ | $\kappa$ |
|---|---|---|---|---|---|---|---|---|
| kaolin clay (Schofield & Wroth, 1968) | | | 0.26 | ≈ 3.265 | | ≈ 1.02 | | 0.05 |
| kaolin clay (Atkinson, 1993) | 65 | 35 | 0.19 | 3.14 | 3.26 | 1.00 | 25° | 0.05 |
| powdered kaolin (Sivakumar et al., 2002) | 72 | 36 | 0.19 | | | ≈ 0.9 | | |
| Speswhite kaolin (Wang & Siu, 2006b) | 58 | 30 | | | | 1.09 | 27.5° | |
| kaolin clay (Prashant & Penumadu, 2005) | 65 | 30 | | | | | | |

### 3.2.2. Portland cement

Portland cement CEM I 42.5 R (Českomoravský cement, a.s., Radotín, CZ) was used in this study. It is a fine grey powder produced by grinding Portland cement clinker, a limited amount of calcium sulphate and up to 5% minor constituents. The main chemical constituents of clinker are CaO, $SiO_2$, $Al_2O_3$ and $Fe_3O_3$. This type of cement has a fast increase of initial strength, with fast and high excess of heat. It is characterized with high strength and mechanical, physical and chemical stability.

## 3.3. Specimens

Reconstituted specimens were prepared from the kaolin powder. According to Burland (1990), a reconstituted clay is one that has been thoroughly mixed at between 1 and 1.5 times the liquid limit and preferably consolidated one-dimensionally. One-dimensional consolidation is generally believed to generate a degree of anisotropy. In the early stages of consolidation, when the clay is more or less in a liquid condition, the particles are able to adjust themselves to the applied loading and drainage conditions (Sivakumar et al., 2002). The standard practice to erase the structure created during one-dimensional loading is to consolidate the specimens isotropically in the triaxial cell.

Sivakumar et al. (2002) reported that the kaolin specimens consolidated isotropically from slurry appear to have evidence of anisotropic microstructure. As a result, such specimens have higher voids ratio in isotropic compression and they are more compressible. However, the results from shear tests suggest isotropy. The differences in the microstructure may not

have a significant influence on the pre-yield (elastic) characteristics of the clay and may have little influence on the shape (and probably position in e/log p´ plots) of the critical state line.

### 3.3.1. Specimens preparation and curing

The kaolin clay was thoroughly mixed at water content equal to the liquid limit $w_L$ (70%). After homogenization for 24 hours, Portland cement was added to the slurry in different quantities. The specimens were prepared without any compaction effort and the water content was the same for all specimens. The time for preparation was always less than 1 hour, which is the initial setting time of the Portland cement. The pozzolanic reaction with kaolinite proceeds at about one hour after cement addition (Osula, 1996).

The oedometer specimens were prepared by placing the treated clay directly into the oedometer rings. After thorough mixing for 10 min, the uniform paste (in appearance) was transferred into the oedometer rings without any compaction. The cement content of 0% (uncemented), 0.5, 1, 2, 4 and 8% of the dry mass were used for introductory one-dimensional compression tests. All samples were submerged in water during the curing periods and they were cured under zero confining stress. The tests of cemented specimens were carried out after 3, 7 and 14 days of curing.

The triaxial specimens contained the admixture of Portland cement of 0% (uncemented) and 4% of the dry mass. The kaolin slurry was consolidated under one-dimensional conditions in a rigid cylinder at a low vertical stress (5 kPa), with permanent watering. The applied loading was low in order to reduce the horizontal arrangement and groupings of the particles in the slurry. After reaching a sufficient strength, the specimens were put into the triaxial cell. The specimens were homogenous in appearance with rare air bubbles and no visible cracks (Figure 3.2). The consolidation of reconstituted kaolin took about 10 days. Cemented specimens were transferred after 3 days of curing. The prepared triaxial specimens were assumed to be isotropic after consolidation in triaxial cell, although the water flow from the specimens was one-dimensional.


*Figure 3.2 Cross section of triaxial specimen after initial consolidation in a rigid cylinder. (a) kaolin clay. (b) cemented kaolin clay.*

### 3.3.2. Scanning Electron Microscope analyses of specimens

The scanning electron microscope CamScan S4 was used to examine the textural and morphological features of pure and cemented specimens. The specimens were prepared by drying at room temperature and carbon coating.

Figure 3.3(a), (b) and (c) shows the SEM photographs taken on kaolin powder, kaolin powder mixed with distilled water and kaolin powder mixed with distilled water and 4% of Portland cement, respectively. The magnifications of the images are 400 × and 1630 ×. The images indicate no significant difference between dry kaolin powder and kaolin powder with distilled water. Both clay samples exhibit a fairly open type of microstructure with randomly oriented particles. A kind of dispersion and horizontal arrangement is more evident in the specimen mixed with distilled water.

The particles of both samples (Figure 3.3(a) and (b)) show irregularities of shapes, sizes and orientation. The shape of kaolinite particles is generally planar with the plate surfaces horizontal. Individual flakes of kaolinite have pseudohexagonal or irregular margins. The typical pseudohexagonal shape appears in the photograph of dry kaolin powder (Figure 3.3(a)) at the magnification of 1630 ×. The edges of detrital grains are visually sharper in the sample of dry kaolin powder.

Significantly different is the image of the cemented sample in Figure 3.3(c). The structure has more flocculated nature with small clay-cement clusters. Such small flakes play a role as a cementing agent in the clay and form the contact cement. Only a slight change of intergranular void space and particle size distribution may be expected in agreement with the results obtained by Chew et al. (2004).

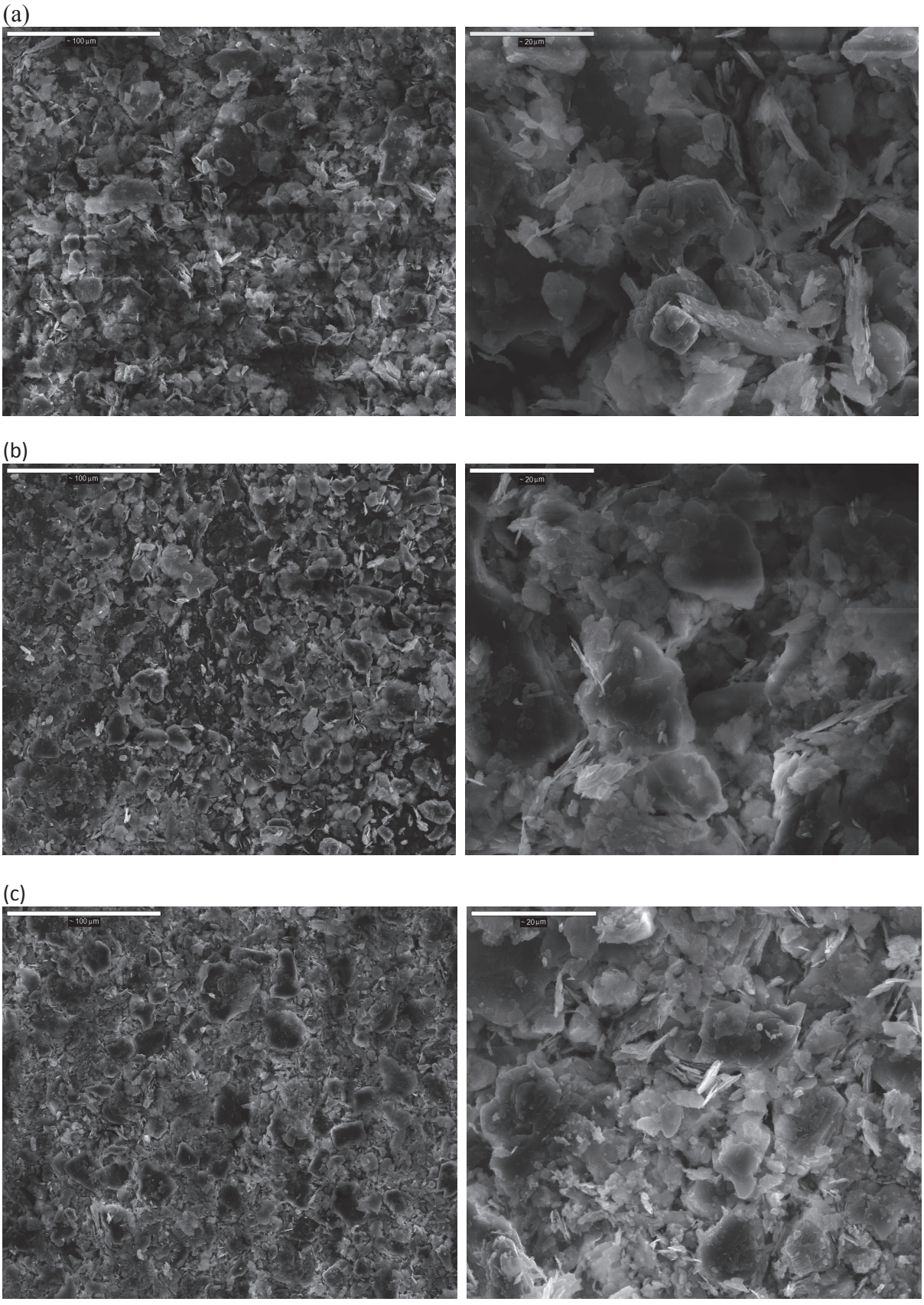


*Figure 3.3 SEM images at a magnification of 400 × and 1630 ×. (a) dry kaolin powder. (b) kaolin powder mixed with distilled water, dried at room temperature. (c) cemented kaolin mixed with distilled water and 4% of Portland cement, dried at room temperature.*

### 3.3.3. XRD analyses of specimens

X-ray powder diffraction analyses of cement-treated and pure kaolin clay were performed on a PANalytical X´Pert Pro diffractometer with CuKα radiation (40 kV and 30 mA), step scanning at 0.05°/150 s in the range 3°- 60° 2$\theta$. Air-dried, powdered, oriented samples of treated and untreated soil were analysed. Sample preparation for the analysis followed the methods of Moore & Reynolds (1997). The mineralogical composition was estimated with X-Pert Highscore software 1.0d, equipped with the JCPDS PDF-2 database (ICDD 2002).

Figures 3.4 and 3.5 show the XRD pattern obtained for pure and cemented clay, respectively. The results from the pure kaolin clay sample indicate the dominant presence of kaolinite with muscovite and quartz. The XRD pattern of cemented clay reveals several new peaks in comparison with the pure clay. The new peaks confirm the presence of calcium, which is presumably present in amorphous form as the cementing products of hydration and pozzolanic reactions such as calcium silicate hydrate (CSH) and calcium aluminium silicate hydrate (CASH). The change in composition of the treated sample is also apparent from the decreasing kaolinite peaks. This suggests that kaolinite is exhausted by the pozzolanic reaction.

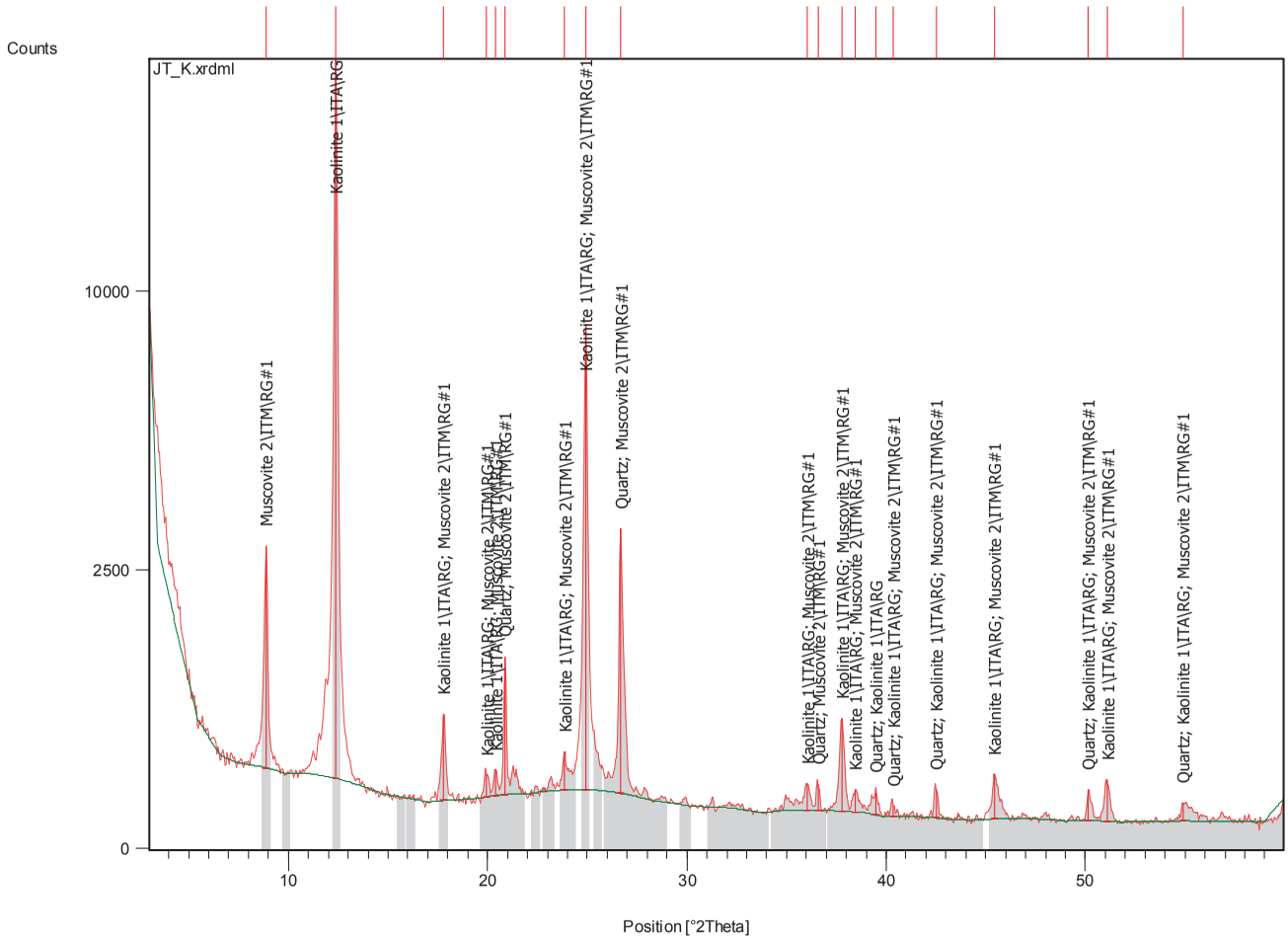


*Figure 3.4 XRD pattern of pure kaolin clay*

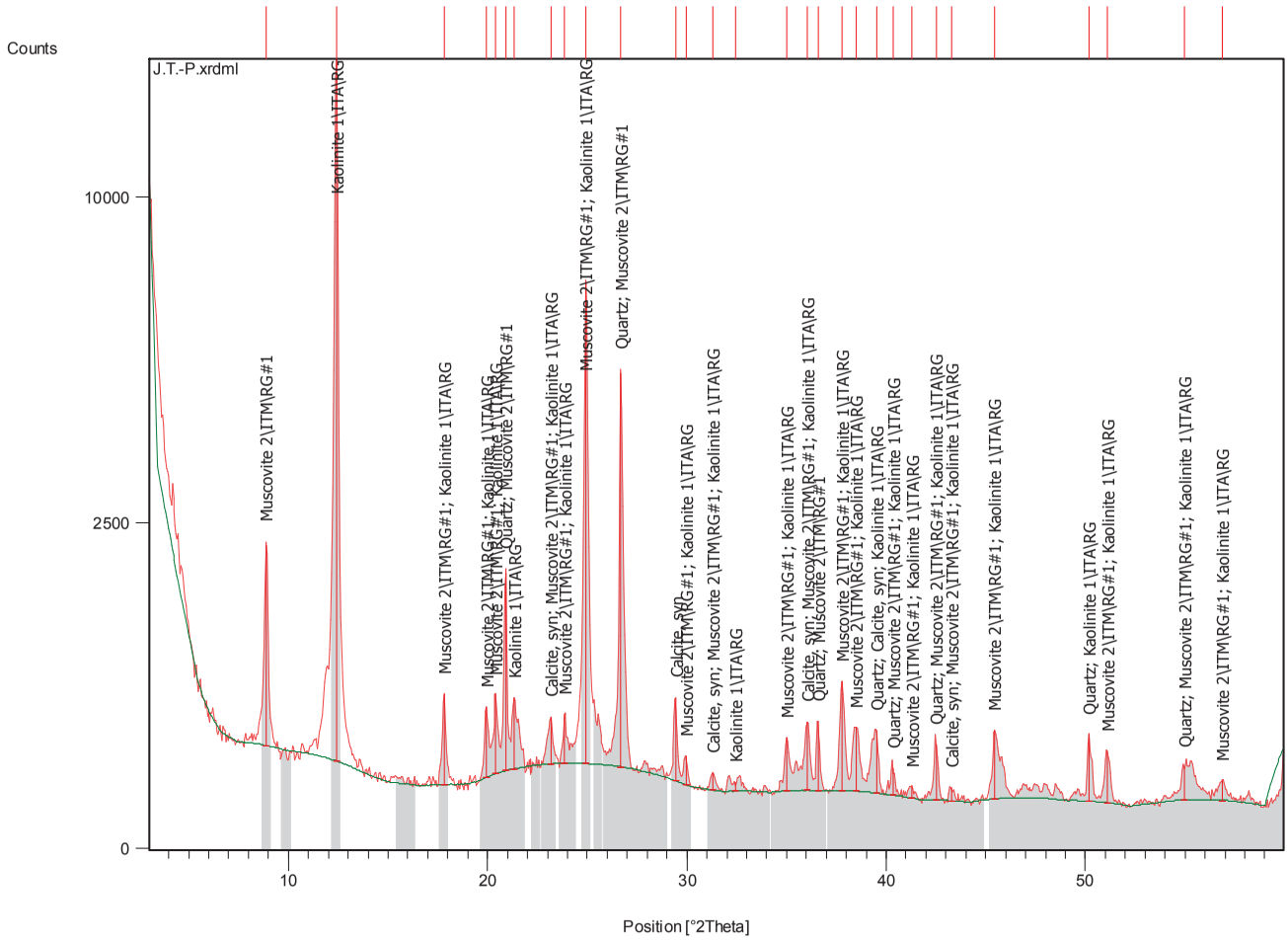


*Figure 3.5 XRD pattern of kaolin clay with 4% of Portland cement*

*Table 3.5 Results of the semi-quantitative analysis – mineral composition of pure and cemented kaolin clay*

| Compound name | kaolin clay | | kaolin clay treated with Portland cement |
|---|---|---|---|
| Quartz ($SiO_2$) | 15.5% | 8% | 15% |
| Kaolinite ($Al_2Si_2O_5(OH)_4$) | 69% | 77% | 64% |
| Calcite | - | - | 2% |
| Mica ($K(Mg,Fe,Al)_3(AlSi_3O_{10})(OH)_2$) | 14.1% | 15% | 18% |
| rest | 1.4% | - | 1% |

Table 3.5 shows the semi-quantitative analysis obtained from XRD patterns using corundum ($Al_2O_3$) as an internal standard. The mineral composition of pure kaolin clay agrees with the results of rational mineral analysis obtained by Lasselsberger laboratory.

# Chapter 4

# Compression

## 4.1. Introduction

A part of the laboratory study was concerned with compression and swelling behaviour of the pure and the cemented specimens. The artificially cemented soil permits the simulation of naturally cemented soil and hence the data obtained from compression of artificial specimens may lead to the understanding of the behaviour of natural soils. The general compressibility behaviour of specimens with the different content of Portland cement was studied by conventional one-dimensional tests. The one-dimensional loading and unloading is characterised with compression and swelling indexes. Properties of reconstituted uncemented clay are denoted by an asterisk.

The differences in the behaviour of uncemented and cemented clay were further studied during isotropic compression of the model materials with the selected content of the admixture. The results of compression tests including one-dimensional and isotropic tests gave the data for cemented and uncemented clay, defining the relationships between void ratio, confining stress, vertical yield stress and cementation.

## 4.2. One-dimensional compression

The aims of the oedometer tests were:

1) To confirm the development of structure in the kaolin specimens with the addition of Portland cement.
2) To evaluate the effects of various cement contents and various periods of curing on the compressibility.
3) To select the model material for further testing.

### 4.2.1. Experimental procedure and specimens

The introductory one-dimensional compression tests were carried out on specimens reconstituted at its liquid limit with the cement content of 0% (uncemented), 0.5, 1, 2, 4 and

8% (see Section 3.3.1). The tests were carried out on 70 mm dia. by 19 mm high specimens by applying standard increments of stress (twice the previous load) to a maximum stress of 800 kPa.

A further series of incremental load oedometer tests were carried out to a maximum stress of about 16 MPa to investigate the compression lines and the effect of cementation at a greater stress interval. To reach the highest stresses, the oedometer specimens had diameters of either 76 mm or 50 mm. The increments of stress differed with stress level. At stresses of up to 3600 kPa, the increments were approximately twice the previous load. At higher stresses, the increments were smaller due to the limitations of oedometer apparatus. The initial water contents of treated specimens varied between 70 – 80%.

To obtain a reliable compression line of the uncemented clay, 6 tests were carried out on different specimens of the pure kaolin clay. Parameters of the specimens, water content $w_0$, voids ratio $e_0$, height $H_0$, thickness $D_0$ and weight $W_0$, are summarised in Table 4.1. The specimens 1, 2 and 3 were compressed by applying increments of stress after placing into the oedometer rings. The specimens 4 and 5 were compressed at stresses of up to 100 kPa, unloaded, taken out to measure the height and weight and reloaded.

The last specimen 6 was cut from the specimen prepared at higher oedometer ring and compressed at stresses of up to 100 kPa to obtain results of compression to higher stresses by reducing the effect of specimen height. After compression and unloading, the specimen (120 mm in diameter and 21 mm in height) was cut with the smaller ring. The obtained specimen (50 mm in diameter and 21 mm in height) was placed into the oedometer ring and again reloaded to 100 kPa.

*Table 4.1 Properties of kaolin clay specimens*

| | $w_0$ | $e_0$ | $H_0$ | $D_0$ | $W_0$ |
|---|---|---|---|---|---|
| 1 | 73% | 1.92 | 0.0200 m | 0.050 m | 0.062 kg |
| 2 | 75% | 1.72 | 0.0182 m | 0.070 m | 0.143 kg |
| 3 | 75% | 1.64 | 0.0199 m | 0.076 m | 0.160 kg |
| 4 | 48% | 1.10 | 0.0168 m | 0.076 m | 0.143 kg |
| 5 | 46% | 1.20 | 0.0146 m | 0.050 m | 0.051 kg |
| 6 | 41% | 1.10 | 0.0210 m | 0.050 m | 0.073 kg |

### 4.2.2. Results

The state of a soil specimen is described by the combination of vertical stress $\sigma'_v$ and void ratio $e$, which was determined from the volume and dry mass of the specimen. The values of initial and final void ratio agreed with the values determined from water contents ($w$) and specific gravity of soil grains ($G_s$). The weighted average of $G_s$ was used for the cemented specimens. The obtained values of $G_s$ vary between 2.65 (0% of cement content) and 2.69 (8% of cement content).

The yield was determined following the procedure suggested by Casagrande (1936) for determining the preconsolidation stress. Figure 4.1 shows the method described in Holtz & Kovacs (1981).

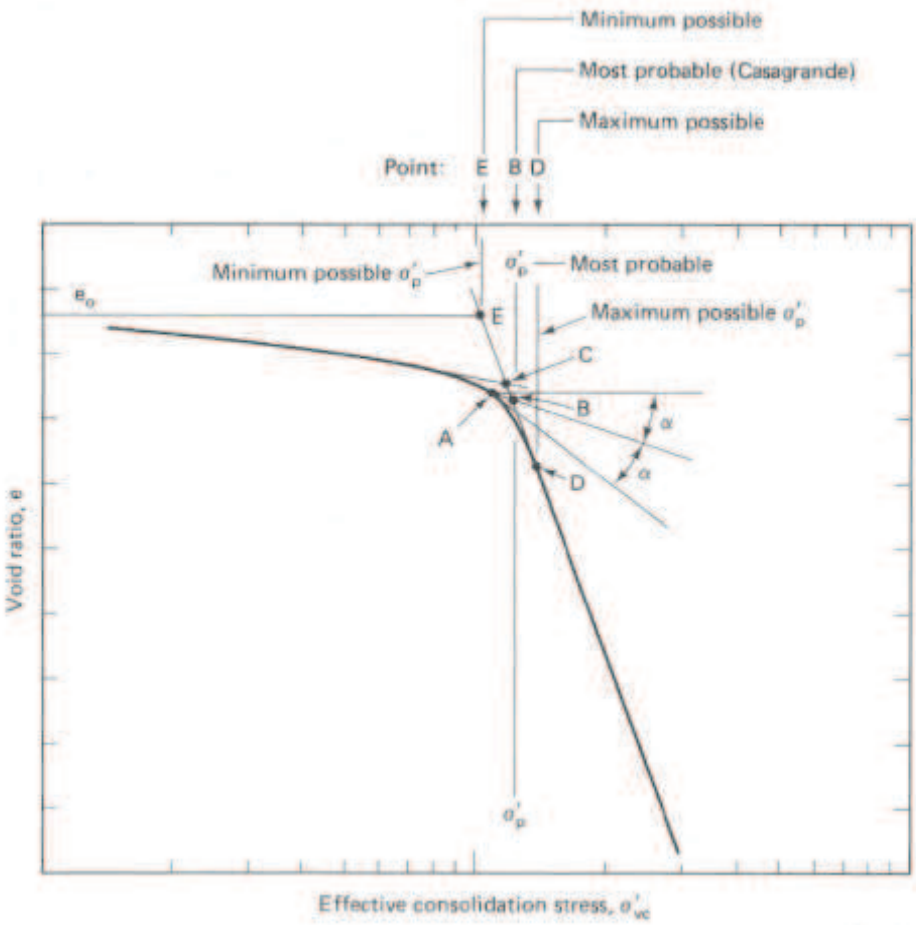


*Figure 4.1 Casagrande's method for determining preconsolidation stress (Holtz & Kovacs, 1981)*

#### 4.2.2.1. One-dimensional compression and swelling of kaolin clay with the different addition of Portland cement

The one-dimensional compression behaviour of uncemented kaolin clay specimens is shown in Figure 4.2. Two groups of compression lines were obtained. The almost identical

compression lines of specimens 1, 2 and 3 are placed in *e* - log $\sigma_v'$ space above the almost identical compression lines of specimens 4, 5 and 6. The difference results from the different preparation. The specimens 4, 5 and 6 were overconsolidated. Thus the structure of reloaded specimens 4, 5 and 6 was different from the structure of specimens 1, 2 and 3 and consequently *e* differed at a given vertical stress. The effect of overconsolidation diminishes at higher stresses, e.g. the compression lines of the specimens 2 and 6 are identical at stresses higher than 1600 kPa. The swelling lines of all untreated specimens are parallel. The results show a good reproducibility of the compression tests.

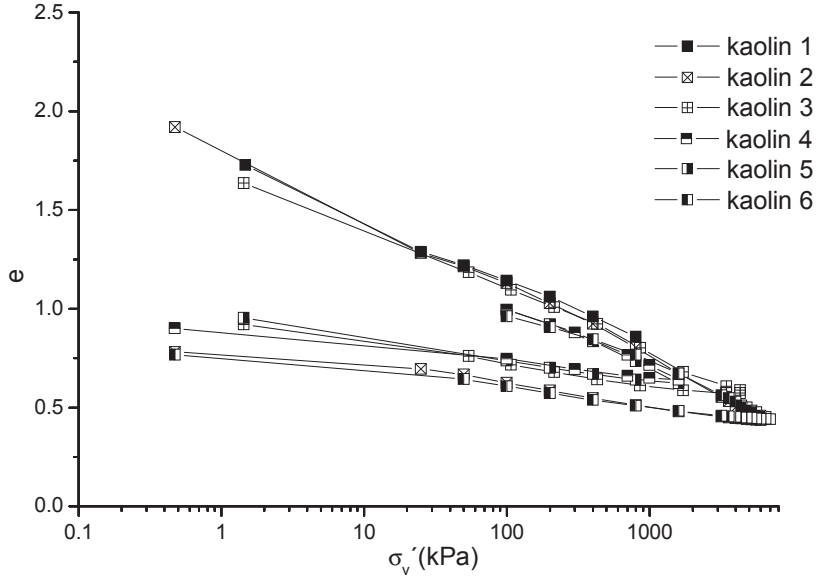


*Figure 4.2 One-dimensional compression and swelling of pure kaolin clay*

The obtained compression behaviour of untreated kaolin clay was compared with the compression behaviour of cemented specimens with the different cement contents. Figure 4.3(a) shows the behaviour of clay specimens with varying amount of Portland cement during one-dimensional compression after 3 days of curing. The initial void ratios are almost the same for most of cemented specimens, independently of the cement content. Moreover, the first points of the curves lie close to the compression curve obtained for the uncemented specimen. It means that the void space of cemented specimens has changed only slightly after addition of Portland cement. The only exception is the specimen with the highest amount of Portland cement (8%).

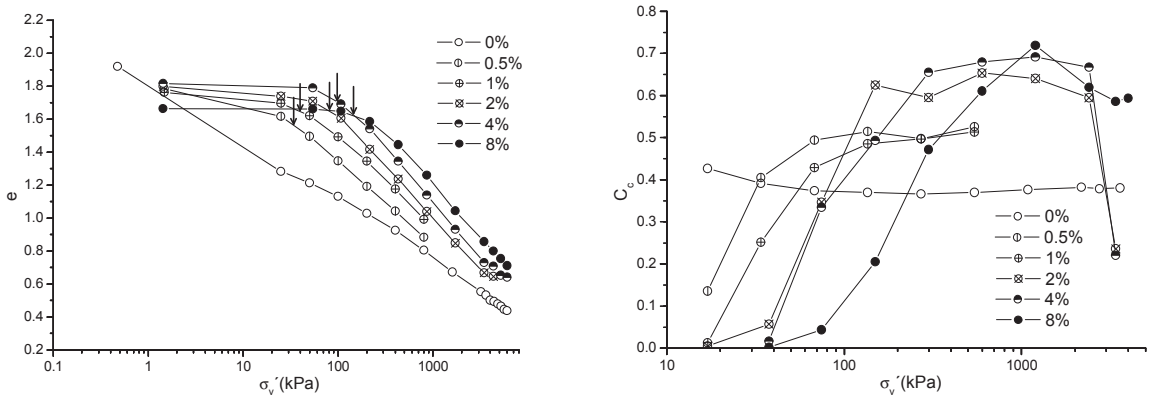


(a) (b)

*Figure 4.3 One-dimensional compression of kaolin clay with 0%, 0.5%, 1%, 2%, 4% and 8% of Portland cement after 3 days of curing: (a) compression curves with arrows indicating the yield points; (b) compression index development*

The states of all cemented specimens in $e$ - log $\sigma_v'$ space (Figure 4.3(a)) are on the right side of the compression curve of the uncemented specimen. The behaviour is governed by the cementation, until the vertical yield stress. The yield, the point in which the compression curve deviates, was identified for the each cement content and is pointed with the arrow. The value of the vertical yield stress is increasing with the increasing cement content.

Following Leroueil & Vaughan (1990), the extent to which the soil is structured can be defined by the extent to which it can exist in structure permitted space. The admixture of Portland cement less than 2% affected the response to compression up to the vertical stress of about 40 kPa and the yield point is insignificant. The higher admixture (2, 4 and 8%) leads to the increase of the structure permitted space, the behaviour is stiffer and the yield becomes sharp. The specimens may be characterised as weakly to moderately cemented soils depending on the classification criteria considered (see also Sec. 1.1.3.3).

After yield, beyond the apparent overconsolidation pressure, $e$ significantly reduces due to the breaking of cementation bonds with the increase in vertical stress for all ranges of cement content. The number of bonds, which were formed after the addition of Portland cement, affects the rate of the reduction. The loading weakens cementation and the states of the cemented specimens are tending to the state of the uncemented specimen in dependence on the content of Portland cement.

The final states of the cemented specimens are above the normal compression line of the untreated kaolin clay and differ according to the amount of Portland cement. After

complete debonding the compression lines of originally cemented specimens are assumed to converge to the compression line of pure kaolin clay. However, the maximum applied stresses were not high enough to confirm the phenomenon.

The observed changes in the compression behaviour of the specimens can be described with the changes of gradient of the normal compression line $C_c$ (Figure 4.3(b)). The vertical stresses on the horizontal axis in Figure 4.3(b) were calculated for the half values of void ratios for individual loading increments to represent tangent $C_c$ of cemented specimens at each load interval. This method expresses more accurately the progress of compression line in logarithmic scale.

The pure kaolin clay shows almost no change of $C_c^*$ in the whole stress range. Conversely, the values of $C_c$ of the cemented specimens are changing significantly. The values of $C_c$ for all treated specimens are lower than the value for untreated specimen at vertical stresses of up to 30 kPa. In this stress range, the behaviour of all cemented specimens is governed by cementation. The debonding with increasing stress increases the values of $C_c$, starting with the specimens with lower cement content (0.5%). This trend continues until reaching the load of about 220 kPa, when the $C_c$ of the last specimen (with 8% of Portland cement) runs over the value of $C_c^*$ for untreated specimen.

The last calculated values of $C_c$ for specimens with 2 and 4% of Portland cement decrease to low and almost equal value. It results from the inaccurate measurements due to the excessive inclination of the lever arm. The effect of incorrect determination of vertical stress and void ratio can be also seen on compression lines for specimens with 2 and 4% of Portland cement in Figure 4.3(a). The decreasing trend of $C_c$ is significant at stresses higher than 3000 kPa.

Figure 4.4 shows the effect of cementation on the swelling behaviour of specimens. The lowest values of $e$ on swelling curves in Figure 4.4(a) correspond to the maximum vertical stress applied on the specimens during compression. The state of the specimen with 0.5% of Portland cement lies below the state of the specimen with 1% at vertical stress of 800 kPa. Similarly, the value of $e$ obtained for the specimen with 4% is lower than the value obtained for the specimen with 8% at vertical stress of 6000 kPa. The bonding of the specimens with higher addition of Portland cement is stronger after one-dimensional loading than the bonding of the specimens with the lower addition.

The resistance of cemented specimens, which is significant during pre-yield compression, is also noticeable during swelling. Generally, the more expansive specimen contains less bonds, the most expansive is the untreated specimen. The swelling index $C_s$ of

specimens with 0, 0.5, 1, 2, 4 and 8% of Portland cement was calculated for each unloading interval. The vertical stresses in Figure 4.4(b) were computed for individual unloading increments, in a similar way as in Figure 4.3(b).

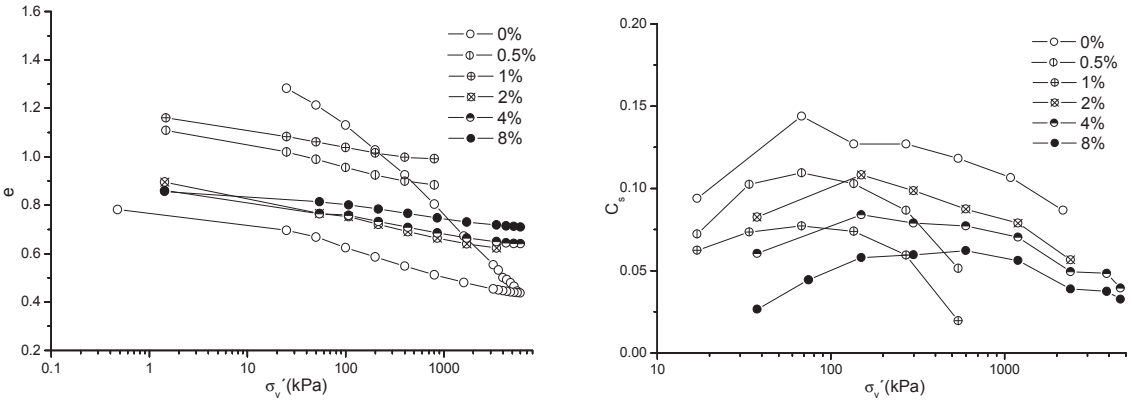


(a) (b)

*Figure 4.4 Behaviour of kaolin clay with 0%, 0.5%, 1%, 2%, 4% and 8% of Portland cement during one-dimensional swelling after 3 days of curing and compression: (a) swelling curves; (b) swelling index development*

Figure 4.4(b) shows that the swelling index determined for cemented specimen with 2, 4 and 8% of Portland cement is increasing during unloading until the vertical stress reaches the value of about 135 kPa and the values obtained for uncemented clay are higher than values obtained for the cemented specimens. The lowest values and the smallest changes in $C_s$ are observed for the specimen with the highest addition of Portland cement, indicating the effect of cementation. The value of swelling index is decreasing at lower stresses than 135 kPa probably due to the inaccurate determination of void ratio at low vertical stress.

The same trend can be seen for swelling curves obtained for the specimens with 0.5 and 1% of Portland cement, which were compressed at lower maximum vertical stress during compression stage and the curves are shifted to the left.

#### 4.2.2.2. One-dimensional compression and swelling of the model artificially cemented clay

On the basis of the obtained results, the cement content of 4% of the dry mass was chosen to model cemented clay. This content allows preparation of specimens with a low variability in the degree of cementation without a significant change of the initial void ratio, and the compression behaviour may be studied from the initial resistance to compression to the final high compressibility due to debonding in a measurable stress interval.

The compression and swelling behaviour of the selected model material with varying curing period is shown in Figure 4.5. The data were obtained from both the introductory and the following one-dimensional compression tests. The compression and swelling curves confirm the high reproducibility of the tests for the model cemented material. The plotted arrows indicate the yield stresses of the cemented material. The vertical yield stresses are almost identical for specimens at each curing period.

After the yielding, the compression curves of cemented specimens show two trends. At first, the change of void ratio increases with the vertical stress as the progressive destructuration takes place. At higher stresses, the change of void ratio of specimens cured for 3 and 7 days decreases and approaches to almost zero (<0.01). It is attributed to the inaccuracies due to an excessive inclination of the lever arm. Nevertheless, the compression curve of the cemented clay cured for 14 days and compressed to higher vertical stress is assumed to get progressively closer towards the compression curve of the uncemented clay and ultimately converge. Leroueil & Vaughan (1990) suggested that even complete removal of structure does not necessarily imply coincidence of the void ratio-stress curves from tests on structured and reconstituted samples. Further straining may be required to establish the same fabric and particle packing.

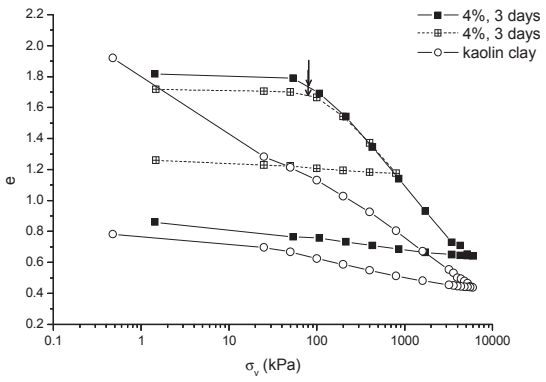


(a)

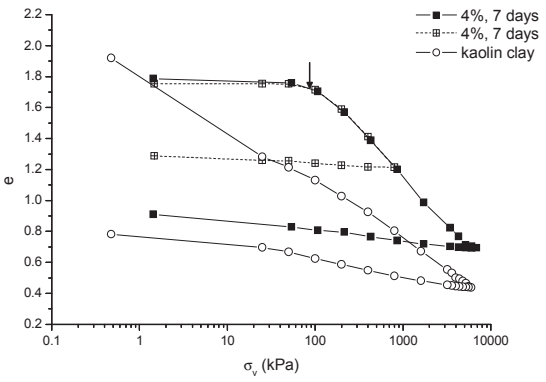


(b)

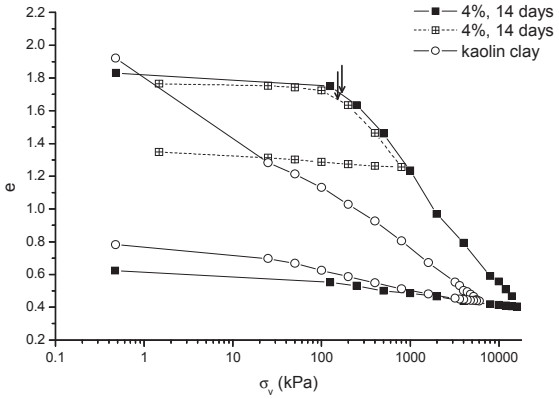


(c)

*Figure 4.5 One-dimensional compression and swelling responses with arrows indicating the yield points for the pure kaolin clay and model material cured for: (a) 3 days; (b) 7 days; (c) 14 days*

The effect of the curing period on the compressibility and swelling behaviour of the selected model material is presented in Figure 4.6. The initial void ratios are almost the same for all specimens, but the results indicate that the vertical yield stress is higher with the longer curing period. The yield point was identified at the threshold of about 82 kPa for 3 days, 90 kPa for 7 days and 170 kPa for 14 days of curing. The increase of the apparent overconsolidation pressure is due to the effect of longer creation of cementation bonds between particles of treated clay.

The post-yield compression line is unique for each curing period. The states of a specimen with a longer curing period are above the states of a specimen with a shorter curing period. The difference between the compression curves is more evident at lower vertical stress range. At stresses higher than 1000 kPa, the convergence of the lines for 7 and 14 days of curing can be seen. It is suggested that the compression curves join a unique compression curve with the increase of vertical stress sufficient to destroy the bonding and the fabric.

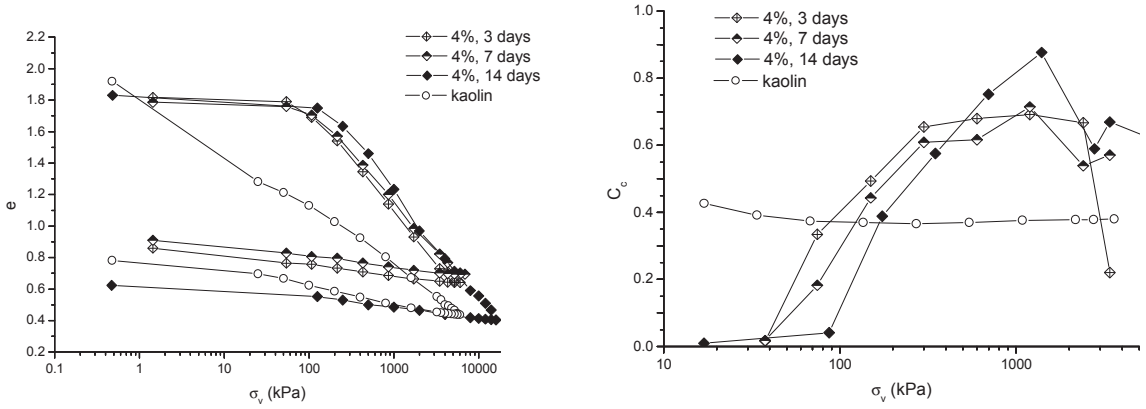


(a) (b)

*Figure 4.6 One-dimensional compression and swelling of the model material cured for 3, 7 and 14 days: (a) compression and swelling curves; (b) compression index development*

The behaviour of the cemented soil cured for varying time was further examined with the development of compression index $C_c$ (Figure 4.6(b)). The values of $C_c$ depend on stress and curing period. At lower stresses, the value of $C_c$ for the specimen after 7 days of curing is lower than that for the specimen after 3 days of curing and higher than that for the specimen after 14 days of curing due to the formation of stronger or weaker cementation, respectively. After yield, the resistance of the cemented soil to compression is decreasing and $C_c$ is increasing with a higher change for the specimen with the longer curing period.

Significant irregularities can be seen on the development of $C_c$ at stresses higher than 3000 kPa. It results from the inaccurate data due to the excessive inclination of the lever arm. The effect can be also seen on the compression lines in Figure 4.6(a).

## 4.3. Isotropic compression

To investigate the effect of cementation on the mechanical behaviour of kaolin clay, the measurements of small strain shear stiffness were carried out on the pure and two model cemented kaolin clay specimens (see Section 5). The two cemented and one pure kaolin clay specimens were compressed isotropically and the isotropic compression properties are presented in this section. The results were used for the numerical modelling of the behaviour of pure and cemented kaolin clay (see Section 7).

### 4.3.1. Experimental setup and specimens

Conventional isotropic drained compression tests were carried out on specimens (38 mm in diameter and 76 mm in height) with 0 and 4% of Portland cement. The properties of all triaxial specimens, including the specimens prepared for shear tests and shear stiffness measurements, are summarised in Table 4.2. In all cases the void ratios were determined from the water contents ($w$) and agreed with the values determined from the volume and dry mass of the specimens. The minimal variability of the values indicates high repeatability of specimens. The specific gravity of soil grains $G_s$ was calculated as the weighted average and the values are 2.65 for uncemented specimens and 2.67 for specimens with 4% of cement content.

*Table 4.2 Properties of triaxial specimens*

| | $w_0$ | $e_0$ | $H_0$ | $D_0$ | $W_0$ |
|---|---|---|---|---|---|
| pure kaolin clay | 53 ± 2% | 1.45 ± 0.05 | ≈ 0.0768 m | ≈ 0.0368 m | ≈ 0.151 kg |
| cemented kaolin clay | 56 ± 2% | 1.55 ± 0.05 | ≈ 0.0767 m | ≈ 0.0374 m | ≈ 0.137 kg |

Specimens, consolidated one dimensionally (see Chapter 4.3.1), were transferred to the triaxial cell. The end of primary consolidation of cemented and uncemented specimens after 3 days and 10 days (respectively) was not checked before removing from the high consolidometer. They were placed inside the membrane, sealed on to the base and to the top cap by O-rings. They were saturated using the back pressure of 100 kPa. The pressure was applied in increments of 3 kPa/hour. The control of saturation is described in Section 5.2.

A continuous isotropic compression was applied to the two cemented specimens (cemented clay 1 and 2) up to the demanded effective stresses of 50, 100, 250, 400, 550, 700, 850, 1000, 1300 and 1500 kPa. The compression at slow rate was preferred to stepwise consolidation to prevent debonding. The compression rate for specimens of cemented clay was 1.25 kPa/hour. The uncemented kaolin specimen was consolidated stepwise. Measurements of water that drained from the specimens were taken during both procedures using the GDS Advanced Pressure/Volume Controller with the stated accuracy of volume ≤ 0.1% measured value. The volume change was considered as stabilized when the volumetric strain rate was lower than $10^{-6}$/min.

### 4.3.2. Results

Figure 4.7 presents the results obtained from the isotropic compression tests carried out on the uncemented and the two cemented specimens. The specimen of pure kaolin clay shows a normally consolidated behaviour during isotropic compression and the behaviour is characterized with the normal compression line (isotropic NCL of the reconstituted kaolin clay).

The isotropic compression behaviour of cemented clays 1 and 2 shows similar trends as the one-dimensional compression behaviour of the cemented kaolin clay. The initial states of the cemented specimens lie close to the obtained isotropic NCL of the uncemented specimen. Thanks to the interparticle bonding, the cemented kaolin clay specimens have more open structure and the compressibility is lower until the yield stress (pointed with arrows in Figure 4.7), at which the cementation structure starts to degrade.

The mean effective stress at yielding and the post-yield compression curve defines the boundary for the possible states of the model cemented soil. The limiting states are represented by the line SBS (state boundary surface), which is parallel with the isotropic NCL of the pure kaolin clay and lies to the right of it.

The yield point of the cemented clay 1 almost coincides with the state boundary line at the threshold value of stress approximately 400 kPa. According to Rotta et al. (2003), the relative contribution of cementation to the yield stress in isotropic compression is higher at higher void ratio. However, the line of the isotropic response of the cemented clay 2 drops towards the line of the cemented clay 1 with lower initial void ratio and lies under the line at stresses higher than 100 kPa. The yield point of the cemented clay 2 lies to the left of the line SBS. The response was probably affected by the method of shear stiffness measurements (see Section 5.3), which were carried out at each effective stress levels of 50, 100, 250, 400, 550, 700, 850, 1000 and 1300 kPa. The deviator stress probes were carried out under constant cell pressure and axial strain rate at standard total stress path $\delta q/\delta p = 3$. The change of the deviator stress was limited to 20 kPa. After probing of the specimen, undrained shear unloading returned the stress path to isotropic compression line. According to the results, the structure seems to be weakened due to the previous strain cycles.

Little convergence of the isotropic compression curves of the cemented and uncemented specimens of kaolin clay can be seen at the isotropic stresses of up to 1500 kPa. Rotta et al. (2003) and Coop & Atkinson (1993) also found slow convergence of isotropic compression curves for uncemented and artificially cemented sands.

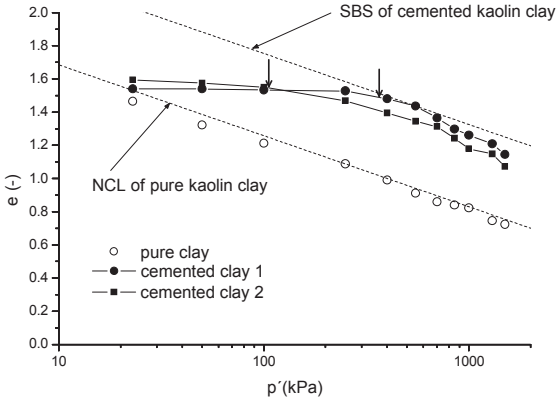


*Figure 4.7 Isotropic compression responses for the uncemented (0% of cement content) and cemented (4% of cement content) kaolin clay with arrows indicating the yield points*

The comparison between isotropic and one-dimensional compression results is shown in Figure 4.8 and 4.9. Figure 4.8 shows the comparison of isotropic compression responses for pure and cemented clay with one-dimensional compression of pure clay in *e* vs. *log p´* space. During one-dimensional loading the vertical stress $\sigma_v'$ and the horizontal stress $\sigma_h'$ are generally unequal and so there are shear stresses in the soil and any comparison between the two types of compression has to take account of the shear stresses (Atkinson, 1993). For the comparison, the value of $p'$ for the characterization of one-dimensional behaviour of pure kaolin clay is obtained from the equation

$$p' = 1/3\ \sigma_z' (1 + 2K_0) \quad (4.1)$$

where $\sigma_z'$ is the effective vertical stress and $K_0$ is the coefficient of earth pressure at rest. The coefficient of earth pressure at rest is defined as the ratio:

$$K_0 = \sigma_h' / \sigma_z' \quad (4.2)$$

Using the relationship of Jaky (1948), for the normally consolidated pure kaolin clay the value of $K_0$ was obtained from the equation

$$K_{0nc} = 1 - \sin \phi_c' \quad (4.3)$$

where $\phi_c'$ is the critical state friction angle ($\phi_c' = 27.5°$).

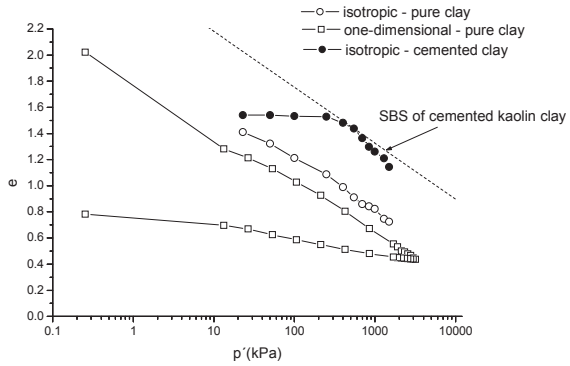


*Figure 4.8 Behaviour of reconstituted cemented kaolin clay during isotropic compression and pure kaolin clay during isotropic and one-dimensional compression*

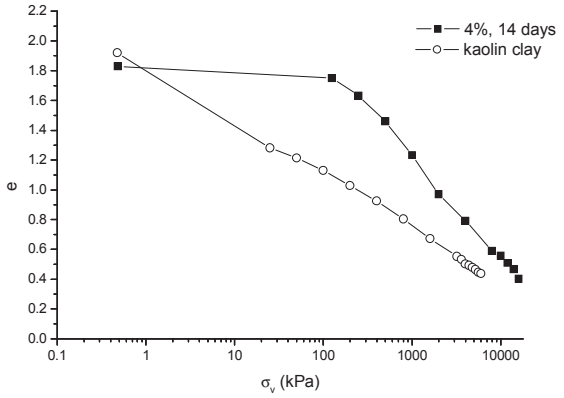


*Figure 4.9 One-dimensional compression line of pure and cemented kaolin clay cured for 14 days*

The one-dimensional compression (swelling) and the isotropic compression (swelling) can be assumed with good approximation to be parallel (Atkinson & Bransby, 1978). In Figure 4.8 both compression lines for the pure kaolin clay, one-dimensional and isotropic, have the same gradient -$\lambda$. The same gradient defines the state boundary line (SBS line) of the cemented kaolin clay.

The one-dimensional compression response of cemented clay cured for 14 days is shown in Figure 4.9 in $e$ vs. $log\ \sigma_v'$ space. The value of $K_0$ for cemented specimen cannot be obtained with the equation (4.3) as the behaviour is affected by the state of structure. After yield the one-dimensional compression curve of the cemented specimen shows a higher compressibility than that observed in the corresponding isotropic compression test (Figure 4.8). This phenomenon is probably due to more significant microstructural changes induced by one-dimensional compression, including compression and shear stresses, and has also been observed by Callisto & Calabresi (1998) and Rampello & Callisto (1998).

## 4.4. Summary

One-dimensional and isotropic compression tests were carried out on uncemented and artificially cemented kaolin clay. The results of the introductory one-dimensional compression test series confirm the development of structure in the kaolin specimens with addition of Portland cement. The cemented clay had a low pre-yield and high post-yield compressibility, which is typical for natural cemented soils.

Cement content and curing period were found the main factors influencing the compressibility of kaolin clay treated with Portland cement. Cemented specimens had almost the same initial void ratio, but the final void ratio was increasing with increasing cement content and curing period. A significant increase in yield stress was observed in the results of oedometer tests as the cement content and curing period increased. Longer curing period and higher content of Portland cement support formation of higher number of bonds, leading to the stronger resistance to compression.

The effect of cementation was described by changes in compression index $C_c$. The specimens with a higher content of cement exhibited low compressibility at low stress level because of the resistance to compression produced by the structure. With increasing load the structure disturbance started, leading to an increase of compression and of compression index $C_c$.

The effect of the cementation on behaviour of the kaolin clay was studied in detail by one-dimensional and isotropic compression of model cemented specimens with the addition of 4% of Portland cement. The results were compared with results obtained for uncemented specimens. The initial influence of cementation is clearly indicated by the low one-dimensional and isotropic compressibility of cemented specimens. The stiff behaviour was followed by yielding at the threshold stress. Subsequently, after surpassing the threshold stress, the compressibility increased owing to the process of debonding. The cementation degraded with loading.

A difference was found between one-dimensional and isotropic compression of the cemented clay at the post-yield convergence of the cemented and uncemented compression curves. After yield the compression curves of originally cemented specimens are assumed to converge for both types of compression to the normal compression lines of pure kaolin clay. However, the maximum applied stress during isotropic compression was not high enough to confirm the phenomenon and the convergence was almost negligible. On the contrary, data from one-dimensional compression tests indicate that the NCLs of cemented and pure clay

ultimately converge at high stresses. Thus the microstructural changes induced by one-dimensional compression (including compression and shear stresses) are more severe than the changes induced by isotropic compression.

# Chapter 5

# Shear tests

## 5.1. Introduction

To characterize the pure and the artificially cemented kaolin clay, laboratory investigation of shear strength and shear stiffness was made. The study was concerned with the different behaviour of model cemented (4% of Portland cement) and uncemented specimens during shearing in the triaxial apparatus. Properties of reconstituted uncemented clay are denoted by an asterisk.

The results of the shear tests enable a comparison of the behaviour in the range from very small to large strains. At very small strains the behaviour of the soil is characterised as approximately linear elastic and the shear modulus has a constant value (Viggiani, 1992). Beyond the elastic threshold strain the stiffness of the soil decreases significantly with shear strain amplitude and there is evidence of elasto-plastic behaviour (Stallebrass, 1990 in Viggiani, 1992). The threshold strain lies between 0.001 and 0.01% depending on the plasticity of the soil (Viggiani, 1992).

In addition, the effect of the amount of Portland cement on the shear strength was studied in the shear box. The effect of curing time was not investigated.

## 5.2. Experimental procedures

Triaxial specimens with the cement content of 0% (uncemented) and 4% (model material) were consolidated one dimensionally in the high consolidometer (see Chapter 3.3.1). After 3 days and 10 days the cemented and uncemented specimens (respectively) were transferred to the triaxial cell. The properties of all triaxial specimens are summarised in Table 4.2 in Section 4.3.1. The specimens were placed inside the membrane, sealed on to the base and to the top cap by O-rings.

All the triaxial tests were conducted using standard triaxial cells. Axial load was measured using a 5 kN load cell manufactured by Wykeham Farrance. The load cell was mounted inside the triaxial cell. Cell water pressure was measured using the GDS Advanced Pressure/Volume Controller with the stated accuracy of pressure measurements < 0.1% full range. The pore pressure at the base of specimens was measured using pressure transducer

with a measuring range of 0 – 1700 kPa. The load cell and the pressure transducer were recalibrated before testing each specimen. Calibration constants were obtained by optimising the readings within the linear scale. The values were incorporated into the computer control program.

The triaxial specimens were saturated using the back pressure of 100 kPa, which was applied in increments of 3 kPa/hour. The saturation was controlled with Skempton´s pore pressure parameter determined as $B = \Delta u/\Delta\sigma_3$ by measuring the pore pressure increase $\Delta u$ due to an increase in cell pressure $\Delta\sigma_3$. Saturation process was continued until the B value achieved for the pure and cemented clay values of 0.95 and 0.9, respectively. According to Muhunthan & Sariosseiri (2008), a value of B around 0.7 and higher tends to achieve a degree of saturation well above 95% for most of the soils.

After saturation, the specimens were consolidated or compressed to the mean effective stresses given in Table 5.1. The specimens with Portland cement were isotropically compressed after an initial one-step consolidation by a small isotropic stress (30 kPa) to determine the rate of loading during isotropic compression. The compression at slow rate was preferred to stepwise consolidation to minimise excess pore pressures and to prevent the debonding. The compression rate for the cemented clay was 1.25 kPa/hour. The pressure on the uncemented kaolin specimens was applied in single increments (stepwise consolidation). Measurements of water that drained from the specimens were taken during both procedures using the GDS Advanced Pressure/Volume Controller with the stated accuracy of volume ≤ 0.1% measured value. The consolidation fulfilment was controlled before each test. The volume change was considered as stabilized when the volumetric strain rate was lower than $10^{-6}$/min.

*Table 5.1 Summary of the applied stresses during isotropic compression tests with the measurements of stiffness and before shearing*

| | 10 | 50 | 100 | 250 | 400 | 500 | 550 | 700 | 850 | 1000 | 1300 | 1500 |
|---|---|---|---|---|---|---|---|---|---|---|---|---|
| Shear tests: | | | | | | | | | | | | |
| *kaolin* | | | x | | | x | | | | x | | |
| *cemented kaolin* | | x | x | | | x | | | | x | | x |
| Stiffness measurements: | x | x | x | x | x | | x | x | x | x | x | x |

The shear box tests were performed on specimens prepared by adding 2, 4 and 8% of Portland cement to the soil in a conventional direct shear box. The mixture was prepared with the same procedure as the mixtures used for one-dimensional compression tests (see Section 4.3.1). The uniform paste was placed into the shear box without any compaction. The tests were carried out after 3 days of curing.

### 5.2.1. Shear testing

Shearing in the triaxial cell under controlled deformation followed after consolidation or compression to the stresses summarised in Table 5.1. When consolidation or compression was completed, drainage was closed and the specimens were sheared under undrained conditions with pore pressure measurements (CIUP tests). The shear tests were conducted at a constant rate of axial displacement of 0.0005 and 0.0008 mm/min for the pure and cemented specimens, respectively. The only exception was the shear test of cemented specimen compressed to the mean effective stress of 50 kPa, which was drained and the shear test was conducted at a constant rate of axial displacement of 0.00008 mm/min.

In addition, shear box tests of soil specimens with various amounts of Portland cement were carried out to investigate the effect of cementation on the shear strength of the soil. At first, the specimens were compressed to an effective vertical pressure of 50 and 100 kPa. After compression, all specimens were sheared at a constant rate of displacement of 0.016 mm/min.

### 5.2.2. Stiffness measurements

During isotropic drained compression, undrained measurements of stiffness were carried out with both static (shear probes using continuous loading and submersible LVDTs) and dynamic method (bender elements) at the given effective stresses (Table 5.1). The maximum shear stiffness was obtained at very small strains (below 0.001%) from the propagation of shear waves through the specimens. At higher strains results from measurements with LVDT´s and shear tests are shown.

The cemented specimens were cured for 3 days in a consolidometer, saturated for 14 days in the triaxial cell and the continuous isotropic compression to effective stress for stiffness measurements lasted 10 days. Thus the time of curing, saturation and consolidation for a loading of 50 kPa was 27 days. After such a long curing period the effect of time on the development of bonding is assumed to be negligible and the development of bonding does not cancel the effect of bond degradation with loading.

In the static method, axial strain was measured using a set of linear variable differential transformers (LVDTs). These internal devices were mounted directly on the specimen (Figure 5.1 (a)). The LVDTs were inserted in two fixing pads, which were glued to the specimen. The shear modulus at very small strains $G_0$ was obtained from

$$G_0 = \delta q/(3\,\delta\varepsilon_a) \tag{5.1}$$

where $\varepsilon_a$ is the axial strain and $q$ is the deviatoric stress.

The LVDT´s were used during the deviatoric stress probes under constant cell pressure and axial strain rate at standard total stress path $\delta q/\delta p = 3$. The change of the deviatoric stress was limited to 20 kPa. After probing of the specimen, undrained shear unloading returned the stress path to isotropic compression line.

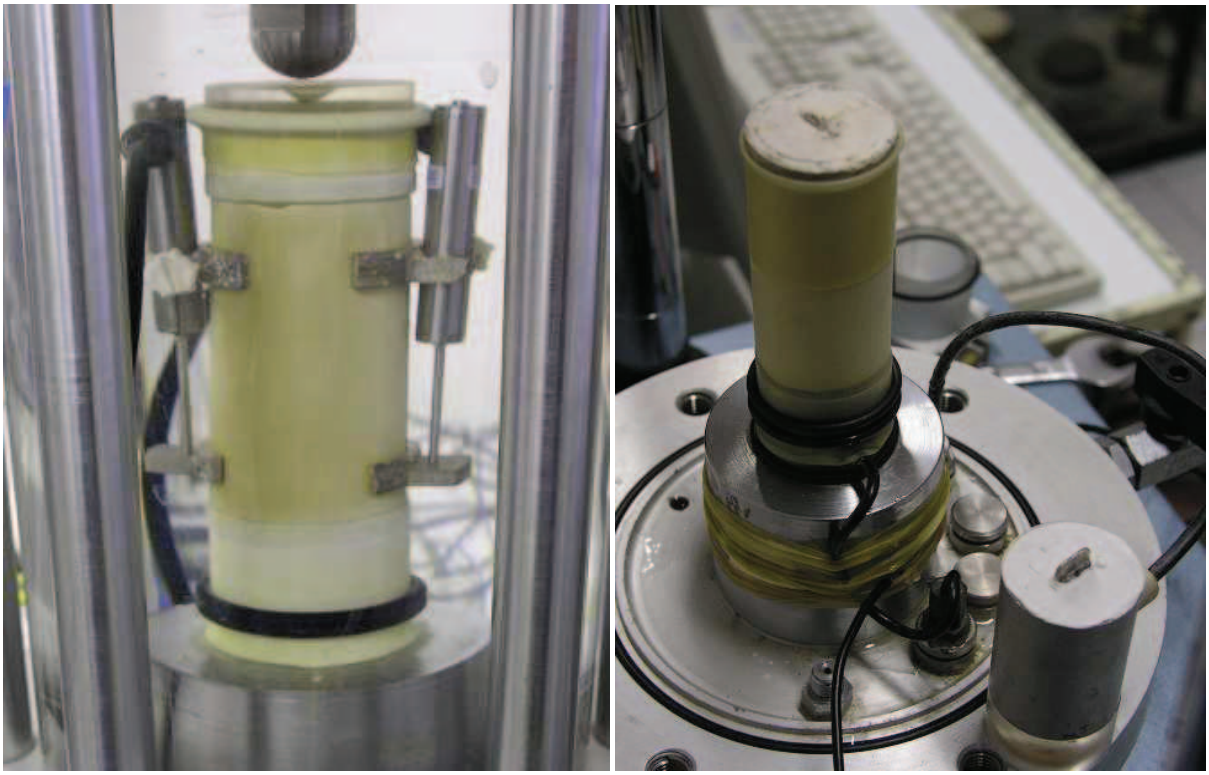

*Figure 5.1 Model cemented kaolin clay specimen: (a) with the set of conventional linear variable differential transformers (LVDTs); (b) with the piezoceramic transducers – bender elements (BE)*

The bender element (BE) setup consisted of piezoceramic transducers fixed to the bottom and top platens (Figure 5.1(b)), signal generator and an oscilloscope card in a personal computer. The measurements were based on transmission of a seismic wave through a soil sample and the shear wave velocity ($V_s$) was determined from the travel times. Single-pulse

sinusoidal input signal was used with frequency of 1 - 25 kHz and peak-to-peak voltage of 1.7 V. The shear modulus at very small strains $G_0$ was obtained directly from

$$G_0 = \rho V_s^2 = \rho L^2/t^2 \quad (5.2)$$

where $\rho$ is the soil density, $V_s$ is the velocity of the shear wave, $t$ is the travel time and $L$ is the effective length. The distance between the tips of the elements was used as effective length (Viggiani & Atkinson, 1995).

The main problem of using BE testing is the interpretation of the results. There is no standard for the testing procedures. An important limitation for certainty of the results is sample-size effect (Arroyo et al., 2006). Different investigators have analyzed the input and output signals from bender element tests using: (i) travel time to first deflection of the output signal; (ii) travel time between characteristic peaks of input and output signals; (iii) travel time by cross-correlation of input to output signals; (iv) travel time by the phase velocity between the input and output signals. Based on the work by Jovicic et al. (1996) and on own experience with BE testing the first significant reversal of polarity of the received signal was considered as the arrival of the shear wave.

For tested relatively stiff soils the near-field effect could not be avoided (Arroyo et al., 2003). Therefore in taking all BE measurements, the input and output signals were of a similar shape with the same frequency (Viggiani & Atkinson, 1997) and the arrival time was determined at several frequencies (1, 2, 3, 5, 7, 9, 11, 15, 20 and 25 kHz). The consistency of the readings was checked (Figure 5.2). Sanchez-Salinero et al. (1987) studied the dependency of near-field effect on the wavelength relative to the distance between the source and receiver. They recommended measurements at frequencies such that the distance from the source to the receiver is at least one wavelength.

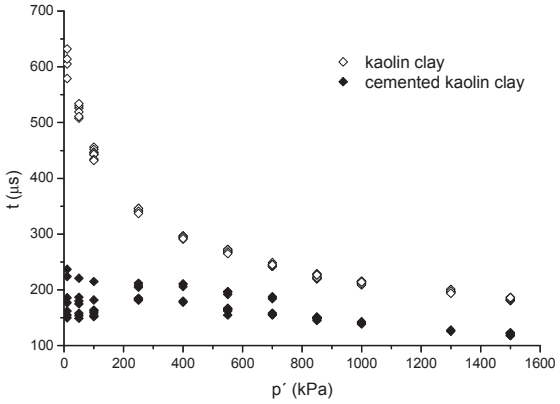


*Figure 5.2 Travel times of sinusoidal waves with the input signal of different frequency during BE testing of pure and cemented kaolin clay at each effective stress level*

## 5.3. Interpretation of data

The shearing behaviour of specimens with 4% of Portland cement was compared with the shearing behaviour of uncemented specimens in the range from very small to large strains.

The small strain behaviour was studied by dynamic and static methods. The results of static method, undrained shear probes, are converted to shear modulus assuming isotropy of the tested specimen. The volumetric strains observed during compression indicated that the excess pore pressures generated in the specimen were less than about 10 kPa. During undrained shear deviatoric probes the pore pressure increase stopped at 10 kPa and after undrained shear unloading the value of pore pressure decreased to the same value as before the deviatoric stress probe. The drained compression followed with no change in volume after opening the drainage valve (Figure 5.3).

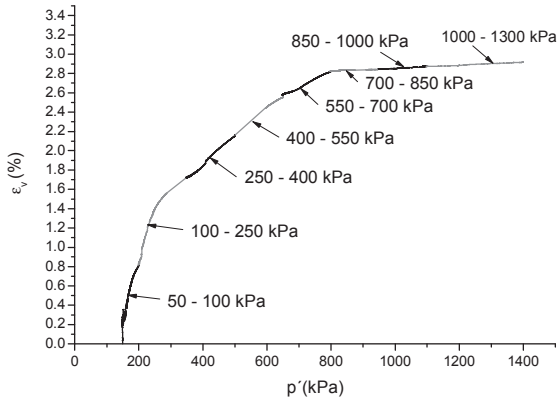


*Figure 5.3 Isotropic drained compression of the cemented specimen up to the demanded effective stresses of 50, 100, 250, 400, 550, 700, 850, 1000, 1300 and 1500 kPa*

### 5.3.1. Shear strength

The results of direct shear tests performed on the specimens with cement admixture of 2, 4 and 8% compressed to an effective pressure of 50 and 100 kPa are shown in Figure 5.4 and 5.5. The shear stress-displacement curves for the tests of the cemented kaolin clay are compared in Figure 5.4(a). The data indicate that the peak shear stress is increasing with increasing cement content and the increase is relatively small. The results of direct shear tests on cemented specimens are highly affected by the relatively short curing period.

All specimens showed contractant volumetric deformation during shearing (Figure 5.4(b)). A difference was found in the dependency of the value of the vertical strain on the applied vertical pressure. The vertical strain of specimens with 2 and 4% of Portland cement is significantly increased by the increase of vertical pressure. On the contrary, both specimens with 8% of cement content achieved very similar values of vertical strain. The resistance to straining of specimen compressed at 100 kPa is almost equal to resistance of specimen compressed at 50 kPa due to the control of cementation.

2% of Portland cement

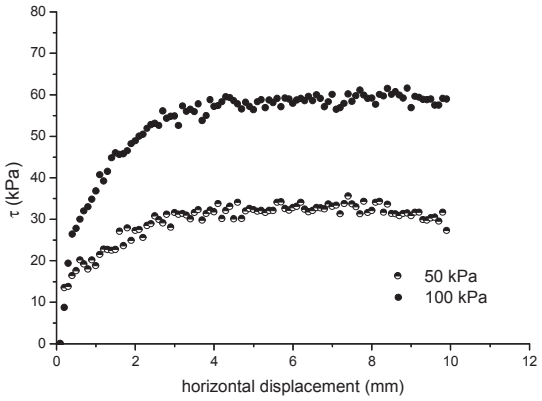


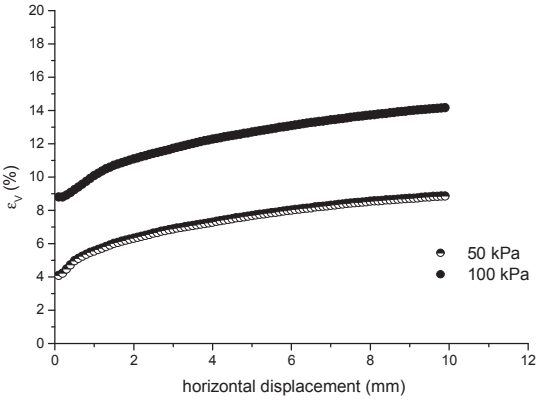


4% of Portland cement

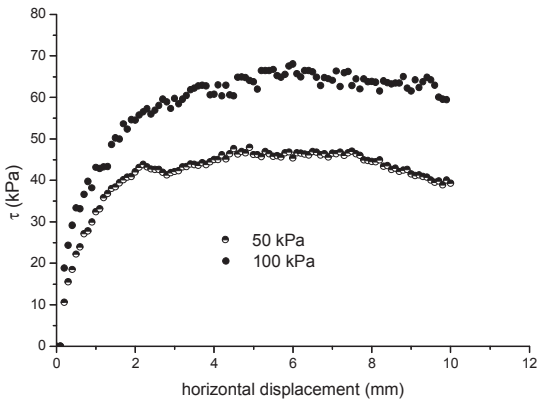


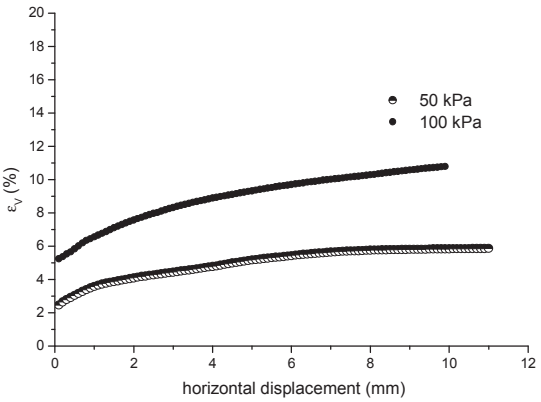

8% of Portland cement

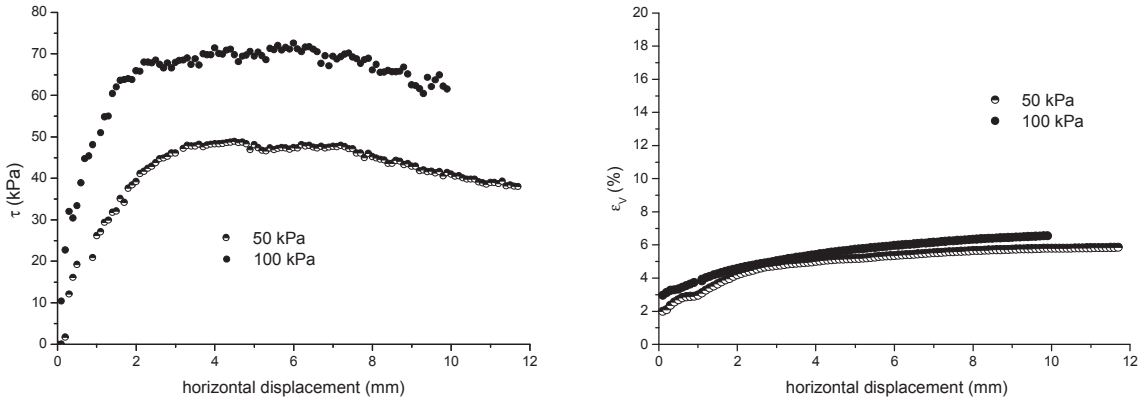


(a) (b)

*Figure 5.4 Direct shear tests on kaolin clay with 2, 4 and 8% of Portland cement: (a) shear stress-displacement curve; (b) strain-displacement curve*

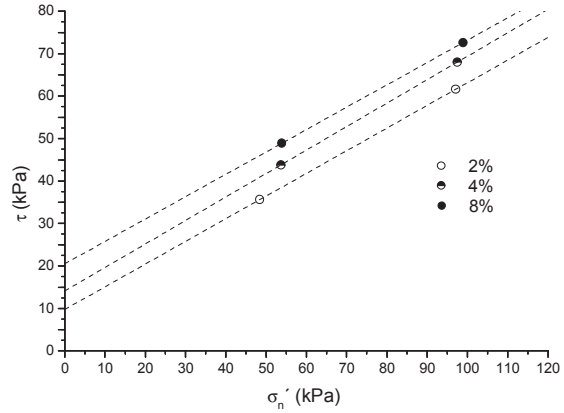


*Figure 5.5 Results of direct shear tests performed on the kaolin specimens with 2, 4 and 8% of Portland cement*

The results in Figure 5.5 indicate that strength envelopes of the specimens with lower addition of Portland cement lie below the envelopes of the specimens with higher addition of Portland cement. The data confirm a significant effect of the amount of Portland cement admixture on the mechanical behaviour of the soil. The cohesion seems to increase with the increasing amount of Portland cement. For the specimens of cemented kaolin clay with 4% of Portland cement the obtained peak friction angle is approximately 28° and the peak cohesion is 14 kPa.

The behaviour of pure and cemented specimens with 4% of Portland cement during shearing in the triaxial apparatus is compared in Figures 5.6, 5.7 and 5.8. Figure 5.6(a) and (b) shows plots for deviatoric stress and axial strain obtained from the tests on pure and cemented

kaolin clay, respectively. The peak deviatoric stress of pure kaolin clay (Figure 5.6(a)) increases with increasing confining pressure. After failure, the stress-strain curve of specimen compressed at 100 kPa is almost flat. In case of specimens compressed at 500 and 1000 kPa, there is a significant drop of deviatoric stress at large strains. This may be related to changes in packing of deflocculated clay particles discussed later.

As Figure 5.6(b) shows, the response of the cemented clay to loading is different due to the cementation. The cemented specimens approach the peak strength and tend to seek the ultimate state via strain softening. The peak deviatoric stress increases with increasing confining pressure and the maximum values are significantly higher than the values obtained for the pure kaolin specimens at corresponding confining pressures.

Figure 5.7 shows plots of pore water pressure ($u$) and axial strain ($\varepsilon_a$). Both types of specimens show predominantly tendency to contractant behaviour, opposite of expectation. The values of $u$ are similar for the pure and the cemented specimen compressed at 100 kPa. In case of the cemented specimens compressed at mean effective stresses of 500 and 1000 kPa the pore pressures are higher than the pore pressures achieved by the corresponding pure specimens. Moreover, the pore pressures of cemented specimens compressed up to 1000 and 1500 kPa rose up to pressures higher than achieved deviatoric stress and decreased with straining after peak.

The differences in the pore pressure development may indicate the differences in structure of the cemented specimens. Sangrey (1972) and Pillai & Muhunthan (1999) reported that naturally cemented soils show a large immediate build-up of pore pressure during shearing. A significant amount of free water is released as a result of breakage of cemented bonds. Similarly, the artificial cemented bonds are destroyed with shearing and the extent of debonding, which is connected with the increase of pore pressure, is affected by the confining pressure.

The pore-water pressure increase in the prepeak phase and the decrease in the post-peak phase were also presented by Feda (1995). The specimens behaved as a pseudocontinuous material because of the specimen´s cementation.

For the specimen, which was compressed to the low mean effective stress of 50 kPa and sheared drained, dilation was observed (Figure 5.8). The presence of bonding prevents the soil from dilating up to yielding. After yielding, the gradual degradation of the bonds inhibits the dilation of the specimen. This suggests a strong effect of cementation at the low confining pressure. Conversely, the dilation was not observed in shear box tests of cemented specimens compressed at 50 kPa (Figure 5.4(b)), which is probably a result of short curing period.

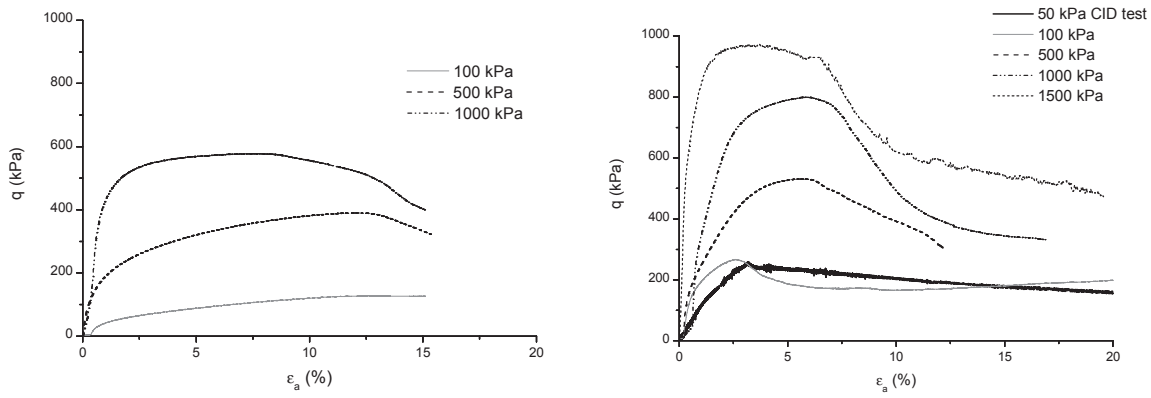


(a) (b)

*Figure 5.6 Stress strain behaviour: (a) pure kaolin clay; (b) kaolin clay with 4% of Portland cement*

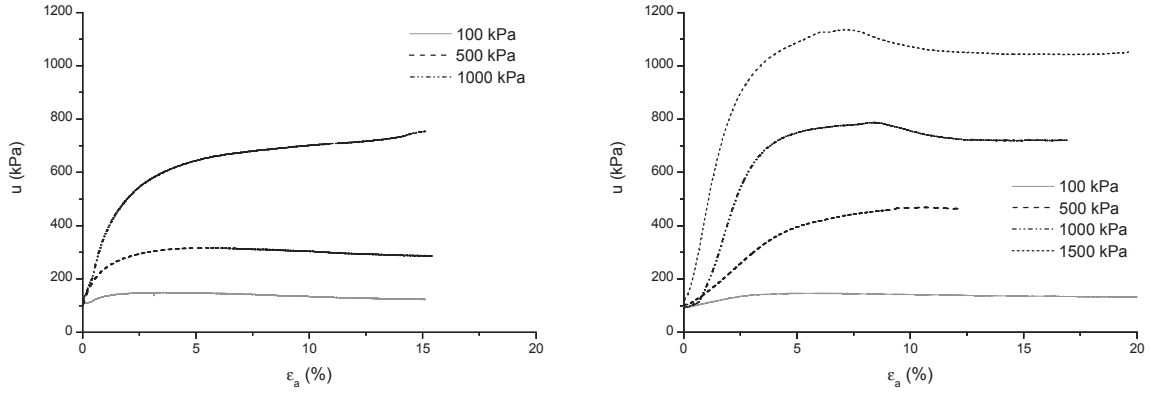


(a) (b)

*Figure 5.7 Pore pressure response against axial strain: (a) pure kaolin clay; (b) kaolin clay with 4% of Portland cement*

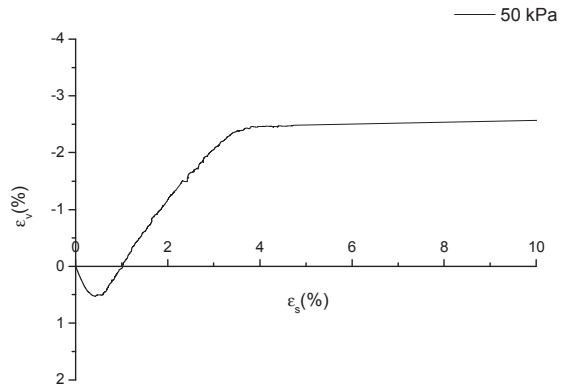


*Figure 5.8 Behaviour of cemented specimen in drained shear test*

The different modes of undrained shearing behaviour are compared in the $\varepsilon_s/(q/p')$ plane in Figure 5.9. Figure 5.9(a) for kaolin specimens shows the typical ductile behaviour of the uncemented clay. This was also reflected in bulging of the specimens near peak (Figure 5.10(a)). The peak deviatoric stress was reached at least at 7.5% strain increment. In contrast, all cemented specimens in Figure 5.9(b) show brittle behaviour. The cemented specimens failed with single shear bands as shown in Figure 5.10(b). The effect of cementation is decreasing with higher mean effective stresses (500, 1000 and 1500 kPa), which are beyond the yield stress identified from isotropic compression tests (at about 400 kPa).

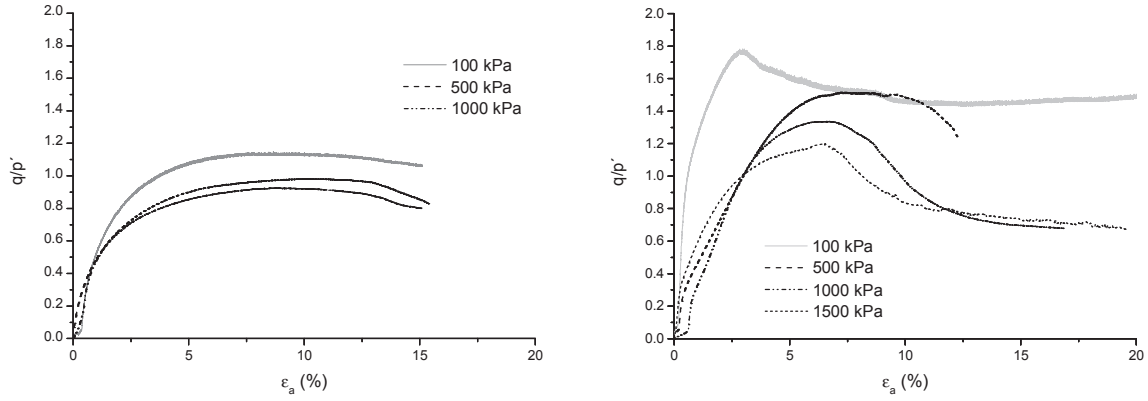


(a) (b)

*Figure 5.9 Modes of undrained shearing behaviour: (a) pure kaolin clay; (b) kaolin clay with 4% of Portland cement*

(a) (b)

*Figure 5.10 Specimens consolidated or compressed up to 100 kPa after rupture: (a) pure kaolin clay; (b) kaolin clay with 4% of Portland cement*

After normalization, two different modes of brittle behaviour could be identified for cemented specimens according to the degree of cementation. The well-cemented specimen compressed at pressure of 100 kPa shows a stiff behaviour until a significant peak. The peak deviatoric stress was reached approximately at 2.6% strain increment. The specimens compressed at higher compression pressures (500, 1000 and 1500 kPa) show less stiff behaviour before peak and become brittle with abrupt drops in postpeak stress ratio with strain. The peak deviatoric stress was approximately at 6% strain increment. For the specimens compressed at 1000 and 1500 kPa the curve of stress ratio versus axial strain falls steeply after peak to a well defined plateau.

The differences in the behaviour of pure and cemented specimens can be also seen in the stress paths plotted in the $q/p'$ plane shown in Figure 5.11(a). The stress paths for specimens of kaolin clay move leftwards as for normally consolidated isotropic clay specimen under undrained conditions. The stress paths of the specimens compressed at the effective stresses of 100 and 500 kPa rise to the ultimate failure line and as peak strength is approached the stress paths bend to the right which is indicative of dilatant behaviour. The contractant behaviour prevails in case of compression at 1000 kPa.

According to Viseras et al. (2007) kaolin dispersions at high solid concentrations show dilatant flow (apparent viscosity increases with increased shear rate). This rheological behaviour is attributed to close packing of deflocculated clay particles, which results in interparticle contacts and interaction during shearing. Once peak strength has been reached the individual packets begin to break down giving rise to contractant behaviour.

Wang & Siu (2006b) studied the effect of pH on the stress-strain behaviour of Speswhite Kaolin. They compared the effective stress paths of specimens at pH 4 and pH 7.8 under three different confining pressures (100, 200 and 300 kPa). The pH 4 specimens exhibit contractive tendencies towards the critical state. The pH 7.8 specimens demonstrated completely different responses, in agreement with the results obtained for specimens of kaolin clay compressed at the effective stresses of 100 and 500 kPa (Figure 5.11(a)): the initial contraction, a phase-transformation state and then the dilation. A distinct transition point, pH 5, was found as a boundary to separate the high and low pH (Wang & Siu, 2006a). The studied kaolin clay falls within the high pH and is characterised with pH 6.6 (see Table 3.1 in Sec. 3.2).

Although the pH 7.8 specimens did not behave the same as the pH 4 specimens, Wang & Siu (2006b) demonstrated that the trends still suggest that the critical stress ratio of the pH 7.8 specimens was close to that of the pH 4 specimens. Interparticle attractive forces do not

have an apparent influence on the shear strength at the critical state. Following their suggestion, critical states were obtained for the pure kaolin clay specimens.

The stress paths of the cemented clay change due to the increase of mean effective stress from almost vertical one, characteristic of overconsolidated state, to the rounded one typical of normally consolidated state. At low mean effective stress (100 kPa), the almost vertical stress path reflects the effect of cementation until approaching the peak strength envelope, followed by breakage of bonds.

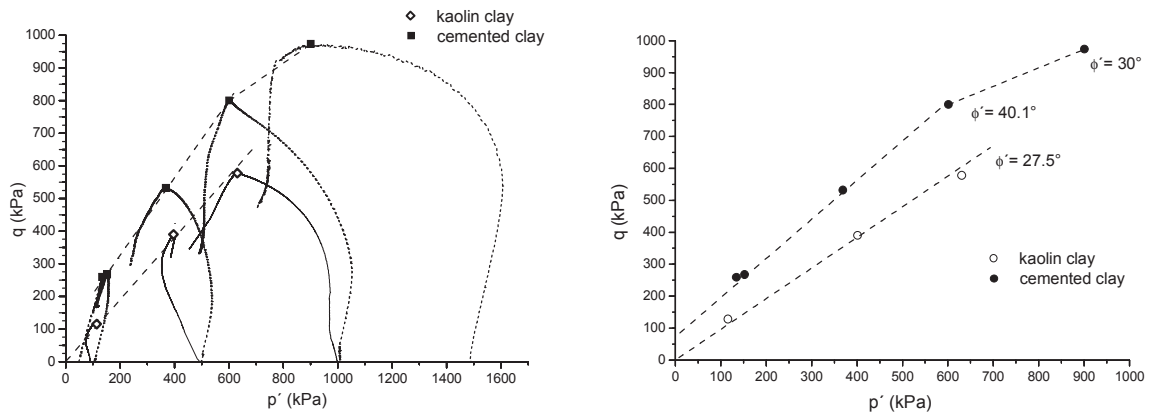


(a) (b)

*Figure 5.11 Results of triaxial shear tests on cemented and pure kaolin clay: (a) stress paths; (b) failure envelopes*

The approximate positions of the failure envelopes are shown in Figure 5.11(b). The obtained critical state friction angle of the pure kaolin clay is approximately $\phi_c' = 27.5°$. All stress paths of cemented specimens crosses the critical state line of the pure clay, indicating that debonding, initiated during isotropic compression beyond yield stress, was not completed. Thus the failure envelope of the cemented clay, derived from the values of peak deviatoric stress, lies above the envelope of the pure clay due to the additional strength of cementing bonds.

The measured peak strength in a cemented specimen is determined by the shape of the initial state boundary surface and the initial stress. The mobilized peak friction angle reduces from 47° at 50 kPa to 30° at 1500 kPa (Figure 5.9(b)). The peak cohesion was obtained by linearization of the failure envelope in the stress range from 100 to 600 kPa and the obtained value was 48.5 kPa. The peak friction angle of the cemented kaolin is $\phi_p' = 39°$ in the given stress range.

The change of the strength could be seen for the cemented specimen compressed at mean effective stress p´= 1500 kPa. The failure envelope of the cemented material becomes nonlinear.

Some of the specimens reached the critical state ($\delta p'/ \delta\varepsilon_s = \delta q/ \delta\varepsilon_s = \delta\varepsilon_v/ \delta\varepsilon_s = \delta u/ \delta\varepsilon_s = 0$). The identification of critical states for all cemented specimens and especially for kaolin clay specimens compressed at 500 and 1000 kPa is questionable due to the shear strain localization. The locations of the "critical" states and isotropic NCL for pure and cemented clay specimens are shown in Figure 5.12. The specimens of pure kaolin clay may be characterised with the "critical" states determined for constant straining at about 13%, which form the critical state line (CSL) parallel with the isotropic NCL and a lower bound to the data at large strains for the cemented soils.

The "critical" states of the cemented specimens were determined for constant straining at about 10% (specimens compressed at 50 and 100 kPa) and 12% (specimens compressed at 1000 and 1500 kPa). In the case of the cemented specimen compressed at the effective stress of 500 kPa the "critical" state was estimated for straining at about 12%. The "critical" states of all cemented specimens lie above the CSL and the NCL of pure kaolin clay. Despite the large strains, the ultimate states were not reached by the cemented kaolin clay specimens, contrary to the pure kaolin clay specimens.

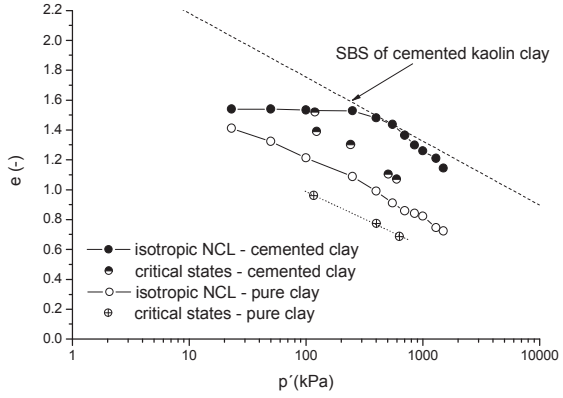


*Figure 5.12 Location of isotropic NCLs and critical states of pure and cemented kaolin clay specimens*

### 5.3.2. Shear modulus

Bender elements (BE) were used to determine the variation of the very small strain shear modulus $G_0$ with stress. The test results for reconstituted kaolin clay are shown in Figure 5.13. The observed value of $G_0$ increases with mean effective stress $p'$ and the obtained values

agree with the data for reconstituted speswhite kaolin clay measured by Viggiani and Atkinson (1995). The values of soil parameters for speswhite kaolin clay are similar to the values obtained for used kaolin clay (see Section 3.2.1, Table 3.4).

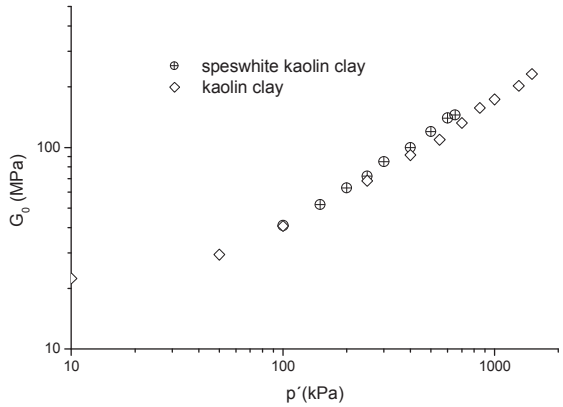


*Figure 5.13 Variation of stiffness with mean effective stress for reconstituted specimens of speswhite kaolin clay (after Viggiani & Atkinson, 1995) and used kaolin clay*

The shear modulus at very small strains ($G_0$) of two specimens with 4% of Portland cement, cemented clay 1 and 2, was measured using "static" (LVDT´s during the deviatoric stress probes) and "dynamic" (BE) methods, respectively. A comparison of the data obtained from both types of measurements is presented in Figure 5.14 together with data from tests on pure kaolin clay. Two strain levels, 0.001% and 0.006%, were chosen from LVDT stiffness measurements for the comparison. Both the axial strains are in the area of elastic behaviour (Figure 5.15).

For the cemented clay both types of measurements are in good agreement at mean effective stress of 50 kPa and the value of $G_0$ is higher than for the pure kaolin clay. According to the measurements obtained for the specimen kaolin clay 2 with bender elements $G_0$ of cemented material is almost constant in the effective stress range up to 400 kPa. The values of $G_0$ are controlled solely by cementation.

At the same stress range (50 – 400 kPa) $G_0$ measured on the specimen cemented clay 1 with LVDT´s is slightly decreasing with the increasing mean effective stress and the decrease is more evident for the measurements at higher strain. As the isotropic stress increases the cemented clay 1 is becoming gradually softer than the specimen cemented clay 2. The structure is weakened due to previous strain cycles. This is an evidence for the effects of debonding on very small strain stiffness. Nevertheless, the effect of structure prevails and the specimen cemented clay 1 is stiffer than the pure kaolin clay.

At stresses higher than 400 kPa values of $G_0$ obtained for both the cemented specimens becomes dependent on $p'$ and the subsequent increase corresponds to the increasing trend of $G_0$ for the pure kaolin clay.

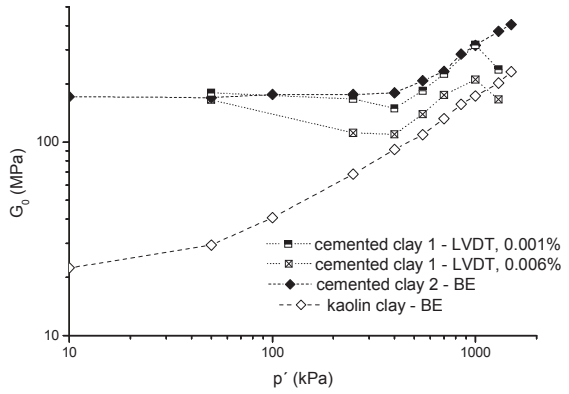


*Figure 5.14 Variation of $G_0$ with mean effective stress for kaolin clay and with mean effective stress and strain for specimens of model cemented kaolin clay*

The yield of the cemented specimens was identified at mean effective stress at about 400 kPa. After yield, the values of $G_0$ obtained for the cemented material remain higher than the values for the pure kaolin clay. The hydration and pozzolanic reaction between cement and clay particles created permanent changes of the treated clay fabric, which were not reversed or destroyed during the compression. However, there is a significant decrease of $G_0$ for the data measured with LVDT´s for the specimen cemented clay 1 compressed up to 1300 kPa, indicating that the differences in small strain behaviour may be reduced by debonding of the specimen caused by previous strain cycles.

The strain dependency of shear modulus ($G$) was studied on the cemented specimens compressed to 50, 100, 500 and 1000 kPa using the results from both types of measurements (Figure 5.15(a)). It is evident that the stiffness of the cemented clay is non-linear. The degradation of stiffness with strain is almost negligible for the specimens compressed up to 50 and 100 kPa until the yield. At the strain of about 0.01% there is a sharp drop of the shear modulus. The reduction in stiffness for specimens compressed at 500 and 1000 kPa is less rapid after yield. The cement bonds gradually degrade with continued straining.

The change in the dependence of stiffness on cementation or mean effective stress may be seen in Figure 5.15(b). The cementation significantly increases the initial stiffness and reduces the effect of confining pressure on $G_0$ for specimens compressed up to 50 and 100

kPa. At higher stress (500 and 1000 kPa) the effect of cementation is reduced and the effect of stress prevails.

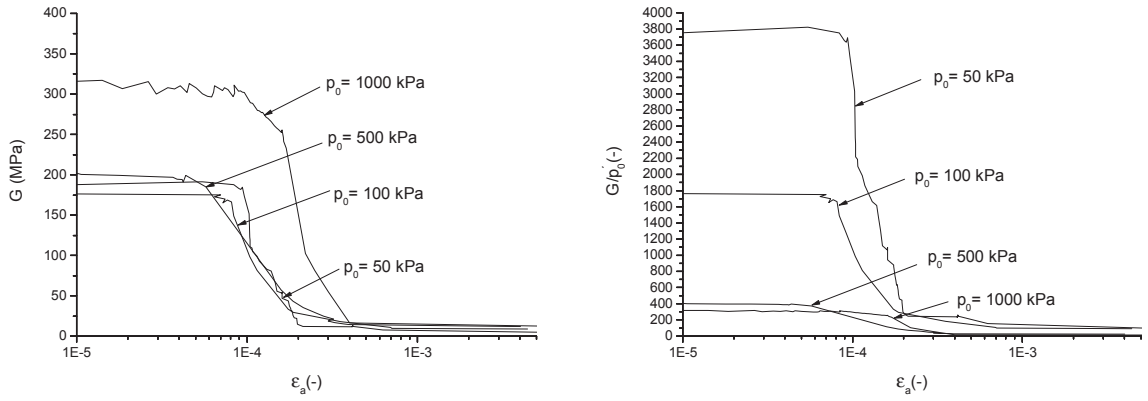


(a) (b)

*Figure 5.15 Variation of stiffness with strain for cemented kaolin clay: (a) original; (b) normalized with p´*

### 5.3.3. Summary

The comparison of shearing behaviour shows significant differences between the specimens with 4% of Portland cement and uncemented specimens in the range from very small to large strains. The addition of Portland cement to the soil leads to the increase of shear strength and initial stiffness of the specimens. The effect of cementation on the mechanical behaviour of the soil is increasing with the increasing amount of Portland cement, similarly to the results of compression tests.

During undrained shearing, kaolin clay shows predominantly ductile behaviour and the peak deviatoric stress increases with increasing mean effective stress. The shearing behaviour is characterised with zero cohesion and the critical state friction angle $\phi_c' = 27.5°$. The stress paths of the kaolin clay specimens correspond to the response of normally consolidated clay. Rheological behaviour at "ultimate" state is dilatant at mean effective stresses of 100 and 500 kPa and contractant at 1000 kPa as a result of differences in packing of deflocculated clay particles in kaolin dispersions. The ultimate state for kaolin clay specimens compressed at 500 and 1000 kPa is approximate due to the shear strain localization.

The cemented specimens exhibited brittle behaviour and the failure took place gradually along a single slip surface. Undrained shear tests of the cemented material indicate

that the strength mobilizes to its peak value at quite a low strain in comparison with the pure kaolin clay and then it gradually decreases with further straining. The strain softening behaviour is more visible for specimens compressed at mean effective stresses of 500, 1000 and 1500 kPa.

The failure envelope of the cemented clay lies above the envelope of the pure kaolin clay demonstrating the enhanced strength of the clay due to bonding. The stress paths reflect the effect of cementation (move rightwards, close to vertical) and its gradual degradation. Tendency to contractant behaviour was observed for the cemented specimens, contrary to expectation. Dilation occurred with the cemented specimen compressed at 50 kPa and sheared drained. This suggests a strong effect of cementation at the low confining pressure.

The effect of mean effective stress on the shear stiffness of pure and cemented kaolin clay was compared. Measurements indicated a significant influence of cementation on the very small strain shear modulus $G_0$. The values of $G_0$ of reconstituted normally consolidated pure clay is dependent on the mean effective stress. On the contrary, $G_0$ of the cemented kaolin clay is stress independent until a threshold. The values of $G_0$ are higher than the values obtained for the pure kaolin clay. The destructuration after the threshold results in the stress dependency of the $G_0$ similar to the pure kaolin clay.

The strength and stiffness parameters for the pure kaolin clay represent the lower bound to the values for the cemented kaolin clay, approached at large strains. The component of shear resistance in the cemented clay is reduced progressively by shear strains or by volume strains. The observations suggest that for specimens compressed up to 400 kPa (yield identified in $G_0$ measurements) the degradation of cementation is more likely to occur with increasing deviatoric stress than with increasing mean effective stress.

# Chapter 6

# Determination of shear modulus at very small strain

## 6.1. Introduction

The initial stiffness studied in this chapter is represented by the shear modulus at very small strains ($G_0$). The value of $G_0$ is a useful parameter for characterizing the highly non-linear stress-strain behaviour of soil for monotonic loading. In the case of uncemented soil shear stiffness is dependent on the mean effective stress, void ratio and overconsolidation ratio (Hardin, 1978).

Cementation generally causes an increase in stiffness and resistance of soils; on the other hand breakage of bonds due to volume or shear strains leads to softening of soils. Thus the values of $G_0$ for cemented soils should be determined on the basis of location of the state of the soil relative to its isotropic state boundary, which represents the threshold isotropic states, rather than to its critical-state or normal compression line. The apparent overconsolidation ratio and the state of structure (sensitivity) give a possibility to define the state of the soil.

The study considered in this chapter is presented in Trhlíková *et al.* (2012).

## 6.2. Equation for calculating shear modulus

For reconstituted soil the influence of the effective stress state and stress history on $G_0$ is expressed by the relationship (Viggiani & Atkinson, 1995)

$$\frac{G_0}{p_r} = A\left(\frac{p'}{p_r}\right)^n \left(\frac{p_p'}{p'}\right)^m \tag{6.1}$$

where $p_r$ is reference pressure (1 kPa) and $p_p'$ is the yield stress. Thus the ratio $p_p'/p'$ defines the isotropic overconsolidation ratio. $A$, $n$ and $m$ are dimensionless soil parameters.

The experimental data indicate that $G_0$ of cemented soils depends significantly on the state of soil structure. The structure can be quantified by the variable *sensitivity ratio s* (Cotecchia & Chandler, 2000), defined as the ratio of the size of the SBS of the cemented soil to that of the corresponding reconstituted soil. In Figure 6.1 adapted from Cotecchia &

Chandler (2000), the position of the SBS of the cemented soil is defined with parameters $N$ and $\lambda^*$. The current SBS relates to $p_e'$, that is the Hvorslev equivalent pressure defined as

$$p_e' = \exp\left(\frac{N - \ln(1+e)}{\lambda^*}\right) \tag{6.2}$$

where $\lambda^*$ is the slope of the NCL, $N$ is the value of $\ln(1+e)$ at $p'=p_r=$ 1 kPa and $e$ is void ratio. For the reconstituted soil the position of the SBS is defined with parameters $N^*$ and $\lambda^*$ (Figure 6.1), which determine the Hvorslev equivalent pressure $p^*_e{}'$ for the reconstituted soil. The current state of the structure can be quantified by the ratio $s = p_e'/p^*_e{}'$.

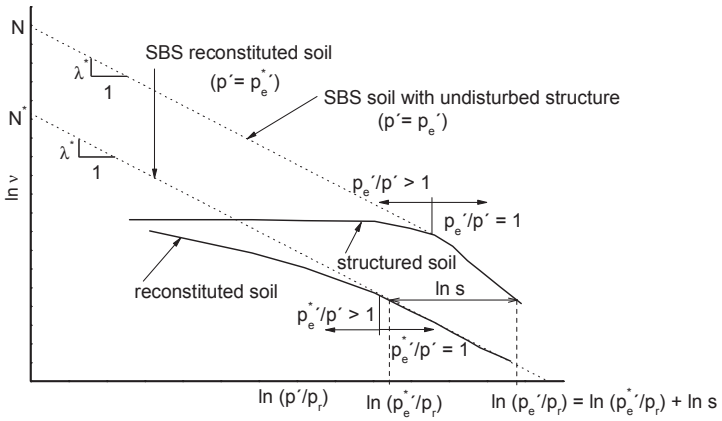


*Figure 6.1 Schematic diagram showing isotropic compression of reconstituted and structured soil with the definition of variables (revisited from Cotecchia & Chandler, 2000)*

To represent the experimental data obtained for the cemented soil, equation (6.1) can be modified to the form including the effect of structure

$$\frac{G_0}{p_r} = A\left(\frac{p'}{p_r}\right)^n \left(\frac{p_e'}{p'}\right)^m \left(\frac{s}{s_f}\right)^l \tag{6.3}$$

where $l$ is a new parameter controlling the influence of soil structure on $G_0$. The equation is equivalent to that proposed by Cafaro & Cotecchia (2001) for natural clays including a diagenized bonding, who explained how this equation results from the conceptual framework reported by Cotecchia & Chandler (2000), based on the selection of the parameter $s$ to represent the comparison between the strength of the natural clay structure and that of the reconstituted clay structure. For the reconstituted soil the values are $s=s_f=1$ and equation (6.3) is reduced to equation (6.1) expressed in terms of the Hvorslev equivalent pressure ($p^*_e{}'$).

Equation (6.3) may be rewritten as

$$\ln\left(\frac{G_0}{p_r}\right) = \ln A + n\ln\left(\frac{p'}{p_r}\right) + m\ln\left(\frac{p_e'}{p'}\right) + l\ln\left(\frac{s}{s_f}\right) \tag{6.4}$$

According to equation (6.4) and Figure 6.2, the value of $A$ represents $G_0$ of the reconstituted soil at $p' = p_r = 1$, the parameter $n$ relates $G_0$ to $p'$ and the parameter $m$ specifies the effect of the overconsolidation ratio (defined as $p^*_e'/p'$). For cemented soil, $G_0$ is increased at the pre-yield state by the apparent overconsolidation ratio (defined as $p_e'/p'$), which is higher than for the corresponding reconstituted soil and is accounted for in the third term of the sum in equation (6.4), and by the sensitivity ($s$). After yield, the effect of the apparent overconsolidation ratio disappears ($p_e' = p'$) and the effect of sensitivity prevails.

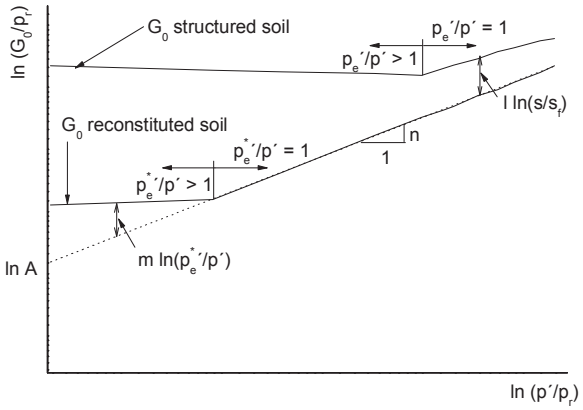


*Figure 6.2 Schematic diagram of the variation of shear modulus at very small strain for reconstituted and structured soil with the definition of variables*

## 6.3. Evaluation of equation

Equation (6.3) was used to calculate $G_0$ for three different soils for which experimental data were available. The number of data sets was limited as void ratio, mean effective stress, very small strain shear stiffness and the position of normal compression line of the reconstituted and cemented soils were required for the present analysis. The results of the laboratory tests on pure and cemented kaolin clay described in Sections 4.3.2 and 5.3.2 and results on two reconstituted and cemented sands reported in literature were used. The characterization of the cemented sands is summarised in Table 6.1.

*Table 6.1 Characterization of cemented sands*

| soil | particles | Cement | specific volume | state | variability of soil |
|---|---|---|---|---|---|
| Calcarenite (Cuccovillo & Coop, 1999) | Weak, hollow and angular shell fragments ($CaCO_3$) | Strong: calcium carbonate, deposition soon after particle deposition | Medium-high $\nu$ = 1.68-2.03 | First loading to current depth | Large variation in specific volume and amount of cement |
| Nevada sand (Yun & Santamarina, 2005) | Uniform, fine, angular sand | Portland cement Type I, 2% and 4% of admixture | Medium-high $\nu$ = 1.636-2.154 | Loose specimens cemented at low vertical sitting pressure | Reconstituted and homogenized specimen |

Figure 6.3 shows the results of isotropic and one-dimensional compression tests on the pure and the cemented kaolin clay (see Section 4.3.2), which were used to determine the parameters for equation (6.3). Values of $G_0$ determined from shear wave velocity measurements (see Section 5.3.2) and from equation (6.3) are shown in Figure 6.4.

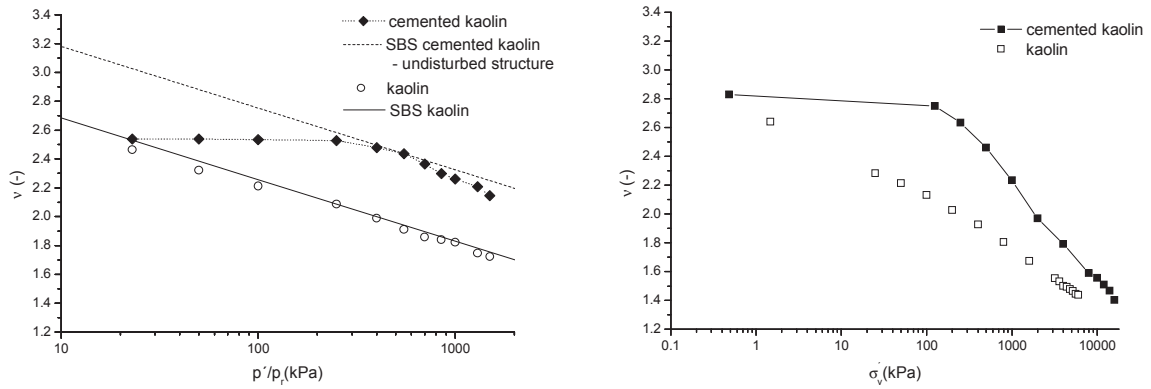


*(a)* *(b)*

*Figure 6.3 Compression lines for pure and cemented kaolin clay: (a) isotropic compression; (b) one-dimensional compression after 14 days*

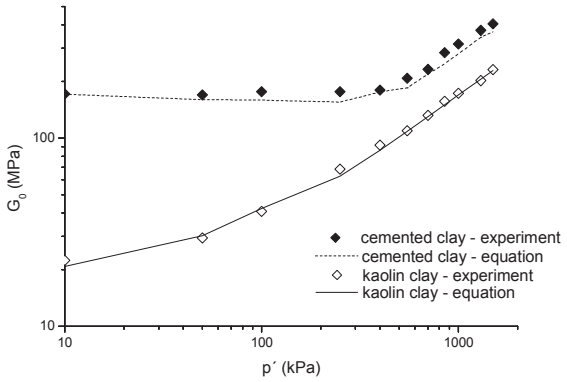


*Figure 6.4 Very small strain shear modulus versus mean effective stress measured on specimens of cemented and pure kaolin clay using bender elements and obtained from the equation (6.3)*

The isotropic compression of intact and reconstituted calcarenite studied by Cuccovillo & Coop (1997) is shown in Figure 6.5(a). Undrained shearing probes were performed and the shear moduli were measured using LVDTs. According to the authors, after accounting for the compressibility of the pore fluid, the effective stress paths followed during undrained shearing were consistent with the material having isotropic properties. Figure 6.5(b) compares the measured values of shear moduli for the intact and reconstituted soil with the calculated values (equation (6.3).

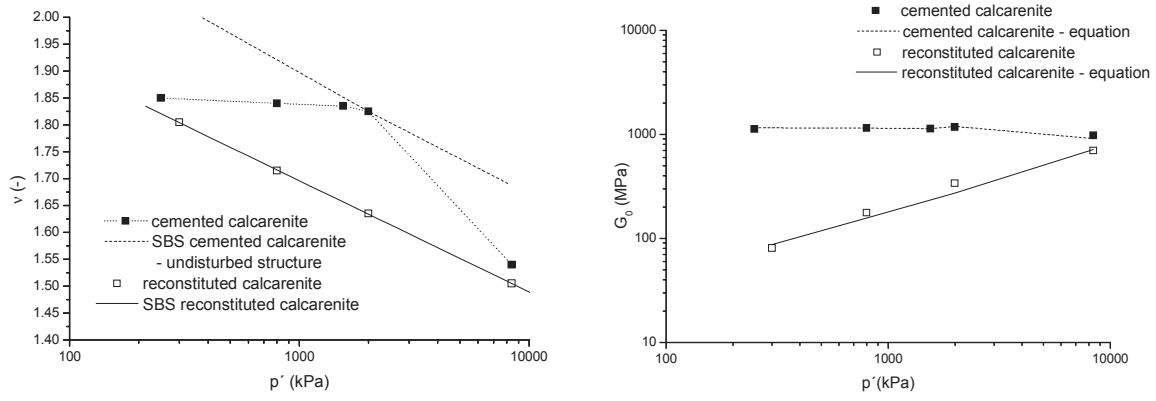


*(a)* *(b)*

*Figure 6.5 Intact and reconstituted calcarenite (experimental data from Cuccovillo & Coop 1997): (a) Isotropic compression lines; (b) very small strain shear modulus versus mean effective stress measured using LVDTs and obtained from the equation (6.3)*

Yun & Santamarina (2005) tested pure and artificially cemented Nevada sand. The small strain shear modulus was measured using shear wave propagation within an oedometer cell. The data for loose uncemented sand and loose sand with 2% and 4% of cement were used in this study. The one-dimensional compression lines are shown in Figure 6.6(a). The

values of $G_0$ were evaluated from the values of shear wave velocities, considering $\rho_s$ = 2.67 g/cm$^3$ and with the equation (6.3) (Figure 6.6(b)). The structure degradation after yielding is more severe for the sample with higher amount of Portland cement.

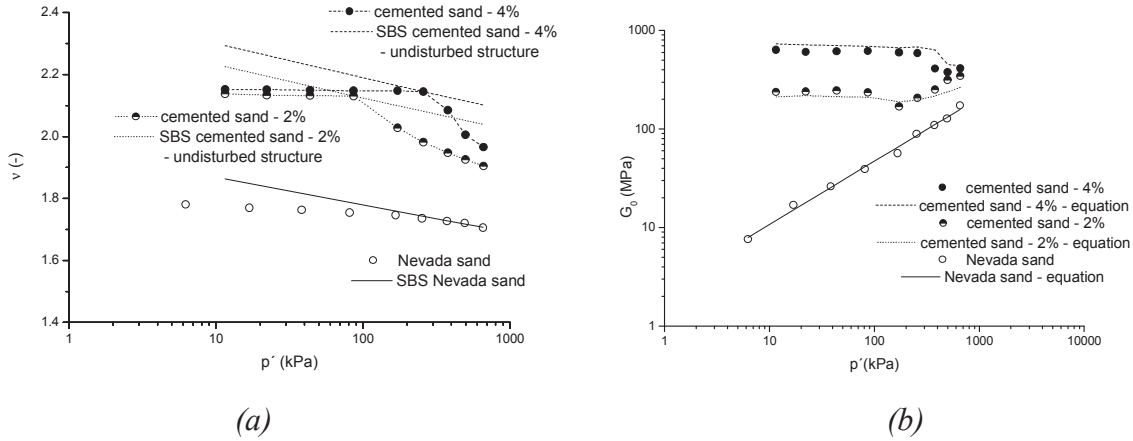


*Figure 6.6 Cemented and pure Nevada sand (experimental data from Yun & Santamarina 2005): (a) Oedometer compression lines; (b) Comparison of results for very small strain shear modulus obtained from the equation (6.3) and from bender element measurements*

The values of the parameters used in equation (6.3) are summarised in Table 6.1. The same values of $A$, $n$ and $m$ were used for the corresponding cemented and reconstituted soils. The parameter $l$ was calibrated by fitting a curve through the experimental data for the structured soil. In the case of Nevada sand the same value of parameter $l$ was used for both amounts of Portland cement. For calcarenite and kaolin clay $s_f$ =1 was considered due to converging NCLs of the cemented and reconstituted specimens (Figures 6.3(b) and 6.5(a)). For Nevada sand $s_f$ = 35 was chosen so that it represents the large distance and slow convergence of the NCLs (Figure 6.6(a)).

The measured and calculated data (equation (6.3)) are compared in Figures 6.4, 6.5(b) and 6.6(b), showing a good fit in the three cases. For the uncemented soils $G_0$ is seen to vary with $p'$. The values of $G_0$ of the cemented specimens, instead, appear to be controlled by cementation, and do not vary with $p'$, until the yield stress. At higher stresses, a significant effect of structure degradation on $G_0$ was observed.

The $G_0$ calculated for the cemented soils decreases slightly before yielding as $p'$ increases and $p_e'/p'$ decreases at the same time. The equation (6.3) thus cannot predict constant $G_0$ pre-yield, measured for strongly cemented soils. The $G_0$ variation with $p'$ is, however, minor due to low pre-yield compressibility of cemented soils and the measurements are relatively well represented. In Figures 6.5(b) and 6.6(b) the irregularities in the decreasing

trend of calculated $G_0$ are attributed to the scatter in the experimental values of $p_e'$ used in equation (6.3).

*Table 6.2 Parameters controlling the shear modulus of soils with cementation bonds used in equation (6.3)*

| material: | A | n | m | l | $s_f$ |
|---|---|---|---|---|---|
| kaolin clay | 1020 | 0.73 | 0.77 | 0.24 | 1 |
| calcarenite | 2326 | 0.631 | 0.7 | 0.7 | 1 |
| Nevada sand | 2454 | 0.642 | 0.7 | 0.34 | 35 |

## 6.4. Discussion

The literature review shows that natural or artificial cementation increases $G_0$ of sands (Acar & El-Tahir 1986; Saxena *et al.* 1988; Chang & Woods 1992; Sharma & Fahey 2004) and clays (Jovičić *et al.* 2006; Puppala *et al.* 2006) in comparison with $G_0$ of the corresponding reconstituted soil at the same mean effective stress. According to Acar & El-Tahir (1986) and Delfosse-Ribay *et al.* (2004), $G_0$ of cemented sands increased with confining stress in the whole applied range. Conversely, Cuccovillo & Coop (1997), Baig *et al.* (1997), Fernandez & Santamarina (2001) and Sharma & Fahey (2004) reported $G_0$ to be for cemented sands practically independent of the mean stress and dependent on cementation until a threshold stress was reached corresponding to the onset of major structure degradation. Cementation appears to control only $G_0$ of clays below isotropic or vertical yield stress and the pressure dependency appears to prevail at higher stresses accordingly (Jovičić *et al.* 2006; Hird & Chan 2008). The latter findings are consistent with the predictions of a micromechanical model for cemented granular material developed by Dvorkin *et al.* (1991), leading to the conclusion that the stiffness of the cemented system is strongly increased by cementation and independent of confining pressure.

The connection between deterioration of bonding and initiation of the pressure dependency of $G_0$ was reported for naturally cemented carbonate sand (i.e. calcarenite; Cuccovillo & Coop 1997), loose cement treated sand (Yun & Santamarina 2005), cement treated clay (Hird & Chan 2008) and natural clay with carbonate bonding (Cafaro & Cotecchia 2001). After yielding, Cuccovillo & Coop (1997) and Cafaro & Cotecchia (2001) reported the reduction of $G_0$, associated with degradation of the natural structure with increasing mean stress. Conversely, Yun & Santamarina (2005) and Hird & Chan (2008) indicated for artificially cemented soils an increase of $G_0$ with increasing stress after yielding

and the values of $G_0$ remained higher than for the reconstituted soils. Thus for cemented soils either reduction or increase of $G_0$ after yielding was reported.

To explain this phenomenon, various isotropic compression curves (Figure 6.7(a)) were simulated with the model for structured clays (Mašín 2007). Behaviour of cemented soils in the post-yield stress regime depends significantly on the current state of structure. The model enables to control the rate of structure degradation by a parameter $k$. The current value of $s$ may be expressed by the relationship

$$s = s_f + (s_0 - s_f)\exp\left[-\frac{k}{\lambda^*}\varepsilon^d\right] \tag{6.5}$$

where $s_0$ is initial sensitivity, $k$ is the rate of structure degradation, $\lambda^*$ is the gradient of NCL of reconstituted soil and $\varepsilon^d$ is damage strain rate.

Figure 6.7(b) shows the development of $G_0$ calculated from the simulated data using equation (6.3). The results indicate that after yield $G_0$ increases with $p'$ at low rates of structure degradation ($k$ = 0.3) and drops at high rates ($k$ = 1).

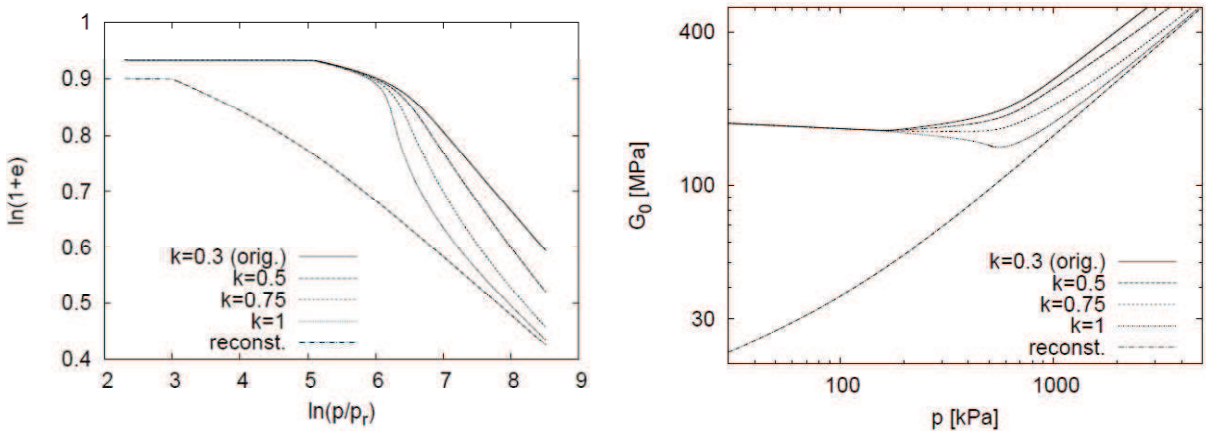


*Figure 6.7 Effect of the rate of structure degradation k on the mechanical behaviour of cemented soil: (a) isotropic compression tests; (b) variation of $G_0$ with p′*

Despite the reported differences, it is shown that a single relationship, which relates $G_0$ to the strength of the bonded structure, mean effective stress and apparent overconsolidation, can be used to predict the variation of $G_0$. The applicability of this equation to cemented soils, either clays or sand is shown. After yield, the development of $G_0$ is interpreted with the rate of structure degradation.

# Chapter 7

# Hypoplastic model for cemented clay

## 7.1. Introduction

A hypoplastic constitutive model for clays (Mašín, 2005) was chosen to model the behaviour of the tested kaolin clay. The extended version of the model, hypoplastic model for clays with meta-stable structure (Mašín, 2007), enables to simulate progressive changes in behaviour caused by debonding. Equation (6.3) presented in Section 6.2 was incorporated by Mašín into the extended version of hypoplastic constitutive model to improve the simulation of the behaviour of the cemented kaolin clay.

## 7.2. Classification of the model

The hypoplastic constitutive model for clays was developed by Mašín (2005) on the basis of generalized hypoplasticity principles (Kolymbas, 1991; von Wolffersdorff, 1996) combined with critical state soil mechanics and the Modified Cam clay model. The model was improved with the elastic strain range - intergranular strain concept (Niemunis & Herle, 1997), which reproduces the effects of increasing small strain stiffness with confining stress.

The effects of structure on the mechanical behaviour of clays were implemented to the hypoplastic model by Mašín (2007) with modifications of barotropy and pyknotropy factors. According to Cotecchia & Chandler (2000) the influence of structure in fine-grained soils can be quantified by the different sizes of the state boundary surfaces (SBS) for the structured and reconstituted soil. The hypoplastic model includes a close approximation of the SBS, the swept-out-memory (SOM) surface (Mašín & Herle, 2005).

The extended version for clays with metastable structure is capable of predicting the non-linear behaviour in the range from very small to large strains, including the effects of recent stress history (Atkinson *et al.*, 1990). Its predictions are comparable with predictions by advanced soil models based on kinematic hardening elasto-plasticity (Mašín, 2009).

## 7.3. Model evaluation

At first, the behaviour of the reconstituted kaolin clay was simulated with the hypoplastic constitutive model for clays. In order to model the behaviour of the cemented kaolin clay, the enhanced model for clays with metastable structure was modified by Mašín and calibrated.

### 7.3.1. Scope of the model

As a first hypothesis, it is assumed that the behaviour of the clay, pure or cemented, can be considered as isotropic. This simplification has been made to limit the number of parameters. Secondly, the additional soil stiffness and strength components related to the cementation between particles are taken into account.

Mašín (2005) derived a formula for calculation of the very small strain shear modulus $G_0$ by the hypoplastic model with the known values of the mean effective stress $p'$ and model parameters $m_R$, $r$ and $\lambda^*$:

$$G_0 = \frac{m_R}{r\lambda^*} p' \tag{7.1}$$

In its original formulation the very small strain shear stiffness is linearly dependent on the mean stress and independent of sensitivity and overconsolidation ratio, which does not correspond to the experimental data presented in Section 6.3.2. To overcome the discrepancy, the hypoplastic model was modified by Mašín to incorporate the equation (6.3) by considering $m_R$ as a variable rather than a model parameter. The isotropic apparent overconsolidation pressure is assumed to be the parameter controlling the size of the yield surface and the sensitivity ratio determines the state of the structure. A comparison of equation (6.3) with equation (7.1) led to the following expression of the variable $m_R$:

$$m_R = r\lambda^* A_G \left(\frac{p'}{p_r}\right)^{(n-1)} \left(\frac{p_e'}{p'}\right)^m \left(\frac{s}{s_f}\right)^l \tag{7.2}$$

The rest of the mathematical formulation of the model remains unchanged.

### 7.3.2. Parameters for simulation

The results obtained for the pure reconstituted kaolin clay (see Chapter 4 and 5) were used to derive five parameters of the basic model $N$, $\lambda^*$, $\kappa^*$, $\varphi_c$ and $r$ with procedures outlined in Mašín (2005). Parameters $N$, $\lambda^*$, $\kappa^*$ were derived from the isotropic compression tests. The parameter $\varphi_c$ is the critical state friction angle and the parameter $r$ controls the shear stiffness and it was found with a parametric study. The same values of the parameters were used in

simulations of both the pure and the cemented kaolin clay except the parameter $\kappa^*$, which was calibrated separately.

The enhanced model for cemented clay requires another three parameters. The soil parameters $k$, $A$, $s_f$ are related to the states of structure at large strains. The values were found using results obtained for the cemented kaolin clay following Mašín (2007). The final sensitivity $s_f$ =1 was considered due to converging NCLs of the cemented and reconstituted specimens (see Section 6.3). The parameter $A$ controls importance of volumetric and shear strain components. The effect of the parameter $k$, which controls the rate of structure degradation, is shown in Section 6.4.

In order to predict the soil behaviour in the range from small to very small strains, the model was enhanced by Mašín (2005) with the intergranular strain concept (Niemunis and Herle 1997). In its basic form, the enhancement requires additional parameters $R$, $\beta_r$, $\chi$, $m_R$ and $m_T$. The parameters $m_R$ and $m_T$ (considered in this work of equal value), controlling the very small strain shear modulus, were replaced by the new parameters $A_G$, $n$, $m$ and $l$ (equation (7.2)). The new parameters were calibrated as described in Section 6.2, Figure 6.2. The parameters $R$, $\beta_r$ and $\chi$ control the rate of stiffness degradation with shear strain in the small strain range and they were found based on LVDT measurements during the shear probes on the cemented kaolin clay (see Section 5.3.2). Values of all parameters used in the hypoplastic model are given in Table 7.1 and Table 7.2.

*Table 7.1 Parameters of hypoplastic constitutive model for pure and cemented clay*

| material: | Parameters of the basic model | | | | | Parameters of structure | | | Parameters of the small strain behaviour | | |
|---|---|---|---|---|---|---|---|---|---|---|---|
| | N | λ* | κ* | $\varphi_c$ | r | k | A | $s_f$ | R | $\beta_r$ | χ |
| uncemented | 1.32 | 0.105 | 0.02 | 27.5 | 0.45 | 1 | 0.4 | 1 | 0.00012 | 1.05 | 3 |
| cemented | 1.32 | 0.105 | 0.01 | 27.5 | 0.45 | 0.3 | 0.4 | 1 | 0.00012 | 1.05 | 3 |

*Table 7.2 Parameters controlling the shear modulus of pure and cemented clay*

| material: | $A_G$ | n | m | l | $s_f$ |
|---|---|---|---|---|---|
| uncemented | 1020 | 0.73 | 0.77 | - | - |
| cemented | 1020 | 0.73 | 0.77 | 0.24 | 1 |

### 7.3.3. Fit to laboratory data

The results calculated with the hypoplastic model for clays with metastable structure using the determined parameters are compared with experimental results. Figure 8.1 shows large strain response of the pure and the cemented kaolin clay under isotropic compression. The response

to unloading was adopted from one-dimensional unloading, considering the one-dimensional and isotropic swelling lines to be parallel.

The experimental and calculated behaviour in undrained tests on the pure and cemented specimens are shown in Figure 8.2 and 8.3, respectively. It is interesting to note how the model can reproduce contractant and dilatant behaviour of the pure kaolin clay. In the case of the cemented kaolin clay the model underestimates the peak deviator stress.

The strain dependency of shear modulus is shown in Figure 8.4. The calculated and experimental results are in good agreement.

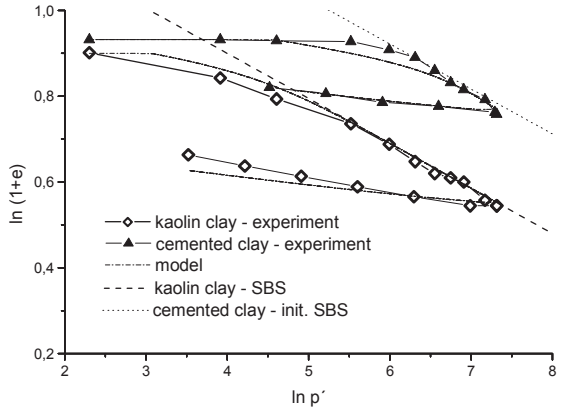


*Figure 8.1 Isotropic compression tests for pure and cemented kaolin clay – experimental and calculated results*

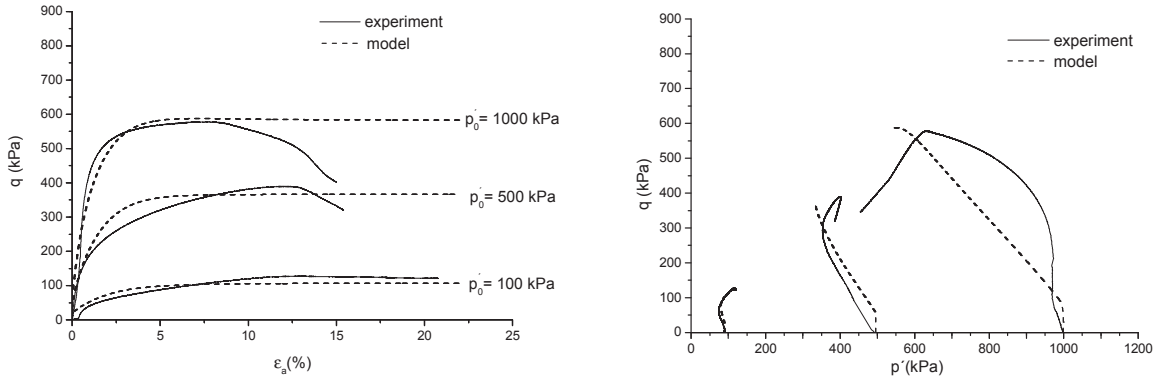


*(a)* *(b)*

*Figure 8.2 Experimental and calculated results of undrained shear tests on pure kaolin clay: (a) stress-strain relationship; (b) stress path*

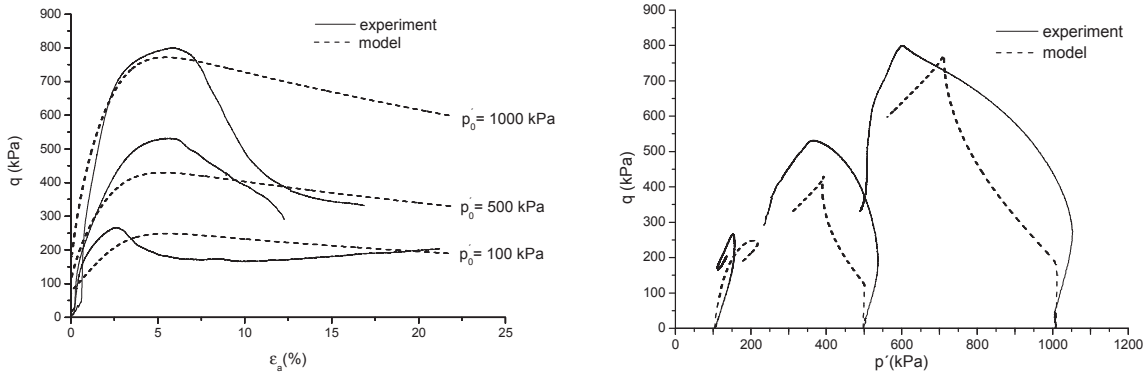


*(a)* *(b)*

*Figure 8.3 Experimental and calculated results of undrained shear tests on cemented kaolin clay: (a) stress-strain relationship; (b) stress path*

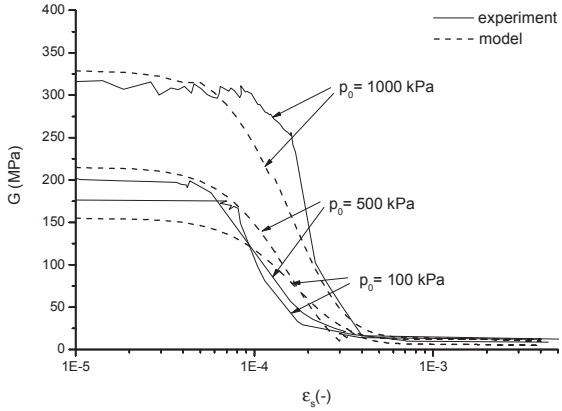


*Figure 8.4 Experimental data and predictions of the shear stiffness degradation with shear strain during undrained shear tests for cemented kaolin clay*

The model is capable of reproducing the behaviour of pure and cemented kaolin clay at very small strains and large strains. The only significant discrepancy is observed in the large-strain response in Figure 8.3(a). The rapid drop of the deviator stress visible in the laboratory tests was caused by the development of shear zones. This effect is not well captured with the single element simulations by the hypoplastic model.

## 7.4. Summary

The results obtained from compression and shear tests of the pure and cemented kaolin clay were modelled by the hypoplastic constitutive model for clays with metastable structure (Mašín, 2007). The model was calibrated by using the available experimental results, including the measurements of the small strain shear modulus.

The experimental behaviour was successfully simulated. A major disagreement was found only in simulating the strain softening.

# Chapter 8

# Conclusions

The thesis focused on the mechanical behaviour of cemented fine-grained soil. The study was based on the comparison of the mechanical behaviour obtained for artificially cemented clay with the behaviour of the corresponding reconstituted clay.

Artificially cemented specimens were prepared by mixing the kaolin clay with the various amount of Portland cement. The results of the introductory one-dimensional compression test series confirmed the development of structure in the kaolin specimens with addition of Portland cement. The cemented clay had a low pre-yield and high post-yield compressibility, which is typical for natural cemented soils. The position of yield was affected by the cement content and the curing period. Both effects were connected with the amount of bonds. The structure disturbance led to increase of compression index $C_c$.

The cement content of 4% of the dry mass was chosen to model cemented clay. A difference was found between one-dimensional and isotropic compression of the model cemented clay at the post-yield convergence of the cemented and uncemented compression curves. The microstructural changes induced by one-dimensional compression (including compression and shear stresses) were more severe than the changes induced by isotropic compression. The data obtained from one-dimensional compression test indicated that the normal compression line of cemented and pure clay ultimately converge at high stresses.

The comparison of shearing behaviour showed significant differences between the cemented and pure specimens in the range from very small to large strains. The addition of Portland cement to the soil led to the increase of shear strength and initial stiffness of the specimens. During undrained shearing, the pure clay showed predominantly ductile behaviour and the shearing behaviour was characterised with zero cohesion. The cemented specimens exhibited brittle behaviour and gradual strain softening after peak. The mobilized peak friction angle was reduced for the cemented specimens compressed at higher mean effective stress. Tendency to contractant behaviour was observed for the cemented specimens as a result of gradual destructuration.

The shear modulus at very small strains ($G_0$) of reconstituted normally consolidated pure clay was dependent on the mean effective stress. On the contrary, $G_0$ of the cemented

kaolin clay was stress independent until a threshold. The values of $G_0$ were higher than the values obtained for the pure kaolin clay. The destructuration after the threshold resulted in the stress dependency of the $G_0$ similar to the pure kaolin clay.

According to the results obtained for the compression and shearing behaviour, parameters such as yield stress, peak strength, pre-yield and post-yield compressibility and small-strain stiffness are sensitive to cementation. The sensitivity varies with stress and strains. The observations suggested that for specimens compressed up to yield the degradation of cementation is more likely to occur with increasing strain than with increasing stress.

The experimental behaviour was successfully simulated by the hypoplastic constitutive model for clays with meta-stable structure. A major disagreement was found only in simulating the strain softening during shear tests.

Finally, the agreement between the test results and an equation from the literature, relating $G_0$ to the mean stress, apparent overconsolidation ratio and sensitivity was obtained. Moreover, the applicability of the equation to cemented sands was shown. After yield, the development of $G_0$ was interpreted with the rate of structure degradation.

Thanks to the detailed laboratory study carried out on the artificially cemented kaolin clay, a complete picture of the mechanical behaviour of cemented clayey soil was obtained. The results confirmed the possibility to simulate the mechanical behaviour of natural cemented soil using artificially cemented specimens. The understanding of the complex mechanical behaviour of cemented soils is an important point in the mechanics of soils and the reported data may be found useful for further study.

# References


Acar, Y. B. & El-Tahir, A. E. 1986. Low strain dynamic properties of artificially cemented sand. *J. Geotech. Eng.* 112 (11): 1001-1015.

Arroyo, M., Wood D., M. & Greening, P. D. 2003. Source near-field effects and pulse tests in soil samples. *Géotechnique* 53 (3): 337 – 345.

Arroyo, M., Wood D. M., Greening, P. D., Medina, L. & Rio, J. 2006. Effects of sample size on bander-based axial $G_0$ measurements. *Géotechnique* 56 (1): 39 – 52.

Atkinson, J. H. & Bransby, P. L. 1978. The mechanics of soils, an introduction to critical state soil mechanics. McGraw-Hill, London.

Atkinson, J. H., Richardson, D. & Stallebrass, S. E. 1990. Effect of recent stress history on the stiffness of overconsolidated soil. *Géotechnique* 40 (4): 531-540.

Atkinson, J. 1993. An introduction to the mechanics of soils and foundations: Through critical state soil mechanics. McGraw-Hill book company.

Baig, S., Picornell, M. & Nazarian, S. 1997. Low strain shear moduli of cemented sands. *J. Geotech. Geoenviron. Eng.* 123 (6): 540-545.

Baudet, B. & Stallebrass, S. 2004. A constitutive model for structured clays. *Géotechnique* 54 (4): 269-278.

Boardman, D. I., Glendinning, S. & Rogers, C. D. F. 2001. Development of stabilisation and solidification in lime-clay mixes. *Géotechnique* 50 (6): 533-543.

Boone, S. J. & Lutenegger, A. J. 1997. Carbonates and cementation of glacially derived cohesive soils in New York State and southern Ontario. *Can. Geotech. J.* 34: 534-550.

Buatier, M. D., Karpoff, A. M. & Charpentier, D. 2002. Clays and zeolite authigenesis in sediments from the flank of the Juan de Fuca Ridge. *Clay minerals* 37: 143-155.

Burland, J. B. 1990. On the compressibility and shear strength of natural clays. *Géotechnique* 40 (3): 329-378.

Burland, J. B., Rampello, S., Georgiannou, V. N. & Calabresi, G. 1996. A laboratory study of the strength of four stiff clays. *Géotechnique* 46 (3): 491-514.

Cafaro, F. & Cotecchia, F. 2001. Structure degradation and changes in the mechanical behaviour of a stiff clay due to weathering. *Géotechnique* 51 (5): 441-453.

Callisto, L., Gajo, A. & Muir Wood , D. 2002. Simulation of triaxial and true triaxial tests on natural and reconstituted Pisa clay. *Géotechnique* 52 (9): 649-666.

Callisto, L. & Rampello, S. 2004. An interpretation of structural degradation for three natural clays. *Can. Geotech. J.* 41: 392-407.

Casagrande, A. 1936. The determination of the pre-consolidation load and its practical significance. *Proc. 1st Int. Conf. Soil Mech.*. Cambridge, Mass., 3: 60-64.

Chang, T. S. & Woods R. D. 1992. Effect of particle contact bond on shear modulus. *J. Geotech. Eng.* **118**, No. 2, 1216-1233.

Chew, S. H., Kamruzzaman, A. H. M. & Lee, F. H. 2004. Physicochemical and engineering behavior of cement treated clays. *Journal of Geotechnical and Geoenvironmental Engineering* 130 (7): 696-706.

Clough, G. W., Sitar, N., Bachus, R. C. & Rad, N. S. 1981. Cemented sands under static loading. *J. Geotech. Eng.* 107 (6): 799-817.

Coop, M. R. & Atkinson, J. H. 1993. The mechanics of cemented carbonate sands. *Géotechnique* 43 (1): 53-67.

Cotecchia, F. & Chandler, R. J. 1997. The influence of structure on the pre-failure behaviour of a natural clay. *Géotechnique* 47 (3): 523-544.

Cotecchia, F. & Chandler, R. J. 2000. A general framework for the mechanical behaviour of clays. *Géotechnique* 50 (4): 431-447.

Chang, T. S. & Woods, R. D. 1992. Effect of particle contact bond on shear modulus. *Journal of Geotechnical Engineering* 118 (8): 1216-1233.

Cookenboo, H. O. & Bustin, R. M. 1999. Pore water evolution in sandstones of the Groundhog Coalfield, northern Bowser Basin, British Columbia. *Sedimentary Geology* 123: 129-146.

Cravero, F., Gonzalez, I., Galan, E. & Dominguez, E. 1997. Geology, mineralogy, origin and possible applications of some Argentinian kaolins in the Neuquen basin. *Applied Clay Science* 12: 27-42.

Cuccovillo, T. & Coop, M. R. 1997. Yielding and pre-failure deformation of structured sands. *Géotechnique* 47 (3): 491-508.

Cuccovillo, T. & Coop, M. R. 1999. On the mechanics of structured sands. *Géotechnique* 49 (6): 741-760.

Cudny, M. 2003. Simple multi-laminate model for soft soils incorporating structural anisotropy and destructuration. In Vermeer, Schweiger, Karstunen & Cudny (eds.) Int. Workshop on Geotechnics of Soft Soils – Theory and Practice.

Delfosse-Ribay, E., Djeran-Maigre, I., Cabrillac, R. & Gouvenot, D. 2004. Shear modulus and damping ratio of grouted sand. *Soil Dynamics and Earthquake Engineering* 24: 461-471.

Dvorkin, J., Mavko, G. & Nur, A. 1991. The effect of cementation on the elastic properties of granular material. *Mechanics of Materials* 12: 207-217.

Dvorkin, J. & Yin, H. 1995. Contact laws for cemented grains: implications for grain and cement failure. *Int. J. Solids Structures* 32 (17/18): 2497-2510.

Dworkin, S. I. & Land, L. S. 1994. Petrographic and geochemical constraints on the formation and diagenesis of anhydrite cements, smackover sandstones, Gulf of Mexico. *Journal of Sedimentary Research* A64 (2): 339-348.

Einsele, G. 1992. Sedimentary basins: evolution, facies, and sediment budget. Berlin – Springer-Verlag.

Ellis, P. M. 1986. Post-Miocene carbonate diagenesis of the Lower Cretaceous Edwards Group in the Balcones fault zone area, south-central Texas. In P. L. Abbott and C. M. Woodruff, Jr. (eds.) The Balcones Escarpment, Central Texas: Geological Society of America: 101-114.

Feda, J. 1995. Behaviour of a cemented clay. *Can. Geotech. J.* 32: 899-904.

Feda, J. 2002. Simulation of behaviour of undisturbed soil samples – in Czech. *Geotechnika* 1: 3-5.

Fernandez, A. L. & Santamarina, J. C. 2001. Effect of cementation on the small-strain parameters of sands. *Can. Geotech. J.* 38: 191-199.

Folk, R. L. 1980. Petrology of sedimentary rocks. Austin – Hemphill.

Gens, A. & Nova, R. 1993. Conceptual bases for a constitutive model for bonded soils and weak rocks. In A. Anagnostopoulos, F. Schlosser, N. Kalteziotis & R. Frank (eds.) Proc. Symp. on Geotechnical Eng. of Hard Soils – Soft Rocks, Balkema Rotterdam, 485-494.

Ginsburg, R.N. 1953. Beachrock in south Florida. *Journal of Sedimentary Petrology* 23 (2): 85-92.

Gluyas, J., Jolley, L. & Primmer, T. 1997. Element mobility during diagenesis: sulphate cementation of Rotliegend sandstones, Southern North Sea. *Marine and Petroleum Geology* 14 (7/8): 1001-1011.

Grant, S. M. & Oxtoby, N. H. 1992. The timing of quartz cementation in Mesozoic sandstones from Haltenbanken, offshore mid-Norway: fluid inclusion evidence. *Journal of the Geological Society, London* 149: 479-482.

Guorui, G. 1991. Application of microstructure classification of marine sediment to engineering geological evaluation. In R. H. Bennett, W. R. Bryant and M.H. Hulbert (eds.) Microstructure of fine-grained sediments: from mud to shale, Springer-Verlag New York, 531-537.

Haddad, S. C., Worden, R. H., Prior, D. J. & Smalley, P. C. 2006. Quartz cement in the Fontainebleau sandstone, Paris basin, France: crystallography and implications for mechanisms of cement growth. *Journal of Sedimentary Research* 76: 244-256.

Hardin, B. O. 1978. The nature of stress-strain behaviour for soils. Proc. ASCE Geotech Engrg Div Speciality Conf on Earthquake Engineering and Soil Dynamics, vol. 1, 3- 90.

He, C., Osbæck, B. & Makovicky, E. 1995. Pozzolanic reactions of six principal clay minerals: activation, reactivity assessments and technological effects. *Cement and Concrete Research* 25 (8): 1691-1702.

Hight, D. W., Böese, R., Butcher, A. P., Clayton, C. R. I. & Smith, P. R. 1992a. Disturbance of the Bothkennar clay prior to laboratory testing. *Géotechnique* 42 (2): 199-217.

Hight, D. W., Bond, A. J. & Legge, J. D. 1992b. Characterization of the Bothkennar clay: an overview. *Géotechnique* 42 (2): 303-347.

Hird, C. & Chan, C. 2008. One-Dimensional Compression Tests on Stabilized Clays Incorporating Shear Wave Velocity Measurements. *Geotech. Test. J.* 31 (2): 1-9.

Holtz, R. D. & Kovacs, W. D. 1981. An introduction to geotechnical engineering. Prentice-Hall, Inc., New Jersey.

ICDD 2002. JCPDS PDF-2 database. ICDD, Newton Square.

Ismail, M. A., Joer, H. A., Randolph, M. F. & Meritt, A. 2002. Cementation of porous materials using calcite. *Géotechnique* 52 (5): 313-324.

Jovičić, V., Coop, M. & Simić, M. 1996. Objective criteria for determining $G_{max}$ from bender element tests. *Géotechnique* 46 (2): 357 – 362.

Jovičić, V., Coop, M. & Simpson, B. 2006. Interpretation and modelling of deformation characteristics of a stiff North Sea clay. *Can. Geotech. J.* 43: 341-354.

Kamruzzaman, A. H. M., Chew, S. H. & Lee, F. H. 2009. Structuration and destructuration behavior of cement-treated Singapore marine clay. *J. Geotech. Geoenviron. Eng.* 135 (4): 573-589.

Kim, G. Y., Yoo, D. G., Lee, H. J., Lee, Y. J. & Kim, D. C. 2007. The relationship between silica diagenesis and physical properties in the East/Japan Sea: ODP Legs 127/128. *Journal of Asian Earth Sciences* 30: 448-456.

Klein, J. S., Mozley, P., Campbell, A. & Cole, R. 1999. Spatial distribution of carbon and oxygen isotopes in laterally extensive carbonate-cemented layers: implications for mode of growth and subsurface identification. *Journal of Sedimentary Research* 69 (1): 184-191.

Koliji, A., Vulliet, L. & Laloui, L. 2008. New basis for the constitutive modelling of aggregated soils. *Acta Geotechnica* 3: 61-69.

Kolymbas, D. 1991. An outline of hypoplasticity. *Archive of Applied Mechanics* 61: 143-151.

Labuda, E., Cherepakhov, G. & Barkatt, A. 2007. Formation of hard hematite-cemented solids in steam generators: an analog of lithification of Fe-containing sedimentary rocks. *Clays and Clay minerals* 55 (1): 59-70.

Leroueil, S. & Vaughan, P.R. 1990. The general and congruent effects of structure in natural soils and weak rocks. *Géotechnique* 40 (3): 467-488.

Lindholm, R. C. 1974. Fabric and cheistry of pore filling calcite in septarian veins: models for liestone cementation. *Journal of Sedimentary Petrology* 44 (2): 428-440.

Liu, K. W. & Greyling, E. H. 1996. Grain-size distribution and cementation of the Cretaceous Mzamba Formation of Eastern Cape, South Africa: a case study of a storm-influenced offshore sequence. *Sedimentary Geology* 107: 83-97.

Liu, M. D. & Carter, J. P. 1999. Virgin compression of structured soils. *Géotechnique* 49 (1): 43-57.

Lo, S.-C. R., Lade, P. V. & Wardani, S. P. R. 2003. An experimental study of the mechanics of two weakly cemented soils. *Geotechnical Testing Journal* 26 (3).

Lorenzo, G. A., Bergado, D. T. & Soralump, S. 2005. New and economical mixing method of cement-admixed clay for DMM application. *Geotechnical Testing Journal* 29 (1).

Malandraki, V. & Toll, D. G. 2001. Triaxial tests on weakly bonded soil with changes in stress path. *J. Geotech. Geoenviron. Eng.* 127 (3): 282-291.

Mašín, D. 2005. A hypoplastic constitutive model for clays. *International Journal for Numerical and Analytical Methods in Geomechanics* 29 (4): 311-336.

Mašín, D. & Herle, I. 2005. State boundary surface of a hypoplastic model for clays. *Computers and Geotechnics* 32 (6): 400-410.

Mašín, D. 2007. A hypoplastic constitutive model for clays with meta-stable structure. *Can. Geotech. J.* 44: 363-375.

Mašín, D. 2009. Comparison of predictive capabilities of selected elasto-plastic and hypoplastic models for structured clays. *Soils and Foundations* 49 (3): 381-390.

Mederer, J. 1988. The geochemistry of main structural bonds between minerals in argillaceous rocks of the Lower Cretaceous. *Applied Clay Science* 3: 135-144.

Metelková, Z., Boháč, J., Přikryl, R. & Sedlářová, I. 2012. Maturation of loess treated with variable lime admixture: Pore space textural evolution and related phase changes. *Applied Clay Science* 61: 37-43.

Michalowski, R., L., 2005. Coefficient of earth pressure at rest. *Journal of Geotech. and Geoenv. Engineering* 131 (11): 1429 – 1433.

Mitchell, J. K. 1993. Fundamentals of soil behaviour–2nd Edition. New York – Wiley and Sons.

Mitsui, K. & Taguchi, K. 1977. Silica mineral diagenesis in Neogene Tertiary shales in the Tempoku district, Hokkaido, Japan. *Journal of Sedimentary Petrology* 47 (1): 158-167.

Moore, D. M. & Reynolds, R. C. 1997. X-ray diffraction and the identification and analysis of clay minerals, 2nd edition, Oxford University Press, Oxford.

Muhunthan, B. & Sariosseiri, F. 2008. Interpretation of geotechnical properties of cement treated soils. Research Report FHWA Contract DTFH61-05-C-00008. Washington State University, Pullman WA.

Muir Wood, D. 2004. Geotechnical modelling. Spon Press, Taylor & Francis Group.

Niemunis, A. & Herle, I. 1997. Hypoplastic model for cohesionless soils with elastic strain range. *Mech. of Cohes.-Frict. Mater.* 2: 279-299.

Osula, D. O. A. 1996. A comparative evaluation of cement and lime modification of laterite. *Engineering Geology* 42: 71-81.

Pamukcu, S. & Tuncan, M. 1991. Influence of some physicochemical activities on mechanical behavior of clays. In R. H. Bennett, W. R. Bryant & M. H. Hulbert (eds.) Microstructure of fine-grained sediments: from mud to shale, Springer-Verlag New York, 241-253.

Petránek, J. 1993. Small encyclopedia of geology. České Budějovice – Nakladatelství JIH.

Pillai, V. S. & Muhunthan, B. 1999. Landslides in cemented and normally consolidated soils: a review of failure mechanism using stress-path. Proceedings of 13th annual Vancouver Geotechnical Society Symposium, Vancouver, British Columbia.

Prashant, A. & Penumadu, D. 2005. A laboratory study of normally consolidated kaolin clay. *Can. Geotech. J.* 42: 27-37.

Puppala, A. J., Kadam, R., Madhyannapu, R. S. & Hoyos, L. R. 2006. Small-strain shear moduli of chemically stabilized sulfate-bearing cohesive soils. *Journal of Geotechnical and Geoenvironmental Engineering* 132 (3): 322-336.

Pusch, R., Zwahr, H., Gerber, R. & Schomburg, J. 2003. Interaction of cement and smectitic clay-theory and practice. *Applied Clay Science* 23: 203-210.

Read, D., Glasser, F. P., Ayora, C., Guardiola, M. T. & Sneyers, A. 2001. Mineralogical and microstructural changes accompanying the interaction of Boom Clay with ordinary Portland cement. *Advances in Cement Research* 13 (4): 175-183.

Rocchi, G., Fontana, M. & Da Prat, M. 2003. Modelling of natural soft clay destruction processes using viscoplasticity theory. *Géotechnique* 53 (8): 729-745.

Rotta, G. V., Consoli, N. C., Prietto, P. D. M., Coop, M. R. & Graham, J. 2003. Isotropic yielding in an artificially cemented soil cured under stress. *Géotechnique* 53 (5): 493-501.

Saihi, F., Leroueil, S., La Rochelle, P. & French, I. 2002. Behaviour of the stiff and sensitive Saint-Jean-Vianney clay in intact, destructured, and remoulded conditions. *Can. Geotech. J.* 39: 1075-1087.

Sanchez-Salinero, I., Roesset, J. M. & Stokoe, K. H. II. 1987. Analytical studies of body wave propagation and attenuation. *A report on research*, University of Texas at Austin, Austin, TX, USA.

Sangrey, D. A. 1972. Naturally cemented sensitive soils. *Géotechnique* 22 (1): 139-152.

Saxena, S. K., Avramidis, A. S. & Reddy, K. S. 1988. Dynamic moduli and damping ratios for cemented sands at low strains. *Can. Geotech. J.* 25: 353-368.

Schmidt, B., 1966. Earth pressures at rest related to stress history. Discussion. *Can. Geotech. J.*, 3 (4): 239 – 242.

Schofield, A. N. & Wroth, C. P. 1968. Critical state soil mechanics. *McGraw-Hill*, London.

Sharma, S. S. & Fahey, M. 2003. Degradation of stiffness of cemented calcareous soil in cyclic triaxial tests. *Journal of Geotechnical and Geoenvironmental Engineering* 129 (7): 619-629.

Sharma, S. S. & Fahey, M. 2004. Deformation characteristics of two cemented calcareous soils. *Canadian Geotechnical Journal* 41: 1139-1151.

Shaw, J. D. N. 1982. A review of resins used in construction. Types of resin-applications-case histories. *Int. J. Adhesion and Adhesives* April: 77-83.

Sivakumar, V., Doran, I. G. & Graham, J. 2002. Particle orientation and its influence on the mechanical behaviour of isotropically consolidated reconstituted clay. *Engineering geology* 66: 197-209.

Spinelli, G. A., Mozley, P. S., Tobin, H. J., Underwood, M. B., Hoffman, N. W. & Bellew. G. M. 2007. Diagenesis, sediment strength, and pore collapse in sediment approaching the Nankai Trough subduction zone. *GSA Bulletin* 119 (3/4): 377-390.

Stallebrass, S. E. 1990. Modelling the effect of recent stress history on the deformation of overconsolidated soils. Ph.D. Thesis. The City University.

Stutzman P. E. 2001. Scanning Electron Microscopy in Concrete Petrography. In J. Skalny, J. Gebauer and I. Odler (eds.) Proc. Materials Science of Concrete Special Volume: Calcium Hydroxide in Concrete, The American Ceramic Society. November 1-3, 2000, Anna Maria Island, Florida, 59-72.

Tada, R. & Iijima, A. 1983. Petrology and diagenetic changes of Neogene siliceous rocks in northern Japan. *Journal of Sedimentary Petrology* 53 (3): 911-930.

Towe, K. M. 1962. Clay mineral diagenesis as a possible source of silica cement in sedimentary rocks. *Journal of Sedimentary Petrology* 32 (1): 26-28.

Tremblay, H., Leroueil, S. & Locat, J. 2001. Mechanical improvement and vertical yield stress prediction of clayey soils from eastern Canada treated with lime or cement. *Canadian Geotechnical Journal* 38: 567-579.

Trhlíková, J., Mašín, D. & Boháč, J. 2012. Small-strain behaviour of cemented soils. *Géotechnique* 62 (10): 943 – 947.

Tucker, M. E. 2001. Sedimentary petrology–3rd Edition. Oxford - Blackwell Science.

Uddin, M. K. & Buensuceso, B. R. 2002. Lime treated clay: Salient engineering properties and a conceptual model. *Soils and Foundations* 42 (5): 79-89.

van der Perk, M. 2006. Soil and water contamination: from molecular to catchment scale. London – Taylor & Francis.

Vatsala, A., Nova, R. & Srinivasa Murthy, B. R. 2001. Elastoplastic model for cemented soils. *J. Geotech. Geoenviron. Eng.* 127 (8): 679-687.

Vieira, M. M. & De Ros, L. F. 2006. Cementation patterns and genetic implications of Holocene beachrocks from northeastern Brazil. *Sedimentary Geology* 192: 207-230.

Viggiani, G. 1992. Small strain stiffness of fine grained soils. Ph.D. Thesis. The City University.

Viggiani, G. & Atkinson, J. 1995. Stiffness of fine-grained soil at very small strains. *Géotechnique* 45 (2): 249 – 265.

Viggiani, G. & Atkinson, J. 1997. Interpretation of bender element tests. *Géotechnique* 47 (4): 873 – 877.

Viseras, C., Aguzzi, C., Cerezo, P. & Lopez-Galindo, A. 2007. Uses of clay minerals in semisolid health care and therapeutic products. *Applied Clay Science* 36: 37 – 50.

von Wolffersdorff, P. A. 1996. A hypoplastic relation for granular materials with a predefined limit state surface. *Mech. of Cohes.-Frict. Mater.* 1: 251-271.

Wang, Y.-H. & Siu, W.-K. 2006a. Structure characteristics and mechanical properties of kaolinite soils. I. Surface charges and structural characterizations. *Can. Geotech. J.* 43: 587-600.

Wang, Y.-H. & Siu, W.-K. 2006b. Structure characteristics and mechanical properties of kaolinite soils. II. Effects of structure on mechanical properties. *Can. Geotech. J.* 43: 601-617.

Wheeler, S. J., Cudny, M., Neher, H. P. & Wiltafsky, C. 2003. Some developments in constitutive modelling of soft clays. In Vermeer, Schweiger, Karstunen & Cudny (eds.) Int. Workshop on Geotechnics of Soft Soils – Theory and Practice.

Ye, G. 2003. Experimental Study and Numerical Simulation of the Development of the Microstructure and Permeability of Cementitious Materials. PhD Thesis, Delft University, Netherlands.

Yun, T. S. & Santamarina, J. C. 2005. Decementation, Softening, and Collapse: Changes in Small-Strain Shear Stiffness in $k_0$ Loading. *J. Geotech. Geoenviron. Eng.* 131 (3): 350-358.